Asymptotics and scaling analysis of 2-dimensional lattice models of vesicles and polymers

Nils Adrian Haug

Submitted in partial fulfillment of the requirements of the Degree of Doctor of Philosophy

May 2017

I, Nils Adrian Haug, confirm that the research included within this thesis is my own work or that where it has been carried out in collaboration with, or supported by others, that this is duly acknowledged below and my contribution indicated. Previously published material is also acknowledged below.

I attest that I have exercised reasonable care to ensure that the work is original, and does not to the best of my knowledge break any UK law, infringe any third party's copyright or other Intellectual Property Right, or contain any confidential material.

I accept that the College has the right to use plagiarism detection software to check the electronic version of the thesis.

I confirm that this thesis has not been previously submitted for the award of a degree by this or any other university.

Signature: Nils Haug Date: 22 May 2017

Details of collaboration and publications:

The contents of Chapter 3 and Section 6.1 are contained in the paper [35]. This work was carried out together with Gregorz Siudem and Thomas Prellberg.

The content of Chapter 4 largely agrees with the content of the publication [34]. The results were derived in collaboration with Thomas Prellberg.

The content of Chapter 5 is not published yet. Its results were derived in collaboration with Thomas Prellberg.

The results of Chapter 6 were derived by me, and as mentioned above, Section 6.1 was published as a part of the article [35].

The content of Chapter 7 was produced during two consecutive academic visits at the Universität Erlangen-Nürnberg, in collaboration with Christoph Richard.

The content of Chapter 8 appeared in the article [33]. This work was done together with Adri Olde Daalhuis and Thomas Prellberg.

Abstract

The subject of this thesis is the asymptotic behaviour of generating functions of different combinatorial models of two-dimensional lattice walks and polygons, enumerated with respect to different parameters, such as perimeter, number of steps and area. These models occur in various applications in physics, computer science and biology. In particular, they can be seen as simple models of biological vesicles or polymers. Of particular interest is the singular behaviour of the generating functions around special, so-called multicritical points in their parameter space, which correspond physically to phase transitions. The singular behaviour around the multicritical point is described by a scaling function, alongside a small set of critical exponents.

Apart from some non-rigorous heuristics, our asymptotic analysis mainly consists in applying the method of steepest descents to a suitable integral expression for the exact solution for the generating function of a given model. The similar mathematical structure of the exact solutions of the different models allows for a unified treatment. In the saddle point analysis, the multicritical points correspond to points in the parameter space at which several saddle points of the integral kernels coalesce. Generically, two saddle points coalesce, in which case the scaling function is expressible in terms of the Airy function. As we will see, this is the case for Dyck and Schröder paths, directed column-convex polygons and partially directed

self-avoiding walks. The result for Dyck paths also allows for the scaling analysis of Bernoulli meanders (also known as ballot paths).

We then construct the model of deformed Dyck paths, where three saddle points coalesce in the corresponding integral kernel, thereby leading to an asymptotic expression in terms of a bivariate, generalised Airy integral.

To my parents.

Acknowledgements

First of all, I must thank my supervisor, Thomas Prellberg, for his very dedicated, invaluable support throughout the past years. Without his guidance, this work would not exist.

I would also like to thank Christoph Richard and Adri Olde Daalhuis for hosting me at their institutions, for collaborating and discussing research with me, and teaching me new techniques in analytic combinatorics and asymptotic analysis. To Grzegorz Siudem I am thankful for our fruitful joint work on the scaling behaviour of generalised Motzkin paths. I am grateful to Thomas Prellberg and Amanda Cameron for carefully proofreading the manuscript.

On an institutional level, I would like to thank Queen Mary University of London for the support throughout the recent years. The generous funding by the Universität Erlangen-Nürnberg and the Queen Mary Postgraduate Research Fund allowed me to carry out two consecutive visits to Erlangen.

I want to thank my family for their love and continued support during my entire life. Without you, I would not have been able to reach this stage.

Contents

Abstract 4

Acknowledgements 7

1 Introduction 11

2 Background 16

2.1 Formal power series and generating functions 16

2.2 Methods of asymptotic analysis 18

2.2.1 Notation 18

2.2.2 Asymptotic approximation of integrals 19

2.3 Airy function and Airy distribution 22

2.4 Self-avoiding walks and polygons 24

2.4.1 Self-avoiding walks as polymers 26

2.4.2 The Fisher-Guttmann-Whittington vesicle 29

2.4.3 Tricritical scaling 31

2.5 Directed lattice paths 34

3 Area-width scaling of generalised Motzkin paths 37

3.1 Introduction 37

3.2 The model 39

3.3 The conjecture 40

3.4 Functional equation for $G(s, u, p, r)$ 40

3.5 Heuristic scaling ansatz 44

3.5.1 Dyck paths ($\ell = \infty$) 45

3.5.2 Motzkin paths ($\ell = 1$) 48
3.5.3 The case of general ℓ 49

4 Uniform asymptotics of area-width weighted Dyck paths 52

4.1 Introduction 52
4.2 The model 54
4.3 Functional equation for $G(x, q)$ 56
4.4 Solution of the functional equation 58
4.5 Contour integral representation of $\phi(x)$. 60
4.6 Saddle point landscape of the kernel $f(z)$ 68
4.7 Asymptotic analysis of $\phi(q^k x)$ 73
4.8 Uniform asymptotics and scaling function of $G(x, q)$ 80

5 General q-hypergeometric series 84

5.1 Introduction 84
5.2 Basic definitions and notation 84
5.3 Functional equation for $\phi(x)$ and $\Phi(x)$ 85
5.4 Contour integral representation of $\phi(x)$ 88
5.5 Saddle point landscape of the kernel $f(z)$ 92
5.6 Asymptotic analysis of $\phi(q^k x)$ 106

6 Uniform asymptotics of further models 110

6.1 Schröder paths 111
6.1.1 Model definition and functional equation 111
6.1.2 Solution of the functional equation 113
6.1.3 Uniform asymptotics and scaling properties 113
6.2 Interacting partially directed self-avoiding walks 115
6.2.1 Model definition and generating function 115
6.2.2 Uniform asymptotics and scaling properties 117

6.3 Directed column-convex polygons 118
6.3.1 Model definition and generating function 118
6.3.2 Uniform asymptotics and scaling properties 120

7 Area-length scaling of Bernoulli meanders **122**

7.1 Introduction 122
7.2 The model 123
7.3 Functional equation and area-length generating function . 124
7.4 The main result 126
7.5 Uniform asymptotics of $M(x, q)$ 127

8 Higher-order Airy scaling in deformed Dyck paths **135**

8.1 Introduction 135
8.2 The model 137
8.3 Solution of the functional equation 140
8.4 The main result 141
8.5 Contour integral representation of $\phi(a, q^k x, q)$ 142
8.6 Location of the saddle points 143
8.7 Geometry of the paths of steepest descent 145
8.8 Transformation of $f(z)$ into a canonical form 148
8.8.1 Coefficient asymptotics for $\xi \to 0$ and $\delta = 0$ 150
8.8.2 Coefficient asymptotics for $\delta \to 0$ and $\xi = 0$ 152
8.9 Asymptotics of $\phi(a, q^k x, q)$ 152

9 Summary and Outlook **156**

Bibliography **159**

1 Introduction

The objects of study of this thesis are different classes of two-dimensional lattice polygons and one-dimensional lattice walks. These models can be seen as combinatorial objects which are interesting in their own right, but they also occur in many applications in computer science, queuing theory, physics and biology. The fundamental question one is interested in is how a typical object "looks" like.

As a prototypical example, take the model of Dyck paths, also known as Bernoulli excursions, which are going to be introduced formally in Chapter 4. Roughly, a Dyck path is a one-dimensional random walk $(X(t))_{t=0}^{m}$ of $m \in \mathbb{Z}_{\geq 0}$ steps on $\mathbb{Z}_{\geq 0}$, starting and ending at the point 0, i.e. $X(0) = X(m) = 0$, with steps ± 1. An example is shown in Fig. 4.1 on page 54. Dyck paths are related to a continuous stochastic process called the Brownian excursion, a one-dimensional Brownian motion $\mathcal{B}(t)$, conditioned to $\mathcal{B}(0) = \mathcal{B}(1) = 0$ and $\mathcal{B}(t) > 0$ for $t \in (0, 1)$. More precisely, the Brownian excursion is the scaling limit of Dyck paths. Informally this means that if one picks random Dyck path trajectories of increasing number of steps and rescales them to fit their graph on one sheet of paper, then eventually the Dyck paths "look like" a Brownian excursion. The area of the Dyck path $(X(t))_{t=0}^{m}$ is roughly the sum $\sum_{t=0}^{m} X(t)$, and corresponds to the integral $\int_{t=0}^{1} \mathcal{B}(t)dt$ in the scaling limit.

There exists a huge body of literature on the statistical properties of both

Dyck paths and Brownian excursions. For example, a natural question one can ask is the following. Put all Dyck path trajectories of a given number of steps m into a bag and draw one at random. What is the probability distribution of the area of the trajectory you picked? In the limit $m \to \infty$, the appropriately rescaled area was shown in [65] to be (area) Airy distributed. This is the probability distribution of the integral of the Brownian excursion [40, 20]. The (area) Airy distribution appears in a variety of contexts, particularly, it is also the area law of many other lattice polygons and walks [27, 22, 59, 60, 62].

In this thesis, we are interested in a different, but related question. We define the generating function

$$G(x,q) = \sum_{m=0}^{\infty} \sum_{n=0}^{\infty} p_{m,n} x^m q^n, \tag{1.1}$$

where $p_{m,n}$ is the number of Dyck paths with $2m$ steps and area n. On the one hand, this generating function can be seen as a formal object, where x and q are merely symbols to keep track of the indices of the counting coefficients. On the other hand, it can also be beneficial to see $G(x,q)$ as an analytic object where x and q take complex values, since the location and type of the singularities determining the radius of convergence of a power series reflect the asymptotic growth of its coefficients. This is the viewpoint of analytic combinatorics [29]. For example, if we see $G(x,q)$ as a series in q with coefficients depending on x, then the radius of convergence $q_c(x)$ is 1 for $0 < x \leq \frac{1}{4}$ and decreases smoothly for $x > \frac{1}{4}$. The point $x = \frac{1}{4}$, at which the radius of convergence starts to decrease, is called a tricritical point. For a qualitative picture of the radius of convergence, see Fig. 2.3. As we will show, around the tricritical point, the generating function $G(x,q)$ satisfies

a simple scaling relation. Precisely, if we set $x = \frac{1}{4} - s\epsilon^{\frac{2}{3}}$, where $s \in \mathbb{R}$ and $q = 1 - \epsilon$, then in the limit of $\epsilon \to 0^+$,

$$G(x, q) \sim 2 + \epsilon^{\frac{1}{3}} F(s) + \mathcal{O}(\epsilon^{\frac{2}{3}}). \tag{1.2}$$

Here, $F(s)$ is called the scaling function and is expressible in terms of the Airy function. The symbol '$\sim$' indicates asymptotic equality and will be introduced formally in Subsection 2.2.1. Among other things, the scaling function contains information about the asymptotic probability distribution of the area of Dyck paths in the limit of an infinite number of steps.

We note here that the term 'scaling function' is used in two different ways in the literature. On the one hand, the scaling function is a function the asymptotic expansion of which contains the information about the limit distribution of the area of a Dyck path. For a detailed account of this viewpoint, see [57]. In that sense, the scaling function of Dyck paths was known before this thesis. Here, on the other hand, the scaling function is an analytic object, describing the scaling behaviour of the generating function around the tricritical point. The scaling function is the same in both cases, but the analytic result is new and will be derived in Chapter 4.

Dyck paths appear in different applications, for example, Takács related them to a queuing problem in railway traffic [66]. Moreover, there exist combinatorial bijections between Dyck paths and other models, for example, rooted plane (ordered) trees, where the area of the Dyck path corresponds to the total height of the tree, that is the sum of the distances of each vertex of the tree to the root [65]. In this thesis we see a Dyck path as a one dimensional membrane, attached to an impenetrable substrate at its end points, subject to a pressure acting on it from outside. In

the tradition of other works [25, 48], we refer to this system as a vesicle. The generating function $G(x, q)$ can be interpreted as a physical partition function, where the parameter q corresponds to the pressure acting on the vesicle and x is a perimeter fugacity. If on the one hand there is a positive net pressure acting onto the outside of the membrane, then the surface tends to stay close to the substrate. In that case, the average area grows asymptotically proportional to the number of steps of the Dyck path, and the distribution is concentrated around the mean value. A vesicle of this shape is called deflated. On the other hand, if there is a net pressure acting on the membrane from the inside, then the vesicle maximises its distance from the substrate and the average area grows quadratically with the number of steps of the Dyck path. The vesicle is then called inflated, and again, the distribution is concentrated. A non-trivial area distribution is only observed when the pressure acting onto the vesicle vanishes. The phase transition between the deflated and the inflated regime is described by the scaling relation (1.2).

Apart from Dyck paths, we are going to analyse the asymptotic behaviour of the generating functions of generalised Motzkin paths, directed column-convex polygons, Bernoulli meanders, and interacting partially directed walks (IPDSAW). The model of IPDSAW stands out slightly, since here, we do not consider a notion of area but the number of self-interactions of the walk as a parameter, and the walks are seen as a toy model for directed polymer chains. The mathematical treatment is, however, very similar to the other models. For generalised Motzkin paths, we will use a heuristic approach, relying on a detailed balance argument, subject to a conjecture on the asymptotic form of the generating function. For the other models, we will employ a rigorous technique which is based on applying the saddle

point method to suitable integral representations for the generating functions. To this end, we will also derive general results on the asymptotic behaviour of q-hypergeometric series in Chapter 5. The tricritical points which mark the phase transitions of the models correspond mathematically to points of coalescence of saddle points. In the generic case, two saddle points coalesce, leading to asymptotic expressions expressible via the Airy function.

It is natural to ask whether there exist similar lattice models where more than two saddle points coalesce in the kernel of the associated integral representation of the generating function. We discuss the asymptotics of the generating function of a model which we call deformed Dyck paths, that is a model of Dyck paths with one additional step allowed. For a special value of the weight of this additional step, three saddle points coalesce in the corresponding integral kernel, leading to an asymptotic expression in terms of generalised Airy integrals.

We outline a further generalisation of this model to obtain lattice walk models for which the asymptotic expressions of the generating function involve generalised Airy integrals of arbitrary numbers of variables.

2 Background

2.1 Formal power series and generating functions

Formal power series (fps) can be seen as generalisations of polynomials in that a formal power series can have infinitely many terms. More precisely, a fps $P(x)$ over a ring R is the object

$$P(x) = \sum_{m=0}^{\infty} p_m x^m,$$

where $(p_m)_{m=0}^{\infty}$ is a sequence of elements of R and x is a formal symbol. We also say that $P(x)$ *generates* the sequence $(p_m)_{m=0}^{\infty}$, or that $P(x)$ is the *generating function* of this sequence. For two series $A(x)$ and $B(x)$ generating the sequences $(a_m)_{m=0}^{\infty}$ and $(b_m)_{m=0}^{\infty}$, respectively, the *sum* $A(x) + B(x)$ is defined as the series generating the sequence $(a_m + b_m)_{m=0}^{\infty}$; the *product* $A(x) \cdot B(x)$ generates the sequence $(\sum_{k=0}^{m} a_k b_{m-k})_{m=0}^{\infty}$. In this way, the set of fps over a given ring R is itself a ring, denoted by $R[[x]]$. If $P(x)$ generates the sequence $(p_m)_{m=0}^{\infty}$ then for $k \in \mathbb{Z}_{\geq 0}$, the element p_k of the sequence is denoted by $[x^k]P(x)$. The *degree* of a fps $P(x)$ is defined as $\deg P(x) = \min\left\{k \,\middle|\, [x^k]P(x) \neq 0\right\}$. The coefficient $[x^0]P(x)$ is also denoted as $P(0)$. If for a given fps $A(x)$, $A(0) \neq 0$, then there exists a fps $B(x)$ such that $A(x) \cdot B(x) = 1 \equiv 1 \cdot x^0 + \sum_{m=1}^{\infty} 0 \cdot x^m$.

The *composition* $(A \circ B)(x)$ of two fps $A(x) = \sum_{m=0}^{\infty} a_m x^m$ and $B(x) =$

$\sum_{m=0}^{\infty} b_m x^m$ is denoted by $A(B(x))$ and defined as

$$A(B(x)) = \sum_{m=0}^{\infty} c_m x^m,$$

where $c_m = \sum_{n=0}^{\infty} a_n \sum_{\sum k_j = m} \prod_{j=1}^{n} b_{k_j}$. The composition exists if $A(x)$ is a polynomial or $B(0) = 0$.

The ring $R[[x]]$ can be endowed with a distance d, defined for two fps $A(x) = \sum_{m=0}^{\infty} a_m x^m$ and $B(x) = \sum_{m=0}^{\infty} b_m x^m$ as $d(A(x), B(x)) = 0$ if $A(x) = B(x)$ and otherwise $d(A(x), B(x)) = 2^{-k}$, where $k = \min\{m \mid a_m \neq b_m\}$. Since the metric space $(R[[x]], d)$ is complete, it is possible to prove the uniqueness of fixed points of functional equations for formal power series. For example, consider the ring $\mathbb{Z}[[x]]$, and the map $\varphi : \mathbb{Z}[[x]] \to \mathbb{Z}[[x]]$, defined for $A(x) \in \mathbb{Z}[[x]]$ as

$$\varphi(A) = 1 + xA^2.$$

From the definition of multiplication of fps one easily verifies that φ is strictly contractive with respect to d, precisely, for any $A(x), B(x) \in \mathbb{Z}[[x]]$,

$$d(\varphi(A(x)), \varphi(B(x))) \leq \frac{1}{2} d(A(x), B(x)).$$

From this we can conclude via the Banach fixed-point theorem [4] that the functional equation $A(x) = 1 + xA(x)^2$ has a unique solution in $\mathbb{Z}[[x]]$.

Formal power series of more than one variable can be defined in a recursive way. For example, a bivariate fps generating a double sequence $(c_{m,n})_{m,n=0}^{\infty}$ is a fps

$$C(x, y) = \sum_{m=0}^{\infty} C_m(y) x^m,$$

where for all m, $C_m(y) = \sum_{n=0}^{\infty} c_{m,n} y^n$.

The use of formal power series makes it possible to talk in a clean way about series, without initially having to worry for which values they converge. But of course, the above definitions of addition and multiplication are compatible with the sum and product of two convergent series. For further references on fps, we refer to [1, Chapter 2] or [29, Appendix 5].

2.2 Methods of asymptotic analysis

In this section we will give the theorems which we will use in our asymptotic analysis of q-hypergeometric series. First we need to define our notation.

2.2.1 Notation

For the following standard notation see [46] or [21, §2.1].

Let f and g be two functions from $\mathbb{R}$ to $\mathbb{C}$, and let $x_0 \in \mathbb{R}$.

(i) We say that f is *asymptotically equivalent* to g in the limit $x \to x_0$, denoted by

$$f(x) \sim g(x) \quad (x \to x_0), \tag{2.1}$$

if and only if $\lim_{x \to x_0} f(x)/g(x) = 1$.

(ii) We say f *is of order less than* g *in the limit* $x \to x_0$, denoted by

$$f(x) = o\big(g(x)\big) \quad (x \to x_0), \tag{2.2}$$

if $\lim_{x \to x_0} f(x)/g(x) = 0$.

(iii) We say f *is of order not exceeding* g *in the limit* $x \to x_0$, denoted by

$$f(x) = \mathcal{O}\big(g(x)\big) \quad (x \to x_0), \tag{2.3}$$

if there is a constant $C \geq 0$ and a value $\delta > 0$ such that $\big|f(x)/g(x)\big| \leq C$ for all $x \in (x_0 - \delta, x_0 + \delta)$.

The above definitions can be adapted mutatis mutandis to the cases $x \to \pm\infty$ and limits taken strictly from above or below, denoted by $x \to x_0^+$ and $x \to x_0^-$, respectively. We occasionally use the symbols $\mathcal{O}, o$ and $\sim$ without specifying the associated limit point x_0, if it is clear from the context which limit we are referring to. Note that if for $x \to x_0$, $f(x) = o(g(x))$, then $f(x) = \mathcal{O}(g(x))$, but not $g(x) = \mathcal{O}(f(x))$.

Let $(a_n)_{n=1}^{\infty}$ be a sequence of real numbers and $\big(\varphi_n(x)\big)_{n=1}^{\infty}$ a sequence of functions from $\mathbb{R}$ to $\mathbb{C}$ such that, for $n \in \mathbb{N}$, $\varphi_{n+1}(x) = o(\varphi_n(x))$ as $x \to x_0$. Then $\big(\varphi_n(x)\big)_{n=0}^{\infty}$ yields an *asymptotic expansion* of a function f as $x \to x_0$ if for $N \in \mathbb{N}$, $f(x) = \sum_{n=1}^{N} a_n \varphi_n(x) + R_{N+1}(x)$, where $R_{N+1}(x) = \mathcal{O}(\varphi_{N+1}(x))$ $(x \to x_0)$. This is denoted by

$$f(x) \sim \sum_{n=1}^{\infty} a_n \varphi_n(x) \quad (x \to x_0). \tag{2.4}$$

Note that the asymptotic series $\sum_{n=1}^{\infty} a_n \varphi_n(x)$ need not converge.

2.2.2 Asymptotic approximation of integrals

In this subsection we give a collection of results which we will apply in the main part. Despite its importance, the following result is called a lemma.

Lemma 2.2.1 (Watson's Lemma [21, §2.4])**.** *Let* $g : (0, \infty) \to \mathbb{R}$ *such*

that for $x \to 0^+$,

$$g(x) \sim \sum_{k=0}^{\infty} p_k x^{(k+\lambda-\mu)/\mu}, \tag{2.5}$$

where $\lambda, \mu > 0$. *Then for* $\epsilon \to 0^+$,

$$\int_0^\infty \exp\left(-\frac{v}{\epsilon}\right) g(v)dv \sim \sum_{k=0}^{\infty} \Gamma\left(\frac{k+\lambda}{\mu}\right) p_k \epsilon^{(k+\lambda)/\mu}. \tag{2.6}$$

With Watson's Lemma, the following theorem can be proven.

Theorem 2.2.1 ([21, §2.4])**.** *Let* C *be a contour in the complex plane. Consider the integral*

$$I(\epsilon) = \int_C e^{\frac{1}{\epsilon}f(z)} g(z)dz, \tag{2.7}$$

where $\epsilon > 0$, f *and* g *are analytic on* C, *and the maximum of* $\mathrm{Re}(f(z))$ *on* C *is assumed on an interior point* z_0. *If* $f'(z_0) = 0$ *and* $f''(z_0) \neq 0$, *then for* $\epsilon \to 0^+$,

$$I(\epsilon) = 2\exp\left(\frac{1}{\epsilon}f(z_0)\right)\sqrt{\pi}\frac{g(z_0)}{\sqrt{-2f''(z_0)}}\epsilon^{\frac{1}{2}} + \mathcal{O}(\epsilon^{\frac{3}{2}}). \tag{2.8}$$

Here, the branch of $\omega_0 = \arg(-f''(z_0))$ *has to be chosen such that* $|\omega_0 + 2\omega| \leq \frac{1}{2}\pi$, *where* ω *is the limiting value of* $\arg(z - z_0)$ *when* $z \to z_0$ *from the end point of* C.

The above theorem can be generalised to cases in which the function f has a saddle point of higher order, for example if $f'(z_0) = f''(z_0) = 0$ and $f'''(z_0) \neq 0$.

If the function f has a further parameter t such that for a given value t_0 of t, the order of the saddle point in the integral (2.7) changes from one to two, then the above theorem does not yield an asymptotic expression

which is valid uniformly for a range of values of t including t_0, since the RHS of Eq. (2.8) diverges for $t = t_0$. To obtain a uniform asymptotic expression, one uses the following theorem, which was proven in [19].

Theorem 2.2.2 ([19]). *Let $f(z,t)$ be an analytic function of z and t and suppose f has two ordinary saddle points z_1 and z_2, coalescing for $t = t_0$ in the point z_c. Define the functions*

$$\alpha = \left\{\frac{3}{4}\big(f(z_2,t) - f(z_1,t)\big)\right\}^{\frac{2}{3}} \text{ and } \beta = \frac{1}{2}\left(f(z_1,t) + f(z_2,t)\right). \tag{2.9}$$

For a given choice of the root for α, there exists a unique transformation $\mathrm{T} : z \mapsto u(z)$, such that

$$f(z,t) = \frac{u^3}{3} - \alpha u + \beta, \tag{2.10}$$

which is analytic and bijective if z and t are in small disks centred at z_0 and t_0, respectively. Under the transformation T, the saddle points z_1 and z_2 are mapped onto $+\sqrt{\alpha}$ and $-\sqrt{\alpha}$, respectively.

By applying a theorem by Levinson [39], Theorem 2.2.2 was generalised in [73] to arbitrarily many coalescing saddle points. Below we give the special case of three coalescing saddle points.

Theorem 2.2.3 ([73]). *Let $f(z,s,t)$ be an analytic function of z, s and t and suppose f has three ordinary saddle points z_1, z_2 and z_3, coalescing for $t = t_0$ and $s = s_0$ in the point z_c. Then there exists a transformation $\mathrm{T} : z \mapsto u(z)$ such that*

$$f(z,s,t) = \frac{u^4}{4} - \alpha u^2 - \beta u + \gamma \tag{2.11}$$

is analytic and bijective if z, s and t lie in small disks centred at z_c, s_0 and t_0, respectively. The image domain of T *in the u-plane contains a small disk centred at the origin and the coefficients α, β and γ are analytic functions of s and t for all s, t in the relevant region.*

2.3 Airy function and Airy distribution

The *Airy function* $\mathrm{Ai}(z)$ [21, Chapter 9] is defined for complex z as the integral

$$\mathrm{Ai}(z) = \frac{1}{2\pi i} \int_{e^{-\frac{i\pi}{3}}\infty}^{e^{\frac{i\pi}{3}}\infty} \exp\left(\frac{u^3}{3} - zu\right) du. \tag{2.12}$$

It is a solution of the ODE

$$y'' - zy = 0. \tag{2.13}$$

The *Airy distribution* occurs in many models studied in this thesis. In [27] it is defined as follows.

Definition 2.3.1. *The Airy distribution (of the area type) is the probability distribution of a random variable X with moments*

$$\mathbb{E}[X^k] = -\frac{\Gamma(-\frac{1}{2})}{\Gamma((3k-1)/2)}\Omega_k \quad (k \geq 1), \tag{2.14}$$

with the constants Ω_k being determined by the recurrence

$$2\Omega_k = (2k-4)k\Omega_{k-1} + \sum_{j=1}^{k-1} \binom{r}{j} \Omega_j \Omega_{k-j} \quad (k \geq 1) \tag{2.15}$$

and $\Omega_0 = -1$.

The fact that the Airy distribution is determined uniquely by its mo-

ments was proven in [27] via an application of Carleman's condition [29, Appendix C]. In [66], also an expression for the density of the Airy distribution in terms of the confluent hypergeometric function was given. The distribution owes its name to the fact that the logarithmic derivative of the Airy function has the asymptotic expansion

$$\frac{\mathrm{Ai}'(z)}{\mathrm{Ai}(z)} \sim \sum_{k=0}^{\infty} \frac{\Omega_k}{2^k} \frac{(-1)^k z^{-\frac{3k-1}{2}}}{k!} \quad (z \to +\infty). \tag{2.16}$$

The Airy distribution of area type appears in a variety of contexts. The word area in its name is due to the fact that it is the distribution of the area $A = \int_{t=0}^{1} X(t)dt$ of a Brownian excursion $X(t)$, that is a one dimensional Brownian motion such that $X(0) = X(1) = 0$, conditioned to satisfy $X(t) > 0$ for $0 < t < 1$ [40]; the integrals of related processes have similar distributions [67, 69, 18]. Consistently with this, it is the limit distribution of the (appropriately rescaled) area of Dyck paths, which we are going to consider in Chapter 4 [65]. It is also the conjectured limit distribution of the area of self-avoiding polygons which will be introduced below [59, 60] and has been shown to be the limit distribution of the area of several subclasses of self-avoiding polygons and one dimensional lattice paths [22, 44, 62]. It is also the probability distribution of the total height of the nodes of random binary trees [68]. Further, the Airy distribution is the limit distribution of the total displacement in parking sequences or the construction cost of hash tables [28]. The moments of the Airy distribution also appear in the asymptotic formula for the number of labelled connected graphs on n nodes and $n + k - 1$ edges, where k is fixed [75, 36, 64]. In [42], it was shown that the Airy distribution function is the distribution of the maximal height in a model of fluctuating interfaces.

The Airy function also appears in the Tracy-Widom distribution, describing the density of the largest eigenvalues in certain random matrix ensembles [70] and the Airy distribution of map type for the size of the largest connected component in random maps [6]. For further occurrences of the Airy function in physics, in particular in optics and quantum mechanics, see [74].

2.4 Self-avoiding walks and polygons

In this thesis we are not going to consider the general models of self-avoiding walks and polygons. However, we deem it useful to begin with the definitions of the most general combinatorial classes, in order to give a better understanding of the broader background of our work.

A self-avoiding walk of length m on a given lattice is a sequence of points such that two consecutive points are nearest neighbours on the lattice and no two points are visited twice. To fix ideas, consider the lattice $\mathbb{Z}^2$, also referred to as the square lattice. Then we have the following formal definition.

Definition 2.4.1. *For $m \in \mathbb{Z}_{\geq 0}$, a self-avoiding walk (SAW) of length m on the square lattice is a sequence of points $(\mathbf{r}_j)_{j=0}^{m}$ on $\mathbb{Z}^2$ such that for $0 \leq j < m$, $\|\mathbf{r}_{j+1} - \mathbf{r}_j\| = 1$, where $\|\cdot\|$ denotes the Euclidean norm, and $\mathbf{r}_j \neq \mathbf{r}_k$ for $0 \leq j < k \leq m$.*

In Fig. 2.1 we show an example of an SAW. For a detailed account on the mathematical understanding of the model, in particular its properties in higher dimensions, we refer to the book [41].

Self-avoiding walks are closely related to self-avoiding polygons (SAP). Informally, an SAP is obtained by taking an SAW which ends at a nearest-

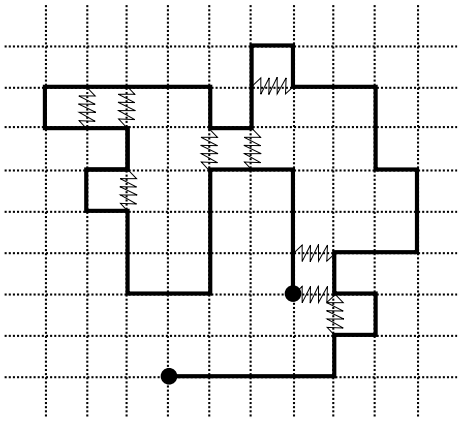

Figure 2.1: A self-avoiding walk (SAW) of length 47 with 9 interactions.

neighbour site of its origin and then connecting the end point with the start point to obtain a polygon. We again consider the square lattice, in which case SAP are formally defined as follows.

Definition 2.4.2. *For $m \in \mathbb{N}$, a self-avoiding polygon on the square lattice of perimeter m is a sequence of points $(\mathbf{r}_j)_{j=0}^{m-1}$ such that $(\mathbf{r}_j)_{j=0}^{m-1}$ is a self-avoiding walk and $\|\mathbf{r}_{m-1} - \mathbf{r}_0\| = 1$.*

Figure 2.2 shows an SAP of perimeter 52. We consider two self-avoiding polygons identical if they are the same up to translation. In other words, if for a given $m \in \mathbb{N}$, $(\mathbf{v}_j)_{j=0}^{m-1}$ and $(\mathbf{w}_j)_{j=0}^{m-1}$ are self-avoiding polygons, then we consider them equal if there exists a $\mathbf{k} \in \mathbb{Z}^2$ such that $(\mathbf{v}_j)_{j=0}^{m-1} = (\mathbf{w}_j + \mathbf{k})_{j=0}^{m-1}$. If we consider self-avoiding polygons which are not *rooted*, then the above self-avoiding polygons are also identified if they are the same up to cyclic shift of indices, meaning that there exists a d with $0 < d < m$ such that

$$\mathbf{v}_j = \begin{cases} \mathbf{w}_{j+d} \text{ for } 0 \leq j < m-d, \text{ and} \\ \mathbf{w}_{j-m+d} \text{ for } m-d \leq j < m. \end{cases}$$

On the other hand, for *rooted* self-avoiding polygons, this identification is not made, meaning that two polygons which have different start points but

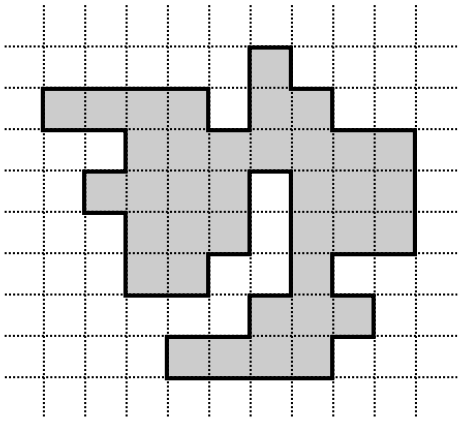

Figure 2.2: A self-avoiding polygon (SAP) of perimeter 52 and area 37.

contain the same points of the lattice, are not identified. In other words, the perimeter of a rooted self-avoiding polygon contains one distinguished point.

We mention that self-avoiding polygons form a subset of the bigger set of polyominoes, which comprises all collections of unit cells of the square lattice [32]. Informally, a self-avoiding polygon is a polyomino without holes.

Both self-avoiding walks and polygons are combinatorial objects which are interesting in their own right, but they are also used in many applications. Apart from the interpretation of SAW and SAP as polymers and vesicles explained in the following subsections, interacting self-avoiding walks can, for example, also model the trajectories of passengers in a public transport network [77] and self-avoiding polygons are related to the so-called $O(n)$ lattice spin model [13].

2.4.1 Self-avoiding walks as polymers

A polymer is a large molecule, consisting of small molecular units called monomers, aligned in a chain, held together by strong physical bonds.

Apart from the bonds between monomers which are neighbours along the chain, non-consecutive monomers can interact via weaker forces if they are spatially close to each other.

Self-avoiding walks have long been used as models for polymer chains which incorporate the effect of excluded volume, that is, the fact that a polymer cannot intersect itself [30, 24]. If a polymer is modelled by an SAW, then the sites visited by the walker represent the monomers, and sites visited consecutively correspond to nearest neighbours in the polymer chain.

With the physical application in mind, we define an *interaction* of an SAW $(\mathbf{r}_j)_{j=0}^m$ as any pair of indices j, k with $0 \leq j < k-1 < m$, such that $\|\mathbf{r}_j - \mathbf{r}_k\| = 1$. For example, the SAW shown in Fig. 2.1 has 9 interactions.

Assume we have a polymer of fixed length, floating in a large heat bath of temperature T, where non-nearest neighbours of the polymer chain attract or repulse each other via van der Waals forces if they are sufficiently close. We model this polymer chain by an SAW of fixed length m, and assign an energy ϵ to each interaction of the walk. Let $w_{m,n}$ be the number of SAW starting at the origin of the lattice with length m and n interactions. The canonical partition function of this polymer system is then given by

$$Z_m = \sum_{n=0}^{\infty} w_{m,n} e^{-\beta n \epsilon} = \sum_{n=0}^{\infty} w_{m,n} \omega^n, \tag{2.17}$$

where $\beta = \frac{1}{k_\mathrm{B}\,\mathrm{T}}$, with $k_\mathrm{B} \simeq 1.38 \cdot 10^{-23}\,\mathrm{J\,K^{-1}}$ being Boltzmann's constant, and $\omega = e^{-\beta\epsilon}$. The relevance of the partition function is due to the fact that in thermal equilibrium, one expects the probability that the polymer

has ν interactions to be given by (see e.g. [8])

$$\mathbb{P}(\#\,\text{interactions} = \nu) = \frac{w_{m,\nu} e^{-\beta\nu\epsilon}}{Z_m}.$$

From the partition function, one can derive the statistics of interesting quantities. For example, the expectation value of the number of interactions of a polymer chain is given by

$$\mathbb{E}(\#\,\text{interactions}) = \frac{1}{Z_m} \sum_{n=0}^{\infty} n w_{m,n} \omega^n = \omega \frac{d}{d\omega} \ln(Z_{\mathrm{m}}).$$

To analyse the behaviour of the SAW model for varying lengths of the chain, one also considers the bivariate power series

$$W(x, \omega) = \sum_{m=0}^{\infty} \sum_{n=0}^{\infty} w_{m,n} x^m \omega^n. \tag{2.18}$$

Physically, this function can be interpreted as the partition function of a polymer system in which both the length of the chain and the number of interactions are allowed to fluctuate.

In the limit in which the length is going to infinity, the polymer undergoes a phase transition as the interaction energy ϵ is varied. Precisely, the polymer is spatially extended when the interaction energy ϵ is low and collapsed for large ϵ. Critical exponents related to the phase transition in between the extended and the collapsed phase were conjectured in [23]. A scaling theory for the collapse transition of a class of geometric cluster models, including interacting self-avoiding walks and the vesicle models introduced below was presented in [12].

2.4.2 The Fisher-Guttmann-Whittington vesicle

Physical vesicles in aqueous solution are closed membranes consisting of lipid molecules composed of hydrophobic chains attached to hydrophilic heads, aggregated in bilayers such that the hydrophilic heads are in contact with the water. The thickness of the membranes is of the order of 10^{-9} m, but the size of the vesicles reaches the order of 10^{-4} m. Since the extension of the vesicles and the thickness of the membrane differ by several orders of magnitude, on mesoscopic scales the vesicles can be considered as two-dimensional surfaces, embedded in three-dimensional space; these surfaces can have both spherical and non-spherical geometry [63]. The understanding of the physical properties of vesicles is of relevance in biology, since also the walls of biological cells consist of lipid bilayers [2]. Moreover, vesicles are used in drug delivery, where they are called liposomes [3].

Depending on parameters such as temperature and the pressure acting onto the membrane, the vesicles can be found in a large variety of shapes. Experimentally, the pressure can be controlled by varying the concentration of large molecules such as sugar, to which the membrane is impenetrable, in the water. Subject to size and volume constraints, the vesicles choose conformations which minimise the curvature energy of the membrane.

In a two-dimensional setting, vesicles can be modelled as planar, self-avoiding polygons, either on the continuum or on the lattice. In this case, the surface area of the membrane becomes the perimeter of the polygon, and the volume enclosed by the membrane is the area enclosed by the perimeter. In [38], Leibler, Singh and Fisher studied the properties of two-dimensional vesicles, modelled as self-avoiding chains in the continuum,

depending on external pressure and bending rigidity via Monte Carlo simulations. In the case of zero bending rigidity, the dependence of the area and radius of gyration of a vesicle on the pressure acting on the membrane was investigated. The authors observed scaling behaviour for both quantities. In particular, for positive pressure acting onto the outside of the vesicles, the radius of gyration was found to scale as for branched polymers.

In the subsequent work [25], Fisher, Guttmann and Whittington modelled vesicles as self-avoiding polygons on the two-dimensional square lattice. The Fisher-Guttmann-Whittington (FGW) vesicle is a vesicle with zero bending rigidity, subject to an osmotic pressure acting on its wall. Due to the absence of a bending rigidity, the relation to real vesicles is somewhat loose and the model is mainly of mathematical interest.

The bivariate generating function of the FGW vesicle is defined as

$$V(x,q) = \sum_{m=0}^{\infty}\sum_{n=0}^{\infty} v_{m,n} x^m q^n, \tag{2.19}$$

where $v_{m,n}$ is the number of non-rooted self-avoiding polygons (on the two-dimensional square lattice) of perimeter m and area n. Here, the area is simply the number of unit cells of the lattice enclosed by the perimeter of the polygon — for example, the SAP shown in Fig. 2.2 has area 37. The variables x and q referred to as the perimeter and area-generating variables, respectively.

For fixed x, the radius of convergence of $V(x,q)$, seen as a series in q, is denoted by $q_c(x)$. Based on the super-multiplicative inequality

$$v_{m_1+m_2,n} \geq \sum_{n_1=0}^{n} v_{m_1,n_1} v_{m_2,n-n_1}, \tag{2.20}$$

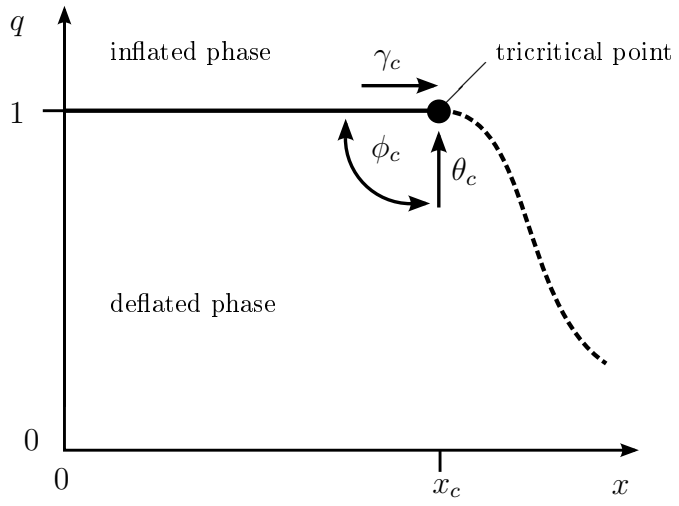

Figure 2.3: The phase diagram of the Fisher-Guttmann-Whittington vesicle model.

the qualitative behaviour of $q_c(x)$ as a function of x was studied in [25]. The authors showed that there exists a value $x_c > 0$ such that for $0 < x \leq x_c$, $q_c(x) = 1$, and such that for $x > x_c$, $q_c(x) < 1$ and $q_c(x)$ is a continuous function of x approaching 0 in the limit $x \to \infty$. The value x_c also determines the radius of convergence of the perimeter generating function $V(x, 1)$, and the point $(x, q) = (x_c, 1)$ is called a tricritical point. Figure 2.3 shows the qualitative behaviour of $q_c(x)$. This is referred to as the phase diagram of the model. For $q > 1$, vesicles of large area obtain a high weight in the generating function (2.19). This is therefore referred to as the inflated phase. Contrariwise, for $q < q_c(x)$, the vesicles which have a small area for a given perimeter are favoured; this is consequently called the deflated phase.

2.4.3 Tricritical scaling

In statistical physics, the so-called renormalisation group theory relates phase transitions to fixed points of transformations which change the char-

acteristic scales of the system while leaving the relevant quantities invariant, and around the fixed points, the free energy of the system satisfies a certain scaling relation. See [13, Chapter 3] for an introduction to the ideas of renormalisation. This somewhat vague idea gives rise to the expectation that in a region around the tricritical point $(x, q) = (x_c, 1)$, the singular behaviour of the area-perimeter generating function of SAP is described by a single variable scaling function and a small set of critical exponents — see Fig. 2.3.

In [59, 60], Richard, Guttmann and Jensen investigated the scaling behaviour of the generating functions of rooted and unrooted SAP based on exact enumeration data. For $m, n \in \mathbb{Z}_{\geq 0}$, there are $mv_{m,n}$ rooted SAP with perimeter m and area n, hence the area-perimeter generating function of rooted SAP is given by $R(x, q) = \frac{d}{dx}V(x, q)$. The numerical analysis in [59, 60] lead to the conjecture that they satisfy a tricritical scaling relation characterised by three critical exponents and a single variable scaling function around the point $(x, q) = (x_c, 1)$. The first exponent, γ_c, describes the singular behaviour of the perimeter generating function $R(x, 1)$ as the value $x = x_c$ is approached. More precisely, for $x \to x_c^-$,

$$R(x, 1) \sim R^{(\mathrm{reg})}(x, 1) + A(x_c - x)^{\gamma_c}, \tag{2.21}$$

where $R^{(\mathrm{reg})}(x, q)$ is analytic at $(x, q) = (x_c, 1)$ and A is a constant. The second exponent, θ_c, characterises the singular behaviour of $R(x_c, q)$. Precisely, for $q = e^{-\epsilon} \to 1^-$,

$$R(x_c, q) \sim R^{(\mathrm{reg})}(x_c, q) + B\epsilon^{\theta_c}, \tag{2.22}$$

where B is another constant. The crossover between these two asymptotic regimes is mediated by a scaling function $F(s)$, such that for $q = e^{-\epsilon} \to 1^-$,

$$R(x_c - s\epsilon^{\phi_c}, q) \sim R^{(\mathrm{reg})}(x_c - s\epsilon^{\phi_c}, q) + \epsilon^{\theta_c} F(s), \tag{2.23}$$

where ϕ_c is called the cross-over exponent. In the limit $s \to \infty$, the curve $(x, q) = (x_c - s(1-q)^{\phi_c}, q)$ approaches the horizontal line $q = 1$ for fixed values of x. From this one gets that for $s \to \infty$, $F(s) \sim s^{\gamma_c}$ and $\gamma_c \phi_c = \theta_c$. The values of the exponents are conjectured as $\gamma_c = \frac{1}{2}, \theta_c = \frac{1}{3}$ and $\phi_c = \frac{2}{3}$, and the scaling function as

$$F(s) = b_0 \frac{d}{ds} \ln\big(\mathrm{Ai}(b_1 s)\big), \tag{2.24}$$

with positive constants b_0 and b_1. The conjectured scaling relation (2.23) also implies that the limit distribution of the area of SAP is the (area) Airy distribution. The singular behaviour of the generating function $V(x, q)$ of unrooted SAP is dominated by a logarithmic singularity in the region around the point $(x, q) = (x_c, 1)$, and the scaling function is, up to prefactors, the logarithm of the Airy function [60].

Shortly after the paper [59], Cardy speculated in [14] that by introducing further interactions in the Fisher-Guttmann-Whittington vesicle, one would be able to observe multicritical points of higher order, described by multivariate scaling functions expressible via higher-order Airy integrals, and a different set of critical exponents.

The tricritical scaling behaviour and the area limit law of SAP are hard to verify, due to the difficulty of rigorous proofs on the SAP problem. Progress can be made by considering subclasses of SAP which are analytically

tractable by imposing conditions such as convexity and directedness onto the model. Examples for subclasses of SAP for which the area-perimeter generating function is known are rectangles, Ferrers diagrams, stack polygons, staircase polygons and directed column-convex polygons. For precise definitions of these models, we refer to [54, 9]. In the case of the first three models, which are also referred to as stacking models, the area-perimeter generating functions are easily obtained and were analysed in [54]; the area-perimeter generating function of staircase polygons was derived in [11]. For stacking models, the phase diagram is qualitatively different to the one of SAP shown in Fig. 2.3. On the other hand, for staircase polygons, the phase diagram has the same qualitative properties as the one of unrestricted SAP. This can be understood from the fact that the derivation of the shape of the phase diagram of SAP in [25] relied on some general properties of the model, including the inequality (2.20). The scaling behaviour of the area-perimeter generating function of staircase polygons was shown in [52] to coincide, up to model-dependent prefactors, with the one conjectured for rooted SAP.

The Airy distribution of area type is also the probability distribution of the area of one-dimensional lattice paths such as Dyck paths and similar models in the limit of infinite perimeter, and they are therefore expected to show the same tricritical scaling behaviour as rooted SAP and staircase polygons.

2.5 Directed lattice paths

For given $m \in \mathbb{N}$, a general lattice path is a sequence $(\mathbf{r}_0, \mathbf{r}_2, \ldots, \mathbf{r}_m)$ of points of $\mathbb{Z}^2$. Geometrically, a lattice path is represented by polygonal lines

obtained by connecting subsequent points by straight lines. Usually, one fixes $\mathbf{r}_0 = (0, 0)$ and considers lattice path models with a restriction on the increments $\mathbf{s}_i = \mathbf{r}_i - \mathbf{r}_{i-1}$ for $0 < i \leq m$. The points on the lattice and the indices of the points are often thought of as positions in a discretised space and time, respectively. If the restrictions on the increments do not depend on the values of $\mathbf{r}_i$ and the index i, then the path is said to be space and time-homogeneous. The subset $\mathcal{S} \subset \mathbb{Z}^2$ of allowed increments is called the step-set of a given path. If the initial point of a lattice path is fixed to $\mathbf{r}_0 = (0, 0)$, then one can represent it by the sequence of increments between successive steps.

A path becomes essentially one-dimensional if for any $0 < i \leq m$, the increment $\mathbf{s}_i = \mathbf{r}_i - \mathbf{r}_{i-1} = (x_i, y_i)$ satisfies $x_i > 0$. In this case, the steps of the path have the horizontal axis as a preferred direction of increase, and the path is accordingly called a directed lattice path. Directed lattice paths occur in many places in probability theory, computer science and formal language theory.

The step-set of a directed path can be both finite and infinite. For example, Dyck paths, which will be considered in Chapter 4 have step-set $\mathcal{S} = \{(1, 1), (1, -1)\}$, whereas the so-called Łukasiewicz paths have step set $\mathcal{S} = \{(1, k) \,|\, k \geq 0\}$. These two examples satisfy the additional constraint that they end on the horizontal axis and are restricted to the upper right quarter plane. Paths satisfying this restriction are called excursions. Paths which stay in the upper right quarter plane but do not have to end on the horizontal axis are called meanders, and paths which are not restricted to the upper right quarter plane but need to end on the horizontal axis are called bridges. These types of lattice paths were studied in the paper [5] by Banderier and Flajolet, with an emphasis on *simple* paths, that is paths

with a step set $\mathcal{S} \subset \{1\} \times \mathbb{Z}$. In this case, the x-coordinate of the last point of the path is called its *length*. The authors characterised the generating functions of directed simple paths, counted with respect to their length and, where appropriate, y-coordinate of the final position, depending on different restrictions. The singularity structure of the generating functions can be used to infer asymptotic properties of the underlying coefficients, and infer properties of the probability distributions of different parameters, such as final altitude and number of contacts with the horizontal axis — see also [29, Part B]).

The *area* of an excursion or meander is roughly the area enclosed between the polygonal line connecting the points of the path and the horizontal axis. The asymptotic of the average area of a large class of paths was given by Banderier and Gittenberger in [7]. Both this paper and the preceding work [5] relied on the so-called kernel method of enumerative combinatorics. Schwertfeger extended the results of [7] in [61] by considering directed paths with a larger step set and by calculating full limit distributions of the area. They involve the area laws of the Brownian excursion and the Brownian meander. For particular step sets, these were already known due to works by Takács [65, 69].

3 Area-width scaling of generalised Motzkin paths

3.1 Introduction

In this section, we are going to introduce a family of lattice walk models called ℓ-Motzkin paths. For a given ℓ, an ℓ-Motzkin path is a path on the square lattice $\mathbb{Z}^2$ with steps $(1,1)$, $(1,-1)$ and $(\ell,0)$, which starts at the origin $(0,0)$, ends on the line $y=0$ and stays above this line all the time. The family of ℓ-Motzkin paths has been studied for general ℓ before in the combinatorics literature with a focus on bijections [51]. The cases $\ell=1$ and $\ell=2$ are known as (standard) Motzkin and Schröder paths, respectively; the case $\ell=\infty$ can be identified with the model of Dyck (or Catalan) paths [1]. Dyck and Schöder paths will be considered again in Chapters 4 and 6, respectively.

For a given ℓ, we consider the ensemble of ℓ-Motzkin paths, weighted with respect to their width, their number of steps $(1,1)$ and $(1,-1)$, and their area. Since the model has the same super-multiplicative property (2.20) as self-avoiding polygons, we expect that, for all ℓ, the phase diagram of ℓ-Motzkin paths has the same qualitative features as the phase diagram of the Fisher-Guttmann-Whittington vesicle. In particular, we expect that there exists a tricritical point, around which the singular behaviour of the

area-width generating function of ℓ-Motzkin paths is described by a single variable scaling function and three critical exponents. The scaling function is, up to ℓ-dependent factors, equal to the logarithmic derivative of the Airy function, and the three critical exponents are $(\gamma_c, \theta_c, \phi_c) = (\frac{1}{2}, \frac{1}{3}, \frac{2}{3})$. Here, the exponent γ_c describes the singular behaviour of the generating function when the area weight is set equal to one; θ_c describes the singular behaviour of the generating function when the weight of the widths is set to its critical value; ϕ_c is the so-called cross-over exponent.

Our approach consists of inserting the expected tricritical scaling form into the derived functional equation for the area-width generating function. By a dominant balance argument, this determines the critical exponents uniquely and leads us to an ODE for the scaling function, which has a unique solution satisfying the appropriate boundary conditions.

After defining the model more precisely, we will analyse the scaling behaviour of Dyck and Motzkin paths, before generalising our results to ℓ-Motzkin paths with arbitrary ℓ. The results of our calculations lead to Conjecture 3.3.1.

The approach as presented here is non-rigorous since it makes an assumption on the asymptotic form of the singular part of the area-width generating function when the tricritical point is approached. However, the scaling ansatz used in this chapter forms part of a rigorous method to analyse the area limit distributions of two-dimensional polygon models [56, 57].

This chapter consists of joint work with Gregorz Siudem and Thomas Prellberg, the results were published in the article [35].

3.2 The model

Definition 3.2.1 (ℓ-Motzkin path)**.** *For $\ell \in \mathbb{N}$ and $s \in \mathbb{Z}_{\geq 0}$, an ℓ-Motzkin path is a lattice walk $(x_k, y_k)_{k=0}^{s}$ on $\mathbb{Z}^2$, such that $y_k \geq 0$ for all $k \in [s]$, and $x_0 = y_0 = y_s = 0$. Moreover, for $0 \leq k < s$, (x_{k+1}, y_{k+1}) is either $(x_k + 1, y_k + 1)$ or $(x_k + 1, y_k - 1)$ or $(x_k + \ell, y_k)$, which correspond to an up-, down-, or horizontal step, respectively.*

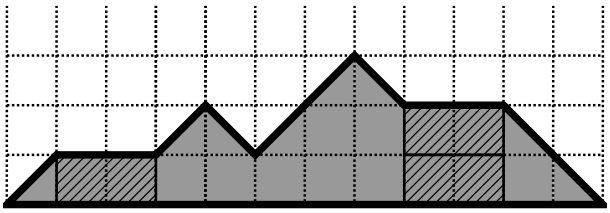

Figure 3.1: A Schröder path ($\ell = 2$) of width 12 with two horizontal steps, three (2×1)-rectangles below these steps (hatched), four pairs of up/down steps, area 12 below these steps, and thus total area 18.

For given ℓ, we define the generating function

$$G(s, u, p, r) = \sum_{k=0}^{\infty} \sum_{l=0}^{\infty} \sum_{v=0}^{\infty} \sum_{w=0}^{\infty} c_{k,l,v,w}\, s^k\, u^l\, p^v\, r^w, \tag{3.1}$$

where $c_{k,l,v,w}$ is the number of paths with k horizontal steps, $\frac{l}{2}$ pairs of up- and down-steps, v $(\ell \times 1)$-rectangles under all the horizontal steps, and w unit squares under all the up- and down-steps (including the half unit squares directly underneath these steps). Thus the weight u is associated to the total number of up- and down-steps, r corresponds to the area under these steps, measured in unit squares of the lattice, and s and p weigh the number of horizontal steps and the number of $(\ell \times 1)$-rectangles directly underneath these steps, respectively. For example, the weight of the trajectory shown in Fig. 3.1 is $s^2u^8p^3r^{12}$. Note that there is no explicit ℓ-dependence in $G(s, u, p, r)$. Instead, the area-width generating functions

for ℓ-paths of different ℓ are obtained by choosing appropriate values for s and p, as will be explained below.

3.3 The conjecture

The results of the calculations done in this chapter lead us to the following conjecture.

Conjecture 3.3.1. *For $\ell \in \mathbb{N}$, let $G^{(\ell)}(a,x,q) = G(x^\ell, \sqrt{a}x, q^\ell, q)$, where $G(s,u,p,r)$ is defined in Eq. (3.1). Define for $a > 0$ and $z \in \mathbb{R}$ the function*

$$F(z) \equiv F^{(\ell)}(a,z) = b_0 \frac{\mathrm{Ai}'(b_1 z)}{\mathrm{Ai}(b_1 z)}, \tag{3.2}$$

with

$$b_0 = \left(\frac{2\sqrt{a} + \ell\, x_c^{\ell-1}}{a^2 x_c^3} \right)^{\frac{1}{3}} \text{ and } b_1 = \sqrt{a}\, b_0, \tag{3.3}$$

where $x_c \in (0,1)$ satisfies the equation $x_c^\ell = 1 - 2\sqrt{a}x_c$. Then we have for $a > 0$ and $z \in \mathbb{R}$ such that $\mathrm{Ai}(b_1 z) \neq 0$, $G_c = (\sqrt{a}x_c)^{-1}$ and $q = 1-\epsilon \to 1^-$,

$$G^{(\ell)}(a, x_c - z\epsilon^{\frac{2}{3}}, 1-\epsilon) = G_c + \epsilon^{\frac{1}{3}} F(z) + \mathcal{O}(\epsilon^{\frac{2}{3}}). \tag{3.4}$$

In the remaining sections of this chapter we are going to carry out the calculations leading to Conjecture 3.3.1. We begin by deriving the functional equation satisfied by $G(s,u,p,r)$.

3.4 Functional equation for $G(s,u,p,r)$

A functional equation for $G(s,u,p,r)$ can be obtained by noting that for a given ℓ, the set of all ℓ-paths can be divided into the following three subsets.

Figure 3.2: Graphical interpretation of Eq. (3.5). An ℓ-path either has length 0, or it starts with a horizontal step, followed by an ℓ-path, or it starts with an up-step, followed by an ℓ-path, followed by a down-step, followed by another ℓ-path.

In Fig. 3.2 we graphically illustrate this decomposition. The first subset only contains the trajectory of zero steps, which has weight 1. The second subset consists of all paths which start with a horizontal step, followed by a path (possibly of zero steps). The weight of a path in this set is thus the weight s of the horizontal step at the beginning, times the weight of the path attached to this initial step. Finally, the third subset contains all the ℓ-paths which start with an up-step. Their weight is given by the weight u of this initial up-step times the weight u of its complimentary down-step, times the weight of the path in between these two steps, times the weight of the path following the down-step. Moreover, the two triangular regions below the initial up-step and the corresponding down-step together contribute one unit of area to the total area underneath the diagonal steps, which is accounted for by a factor r. Since the path between the initial up-step and its complimentary down-step is elevated by one, each up- or down-step in between generates one further area of unit size, weighted by r, and each horizontal step generates an $(\ell \times 1)$-rectangle, weighted by p. Summing over the weights of the paths in all three subsets, this leads to the functional equation

$$G(s,u,p,r) = 1 + s\,G(s,u,p,r) + ru^2 G(ps,ru,p,r)\,G(s,u,p,r). \qquad (3.5)$$

Note that by iteration of Eq. (3.5), we obtain the continued fraction representation

$$G(s,u,p,r) = \cfrac{1}{1-s-\cfrac{ru^2}{1-ps-\cfrac{r^3u^2}{1-p^2s-\cfrac{r^5u^2}{1-p^3s-\ldots}}}}, \tag{3.6}$$

which can be used to approximate $G(s,u,p,r)$ numerically.

The *width* of an ℓ-Motzkin path is the horizontal distance between its starting and end point; the *area* of an ℓ-Motzkin path is the total area enclosed between the trajectory and the line $y=0$, measured in unit cells of the lattice. For example, the path in Fig. 3.1 has width 12 and area 18. We will consider the generating function

$$G^{(\ell)}(a,x,q) = \sum_{k=0}^{\infty}\sum_{l=0}^{\infty}\sum_{m=0}^{\infty} p_{k,m,n}a^k x^m q^n, \tag{3.7}$$

where $p_{k,m,n}$ is the number of paths with $2k$ diagonal steps, width m and an area n enclosed between the trajectory and the bottom line, counted in units of lattice cells. We will refer to $G^{(\ell)}(a,x,q)$ as the area-width generating function. Note, however, that it has an additional parameter a, which counts the number of pairs of up- and down-steps. Since each horizontal step of an ℓ-path increases the width of the path by ℓ and each $(\ell\times 1)$-rectangle increases the total area, measured in units of lattice cells, by ℓ, and each diagonal step increases the total number of pairs of diagonal steps by $\frac{1}{2}$, we have the identity

$$G^{(\ell)}(a,x,q) = G(x^\ell, x\sqrt{a}, q^\ell, q). \tag{3.8}$$

Substituting Eq. (3.8) into Eq. (3.5), we obtain the functional equation

$$G^{(\ell)}(a,x,q) = 1 + x^{\ell} G^{(\ell)}(a,x,q) + aqx^2 G^{(\ell)}(a,qx,q) G^{(\ell)}(a,x,q). \quad (3.9)$$

For $q = 1$, Eq. (3.9) is solved by

$$G^{(\ell)}(a,x,1) = \frac{1 - x^{\ell} - \sqrt{(1-x^{\ell})^2 - 4ax^2}}{2ax^2}, \quad (3.10)$$

and setting $a = 1$ in Eq. (3.10), we obtain the generating functions of the Motzkin numbers for $\ell = 1$ and the large Schröder numbers for $\ell = 2$ [45, A001006 and A006318]).

For a given $\ell \in \mathbb{N}$ and real $a > 0$, we denote the smallest positive value for which the discriminant $(1-x^{\ell})^2 - 4ax^2$ vanishes by x_c and define $G_c = G^{(\ell)}(a, x_c, 1)$. For all $\ell \in \mathbb{N}$ and $a > 0$, $x_c \in (0,1)$. From Eq. (3.10), it follows that

$$G_c = \frac{1 - x_c^{\ell}}{2ax_c^2} = \frac{1}{\sqrt{a}x_c}. \quad (3.11)$$

If $|x| < 1$ and we let ℓ tend to infinity, then the weight x^{ℓ} associated to horizontal steps becomes zero, thus $G^{(\infty)}(a,x,q) = G(0, \sqrt{a}x, 0, q)$ satisfies the functional equation

$$G^{(\infty)}(a,x,q) = 1 + aqx^2 G^{(\infty)}(a,qx,q) G^{(\infty)}(a,x,q). \quad (3.12)$$

In this case, the parameter x only appears in powers of the product ax^2 and therefore a can be set equal to one without loss of generality. We write $G^{(\infty)}(x,q) \equiv G^{(\infty)}(1,x,q)$. Equation (3.12) is then readily identified as the functional equation for the area-width generating function of Dyck paths [26]. If $q = 1$, it is solved by the generating function of the Catalan

numbers [45, A000108]), and for general q, the solution can be found in [26].

In the next section, we are going to analyse the scaling behaviour of $G^{(\ell)}(a,x,q)$ around the point $(a,x,q)=(a,x_c,1)$ by using a heuristic ansatz. We will begin by considering the cases of Dyck paths ($\ell=\infty$) and Motzkin paths ($\ell=1$), before generalising our approach to arbitrary ℓ.

3.5 Heuristic scaling ansatz

The heuristic approach consists in assuming that, in the vicinity of the point $(a,x,q)=(a,x_c,1)$, the area-width generating functions of ℓ-Motzkin paths satisfy a simple scaling relation. More precisely, we expect that there is a value $z_-<0$ such that for $z\in(z_-,\infty)$ and $\epsilon\to 0^+$,

$$G^{(\ell)}\big(a,x(z,\epsilon),1-\epsilon\big)=G_c+\epsilon^{\theta_c}F_0(a,z)+\epsilon^{2\theta_c}F_1(a,z)+\mathcal{O}(\epsilon^{3\theta_c}), \quad (3.13)$$

where $x(z,\epsilon)=x_c-z\,\epsilon^{\phi_c}$, θ_c and ϕ_c are positive, non-integer critical exponents, and $F_0(a,z)$ is the (unknown) scaling function.

For better readability, we omit the index 0 and the dependence of a from now on and write $F_0(a,z)\equiv F(z)$. We define

$$G^{(\ell)}_{sc}(a,z,\epsilon)=G_c+\epsilon^{\theta_c}F(z)+\epsilon^{2\theta_c}F_1(z). \quad (3.14)$$

For $z=\xi\epsilon^{-\phi_c}$ with $0<\xi<x_c$, one gets $x(z,\epsilon)=x_c-\xi$, and the RHS of Eq. (3.13) needs to converge to $G^{(\ell)}(a,x_c-\xi,1)$ in the limit $\epsilon\to 0^+$. It follows from the positivity of the coefficients of the generating function

that $G^{(\ell)}(a, x_c - \xi, 1) < G_c$. This implies that necessarily, for $a > 0$,

$$\lim_{z\to\infty} F(z) = -\infty. \tag{3.15}$$

Following [56], we now insert the RHS of Eq. (3.13) into the functional equation Eq. (3.9). Using a dominant balance argument, this leads to an ODE for the function $F(z)$ and uniquely determines the values of θ_c and ϕ_c.

We will begin by applying this approach to Dyck paths.

3.5.1 Dyck paths ($\ell = \infty$)

The area-width generating function of Dyck paths satisfies Eq. (3.12), where, as explained above, a can be set to one without loss of generality. Substituting $a = 1$ and $x^\ell = 0$ into the solution for $q = 1$ given in Eq. (3.10), we obtain the critical values

$$x_c = \frac{1}{2} \text{ and } G_c = 2. \tag{3.16}$$

Now we define the function

$$\begin{aligned}\Phi_\infty(z,\epsilon) \; &= 1 - G_{sc}^{(\infty)}(z,\epsilon) \\ &\quad + (1-\epsilon)\, x(z,\epsilon)^2\, G_{sc}^{(\infty)}(z + x_c\epsilon^{1-\phi_c} - z\epsilon, \epsilon)\, G_{sc}^{(\infty)}(z,\epsilon),\end{aligned}$$

where $G_{sc}^{(\infty)}(z,\epsilon) \equiv G_{sc}^{(\infty)}(1,z,\epsilon)$ is given by Eq. (3.14), with an unknown function $F(z)$. Under the assumption that Eq. (3.13) holds, it follows from Eq. (3.12) that

$$\Phi_\infty(z,\epsilon) = \mathcal{O}(\epsilon^{3\theta_c}) \quad (\epsilon \to 0^+). \tag{3.17}$$

Expanding $\Phi_\infty(z,\epsilon)$ into a series in ϵ, we obtain

$$\begin{aligned}\Phi_\infty(z,\epsilon) &= (1 - G_c + x_c^2 G_c^2) \\ &+ \epsilon^{\theta_c}\left((2x_c^2 G_c - 1)F(z)\right) \\ &+ \epsilon^{2\theta_c}\left((2x_c^2 G_c - 1)F_1(z) + x_c^2 F(z)^2\right) \\ &+ \epsilon^{\phi_c}\left(-2x_c G_c^2 z\right) \\ &+ \epsilon^{1-\phi_c+\theta_c}(x_c^3 G_c F'(z)) \\ &+ \epsilon^{1-\phi_c+2\theta_c}(x_c^3(F(z)F'(z) + G_c F_1'(z)) \\ &+ \epsilon^{\phi_c+\theta_c}(-4z x_c G_c F(z)) \\ &+ \mathcal{O}(\epsilon^{3\theta_c}).\end{aligned}$$

The constant coefficient and the one of order ϵ^{θ_c} are zero by virtue of Eq. (3.16). For Eq. (3.17) to hold, the coefficient of the order of $\epsilon^{2\theta_c}$ in the above equation needs to be cancelled by another coefficient, hence one of the other exponents needs to equal $2\theta_c$. If $2\theta_c = \phi_c + \theta_c$, thus $\theta_c = \phi_c$, then the term of order ϵ^{ϕ_c} in the above equation could not be cancelled by any other term unless $\theta_c = 1$, which is impossible by the assumption that θ_c is not an integer. Likewise, it is impossible that $2\theta_c = 1 - \phi_c + 2\theta_c$, since ϕ_c is assumed to be non-integer. The third possibility is that $2\theta_c = \phi_c$, in which case the only way to obtain a solution $F(z)$ analytic for $z \in (z_-, \infty)$ is to also have $2\theta_c = 1 - \phi_c + \theta_c$. The critical exponents therefore necessarily satisfy the equations

$$2\theta_c - \phi_c = 0 \text{ and } \theta + \phi_c = 1,$$

and thus $\theta_c = \frac{1}{3}$ and $\phi_c = \frac{2}{3}$. Inserting these exponents and the values for x_c and G_c from Eq. (3.16), the above expansion gives us

$$\Phi_\infty(z,\epsilon) = \left[\frac{1}{4}F'(z) + \frac{1}{4}F(z)^2 - 4z\right]\epsilon^{\frac{2}{3}} + \mathcal{O}(\epsilon).$$

From Eq. (3.17) we thus arrive at the Riccati type ODE

$$F'(z) = Az - BF(z)^2 \tag{3.18}$$

for the scaling function $F(z)$, where $A = 16$ and $B = 1$. In order to solve Eq. (3.18), we linearise it by using the ansatz

$$F(z) = b_0\frac{f'(b_1 z)}{f(b_1 z)}, \tag{3.19}$$

where

$$b_0 = \left(\frac{A}{B^2}\right)^{1/3} \text{ and } b_1 = b_0 B. \tag{3.20}$$

This leads to the second order ODE

$$f''(z) - zf(z) = 0, \tag{3.21}$$

the general solution of which is given by

$$f(z) = \lambda_1 \operatorname{Ai}(z) + \lambda_2 \operatorname{Bi}(z), \tag{3.22}$$

where $\lambda_1, \lambda_2 \in \mathbb{R}$, and

$$\operatorname{Bi}(z) = e^{-i\pi/6}\operatorname{Ai}(ze^{-2i\pi/3}) + e^{i\pi/6}\operatorname{Ai}(ze^{2i\pi/3}). \tag{3.23}$$

Inserting Eq. (3.22) into Eq. (3.19), we obtain the general solution of Eq. (3.18) as

$$F(z) = b_0 \frac{(\lambda+1)\,\mathrm{Ai}'(b_1 z) + (\lambda-1)\,\mathrm{Bi}'(b_1 z)}{(\lambda+1)\,\mathrm{Ai}(b_1 z) + (\lambda-1)\,\mathrm{Bi}(b_1 z)}, \tag{3.24}$$

where $\lambda \in \mathbb{R}$. It now follows from the asymptotic behaviour of $\mathrm{Ai}(z)$, $\mathrm{Bi}(z)$ and their derivatives ([21, §9.7]) that the only possible way to satisfy condition (3.15) is to set $\lambda = 1$. Thus, $F(z)$ has the form given in Eq. (3.2), and inserting the values $A = 16$ and $B = 1$ into Eq. (3.20), we obtain

$$b_0 = b_1 = 2^{\frac{4}{3}}. \tag{3.25}$$

These coefficients agree with those obtained from Eq. (3.3) upon substituting $x_c = \frac{1}{2}$ and letting $\ell \to \infty$.

Now we do the same analysis for (standard) Motzkin paths.

3.5.2 Motzkin paths ($\ell = 1$)

Setting $\ell = 1$ and $q = 1$ in Eq. (3.10), we get the critical values for standard Motzkin paths

$$G_c = \frac{1+2\sqrt{a}}{\sqrt{a}} \text{ and } x_c = \frac{1}{1+2\sqrt{a}}. \tag{3.26}$$

Analogous to the case of Dyck paths, we define $\Phi_1(a, z, \epsilon)$ from Eq. (3.5) as

$$\begin{aligned}\Phi_1(a,z,\epsilon) = {} & 1 - G_{sc}^{(1)}(a,z,\epsilon) + x(z,\epsilon) G_{sc}^{(1)}(a,z,\epsilon) + \\ & + a(1-\epsilon)\, x(z,\epsilon)^2\, G_{sc}^{(1)}(a, z + x_c \epsilon^{1-\phi_c} - z\epsilon, \epsilon)\, G_{sc}^{(1)}(a,z,\epsilon).\end{aligned}$$

Again, assumption Eq. (3.13) implies that $\Phi_1(a,z,\epsilon) = \mathcal{O}(\epsilon^{3\theta_c})$ and requires the critical exponents to be $\theta_c = \frac{1}{3}$ and $\phi_c = \frac{2}{3}$. From the expansion

$$\Phi_1(a,z,\epsilon) = \left[aG_c x_c^3 F'(z) + a x_c^2 F(z)^2 - z(2aG_c^2 x_c + G_c)\right] \epsilon^{\frac{2}{3}} + \mathcal{O}(\epsilon),$$

we are again lead to the ODE Eq. (3.18), now with the coefficients

$$A = \frac{2G_c}{x_c^2} + \frac{1}{a x_c^3} \text{ and } B = \sqrt{a}. \tag{3.27}$$

The final form of the scaling function is given by Eq. (3.2) with

$$b_0 = \left(\frac{2\sqrt{a}+1}{a^2 x_c^3}\right)^{\frac{1}{3}} \text{ and } b_1 = \sqrt{a}\, b_0. \tag{3.28}$$

We will now generalise this result to ℓ-Motzkin paths with arbitrary ℓ.

3.5.3 The case of general ℓ

Now we assume ℓ to be any positive integer. In this general case, it is not possible to give an expression for the critical value x_c as a function of a, so our results will be expressed in terms of x_c.

As in the special cases, we define

$$\begin{aligned}\Phi_\ell(a,z,\epsilon) =& 1 - G_{sc}^{(\ell)}(a,z,\epsilon) + x(z,\epsilon)^\ell G_{sc}^{(\ell)}(a,z,\epsilon) + \\ &+ a(1-\epsilon)x(z,\epsilon)^2\, G_{sc}^{(\ell)}\left(a, z + x_c\epsilon^{1-\phi_c} - z\epsilon, \epsilon\right) G_{sc}^{(\ell)}(a,z,\epsilon)\,,\end{aligned} \tag{3.29}$$

and from the assumption that $\Phi_\ell(a,z,\epsilon) = \mathcal{O}(\epsilon^{3\theta_c})$ one obtains $\theta_c = \frac{1}{3}$ and

$\phi_c = \frac{2}{3}$. Expanding the RHS of Eq. (3.29) in ϵ we get

$$\Phi_\ell(a, z, \epsilon) = \left[aG_c x_c^3 F'(z) + a x_c^2 F(z)^2 - (2aG_c^2 x_c + \ell\, G_c x_c^{\ell-1})z\right] \epsilon^{\frac{2}{3}} + \mathcal{O}(\epsilon),$$

which leads to Eq. (3.18) with

$$A = \frac{2G_c}{x_c^2} + \frac{\ell\, x_c^{\ell-4}}{a} \text{ and } B = \sqrt{a}. \tag{3.30}$$

The solution of this equation is given by Eq. (3.2) with the parameters from Eq. (3.3). This motivates Conjecture 3.3.1.

Rearranging Eq. (3.13), one obtains

$$\left(G^{(\ell)}(a, x_c - z\epsilon^{\frac{2}{3}}, 1-\epsilon) - G_c\right) \epsilon^{-\frac{1}{3}} = F(z) + \mathcal{O}(\epsilon^{\theta_c}). \tag{3.31}$$

From Eq. (3.6), it is possible to numerically evaluate $G^{(\ell)}(a, x, q)$ for any ℓ. In Fig. 3.3, we plot the LHS of Eq. (3.31) for the example of Schröder paths ($\ell = 2$) and $a = 1$ as a function of z for different values of ϵ. This figure shows the close agreement of scaling function and partition function asymptotics for q close to one.

For the cases $\ell = 2$ and $\ell = \infty$, we are going to be able to prove Conjecture 3.3.1 by applying the method of steepest descents in Chapters 4 and 6.

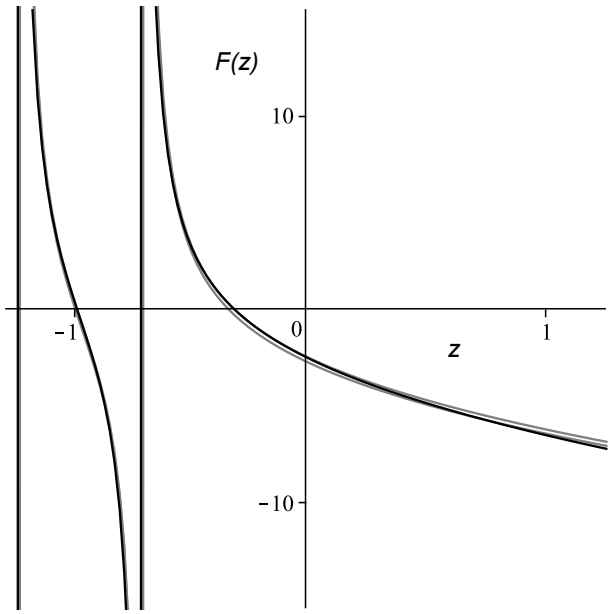

Figure 3.3: Plot of the scaling function $F(z)$ given by Eq. (3.2) with coefficients (3.3) for $a = 1$ and $\ell = 2$ (black) against the approximation of the scaling function obtained directly from the generating function $G^{(2)}(1, x, 1-\epsilon)$ and fixed values $\epsilon = 10^{-3}$ and 10^{-4} (grey).

4 Uniform asymptotics of area-width weighted Dyck paths

4.1 Introduction

The model of Dyck paths (also known as Bernoulli excursions) can be seen as the discrete counterpart of the continuous Brownian excursion, which describes a one-dimensional Brownian particle starting at the point $y = 0$ at time $t = 0$, ending at $y = 0$ at time $t = T$ and staying above the line $y = 0$ in between. It was first shown by Louchard and Darling in [20, 40] that the integral of the Brownian excursion of fixed length is Airy distributed. Takács calculated the moments of the area distribution of Dyck paths and showed that in the limit of infinite length, the distribution of the area of Dyck paths is the Airy distribution of area-type. He also pointed out other problems in which Dyck paths occur, including a problem in railway traffic, and the total height distribution of the vertices of random planar trees [65, 66].

In this chapter, we are going to analyse the asymptotic behaviour of the area-width generating function of Dyck paths, in the limit of the area-generating variable tending towards one. We will obtain an asymptotic expression which is valid uniformly for a range of values of the width-generating variable, including the tricritical point of the model. In partic-

ular, our result proves Conjecture 3.3.1 for the case $\ell = \infty$.

The method which we will apply is based on the method of steepest descents, generalised to the case of two coalescing saddle points. This method has been applied before to the model of staircase polygons by Prellberg [52]. It requires a suitable exact expression for the area-width generating function.

We will begin by defining Dyck paths and derive the functional equation satisfied by their area-width generating function in detail. This functional equation differs from the one which we had in Chapter 3 for Dyck paths, since we now use a slightly different definition for the area of a Dyck path than in that chapter, which is more suitable when considering Dyck paths alone. The results for either of the definitions of area can, however, be easily translated into one another. The solution of this functional equation in terms of q-hypergeometric series is known from [26]. Since its derivation is very straightforward, we will repeat it here. The solution can be written as a fraction of two q-hypergeometric series. We will express these series as contour integrals and analyse the integrals asymptotically by using the method of steepest descents. An asymptotic expression for the area-width generating function is then obtained by taking the fraction of the asymptotic expressions for the two q-hypergeometric series. This expression is uniform with respect to the width-generating variable and gives the scaling behaviour of the singular part of the generating function in the vicinity of the tricritical point. This proves Conjecture 3.3.1 for the limiting case $\ell = \infty$.

The results presented in this chapter are joint work with Thomas Prellberg, and were mostly published in the article [34].

4.2 The model

Although the model of Dyck paths can be seen as a part of the family of ℓ-Motzkin paths considered in the last chapter, we once again define it explicitly.

Definition 4.2.1 (Dyck path)**.** *For $m \in \mathbb{Z}_{\geq 0}$, a Dyck path (DP) is a lattice walk $(x_k, y_k)_{k=0}^{2m}$ on $\mathbb{Z}^2$ such that $(x_0, y_0) = (x_{2m}, y_{2m}) = (0, 0)$, and $y_k \geq 0$ for all $k \in [2m]$. Moreover, for $0 \leq k < 2m$, (x_k, y_k) is either $(x_k + 1, y_k + 1)$ or $(x_k + 1, y_k - 1)$, corresponding to an up- or down-step, respectively.*

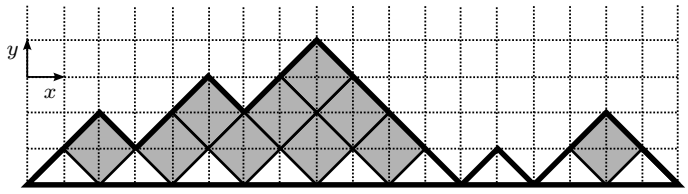

Figure 4.1: A Dyck path of half-width 9 and area 10. The shaded squares have unit area. The dotted grid shows the underlying lattice, and the small arrows indicate the directions of the coordinate axes.

Since the start and end point of a DP are fixed, a DP can also be represented by a sequence of steps, for example, the DP shown in Fig. 4.1 is represented by the sequence

$$\nearrow, \nearrow, \searrow, \nearrow, \nearrow, \searrow, \nearrow, \nearrow, \searrow, \searrow, \searrow, \nearrow, \searrow, \nearrow, \nearrow, \searrow, \searrow,$$

where $\nearrow$ and $\searrow$ stand for up- and down-steps, respectively.

In Fig. 4.1, we show an example for a DP. The *width* of a DP is the number of steps it consists of, and the *half-width* is just the width divided by two. Since the width of a DP is always even, the half-width is always an integer. The trajectory shown in Fig. 4.1 has width 18[1]. In this chapter,

[1] In [34], we used the word length instead of width.

we define the *area* of a DP as the number of squares congruent to the square with corners $(0,1)$, $(1,2)$, $(2,1)$ and $(1,0)$ between the trajectory and the trajectory of same width, consisting of an alternating sequence of up- and down-steps $(\nearrow, \searrow, \ldots, \searrow)$. In Fig. 4.1, the squares contributing to the area of the DP are shaded. Thus, the shown DP has area 10. As mentioned above, this definition of area is different to the one used in Chapter 3, but results obtained using one or the other definition can be translated into each other. We note that the area of a Dyck path is closely related to the sum of the heights of the points of the path, where the height of a point is its distance to the horizontal axis. The generalisation of the area to sums of k-th powers of heights, called rank-k parameters, was considered by Duchon [22] and the existence of a joint limit distribution of these parameters was shown by Richard [58].

Let $\mathcal{D}$ denote the set of all Dyck paths, and for any $d \in \mathcal{D}$, let $h(d)$ be the half-width and $a(d)$ the area of d, respectively. The area-width generating function of Dyck paths is the formal power series

$$G(x,q) = \sum_{m=0}^{\infty} \sum_{n=0}^{\infty} p_{m,n} x^m q^n \tag{4.1}$$

where $p_{m,n}$ is the number of all DP with half-width m and area n, i.e.

$$p_{m,n} = \#\big\{ d \in \mathcal{D} \;\big|\; h(d) = m \;\wedge\; a(d) = n \big\}. \tag{4.2}$$

For example, the DP in Fig. 4.1 contributes a weight $x^9 q^{10}$ to $G(x,q)$. Defining the univariate generating functions

$$Z_m(q) = \sum_{n=0}^{\infty} p_{m,n} q^n \text{ and } Q_n(x) = \sum_{m=0}^{\infty} p_{m,n} x^m, \tag{4.3}$$

we can also write

$$G(x,q) = \sum_{m=0}^{\infty} Z_m(q)x^m = \sum_{n=0}^{\infty} Q_n(x)q^n. \tag{4.4}$$

Note that $p_{m,n} = 0$ for $n > m^2$, therefore $Z_m(q)$ is a polynomial in q for any finite m, whereas, with the given definition of the area, $Q_n(x)$ contains infinitely many terms for any n. For example, for any m, there exists exactly one trajectory of area 0, namely the "zigzag" trajectory $\nearrow$, $\searrow, \ldots, \nearrow, \searrow$. Therefore,

$$Q_0(x) = \sum_{m=0}^{\infty} x^m = \frac{1}{1-x}. \tag{4.5}$$

If we use Dyck paths as a two-dimensional model for biological vesicles, subject to an osmotic pressure acting on the wall of the vesicle, then $Z_m(q)$ and $Q_n(x)$ are the fixed-width and fixed-area partition functions of the model, respectively; the generating function $G(x,q)$ is the partition function of the ensemble where both width and area are allowed to fluctuate.

4.3 Functional equation for $G(x,q)$

To find a functional equation for the generating function defined in Eq. (4.1), we again use a decomposition argument as in Section 3.4. To this end, we first define for a given DP, d, the associated elevated DP as $\nearrow, d, \searrow$. Now note that a DP has either width 0, in which case it contributes a weight 1 to $G(x,q)$, or it starts with an elevated DP, followed by a DP – this decomposition is illustrated in Fig. 4.2. This means that if we call $E_m(q)$

the fixed-width partition function of elevated Dyck paths, then we have

$$Z_m(q) = \begin{cases} 1 & \text{if } m = 1 \\ \sum_{k=1}^{m} E_k(q) Z_{m-k}(q) & \text{if } m > 1. \end{cases} \tag{4.6}$$

Here, $Z_m(q)$ is the fixed-width partition function of DP, defined in Eq. (4.3). If we substitute Eq. (4.6) into Eq. (4.4), this gives us

$$\begin{aligned} G(x,q) &= 1 + \sum_{m=1}^{\infty} \left(\sum_{k=1}^{m} E_k(q) Z_{m-k}(q) \right) x^m \\ &= 1 + \left(\sum_{m_1=1}^{\infty} E_{m_1}(q) x^{m_1} \right) \left(\sum_{m_2=0}^{\infty} Z_{m_2}(q) x^{m_2} \right), \end{aligned}$$

where the left bracket in the last row is the area-width generating function of elevated DP. If the weight of a DP is $x^m q^n$, then the associated elevated DP has weight $x(xq)^m q^n = x^{m+1} q^{m+n}$, where the additional factor of x is due to the two additional steps and the additional factor of q^m is due to the fact that each pair of steps adds an additional unit of area to the area of the path. The generating function of an elevated DP is therefore $xG(qx,q)$. Substituting this into the last equation, this gives us the functional equation

$$G(x,q) = 1 + xG(qx,q)G(x,q). \tag{4.7}$$

Figure 4.2: Graphical interpretation of Eq. (4.7). A Dyck path either has width 0, or it starts with an up-step, followed by an elevated DP, followed by a down-step, followed by another DP.

Equation (4.7) can be rearranged to

$$G(x,q) = \frac{1}{1 - xG(qx,q)}, \tag{4.8}$$

and from iterating this equation one obtains the continued fraction representation

$$G(x,q) = \cfrac{1}{1 - \cfrac{x}{1 - \cfrac{xq}{1 - \cfrac{xq^2}{1 - \cfrac{xq^3}{1 - \ldots}}}}}, \tag{4.9}$$

which was also given in [26]. While this expression is useful for numerical approximations, we need a different expression to approximate $G(x,q)$ asymptotically in the limit $q \to 1^-$. In the next section, we will derive an expression for $G(x,q)$ in term of q-hypergeometric series.

4.4 Solution of the functional equation

First we note that for $q = 1$, Eq. (4.7) becomes the algebraic equation

$$G(x,1) = 1 + xG(x,1)^2, \tag{4.10}$$

which has the two solutions

$$G(x,1) = \frac{1}{2x}\left(1 \pm \sqrt{1-4x}\right). \tag{4.11}$$

The solution with positive sign diverges at $x = 0$, consistent with the fact that the equation is solved by a unique formal power series. Therefore the generating function of Dyck paths is the solution with negative sign, for

which $[x^0]G(x,1) = 1$. For general q, the solution of Eq. (4.7) can be found in [26]. Since the derivation is simple, we restate it here.

One makes the ansatz

$$G(x,q) = \frac{\phi(qx,q)}{\phi(x,q)}, \tag{4.12}$$

where $\phi(x,q)$ is an unknown function. Inserting Eq. (4.12) into Eq. (4.7), we get the linearised functional equation

$$x\phi(q^2x) - \phi(qx) + \phi(x) = 0, \tag{4.13}$$

where we suppressed the explicit q-dependence of ϕ for better readability. Note that the transformation (4.12) is similar to the linearisation of Riccati differential equations (see e.g. [29, Chapter 9]). To solve Eq. (4.13), we write

$$\phi(x) = \sum_{n=0}^{\infty} c_n x^n, \tag{4.14}$$

where the coefficients c_n depend on q. Upon substituting Eq. (4.14) into Eq. (4.13), we get

$$0 = \sum_{n=0}^{\infty} \left(xc_nq^{2n} - c_nq^n + c_n\right) x^n = \sum_{n=1}^{\infty} \left(c_{n-1}q^{2(n-1)} - c_nq^n + c_n\right) x^n.$$

The series of the RHS of the above equation needs to vanish coefficient-wise. This gives us the recursion relation

$$c_n = c_{n-1}\frac{q^{2(n-1)}}{q^n - 1} \quad (n \in \mathbb{N}). \tag{4.15}$$

The value c_0 can be chosen arbitrarily, since it is cancelled out in Eq. (4.12). We choose $c_0 = 1$, since this coincides with the definition of q-hypergeometric

series [31]. Iterating Eq. (4.15), we get

$$c_n = (-1)^n \frac{q^{n^2-n}}{(q;q)_n} \quad (n \in \mathbb{N}), \tag{4.16}$$

where $(q;q)_n$ is the q-Pochhammer symbol, defined for $n \in \mathbb{N}$ as

$$(z;q)_n = \prod_{k=0}^{n-1}(1 - zq^k). \tag{4.17}$$

Inserting Eq. (4.16) into Eq. (4.14), we obtain

$$\phi(x) = \sum_{n=0}^{\infty} \frac{(-1)^n q^{n^2-n}}{(q;q)_n} x^n = {}_0\phi_1 \left(\begin{matrix} - \\ 0 \end{matrix} ; q, -x \right), \tag{4.18}$$

where we use the standard notation for q-hypergeometric series from [31], to be introduced in Chapter 5.

In the next section, we will derive a contour integral expression for $\phi(x)$.

4.5 Contour integral representation of $\phi(x)$.

We begin with the following lemma, which was already used in [52]. Here we give a more detailed proof of it.

Lemma 4.5.1. *For complex q with $0 < |q| < 1$ and $n \in \mathbb{Z}_{\geq 0}$,*

$$\frac{(-1)^{n+1} q^{\binom{n}{2}}}{(q;q)_n (q;q)_\infty} = \operatorname*{Res}_{z=q^{-n}} \left(\frac{1}{(z;q)_\infty} \right). \tag{4.19}$$

Proof. First we notice that, for $|q| < 1$, $(z;q)_\infty = \lim_{n\to\infty}(z;q)_n$ is an

entire function of z. To see this, we use the formula [31]

$$(z;q)_\infty = \sum_{n=0}^{\infty} \frac{(-1)^n q^{\binom{n}{2}} z^n}{(q;q)_n}. \tag{4.20}$$

From the ratio test for convergence, one sees that the radius of convergence of this series is infinite if $|q| < 1$. Since a function defined by a power series is analytic everywhere inside its disk of convergence, $(z;q)_\infty$ is analytic for all $z \in \mathbb{C}$.

Let $n \in \mathbb{Z}_{\geq 0}$. We decompose $(z;q)_\infty^{-1}$ into the product

$$\frac{1}{(z;q)_\infty} = \frac{1}{(z;q)_n} \cdot \frac{1}{(1-zq^n)} \cdot \frac{1}{(zq^{n+1};q)_\infty}. \tag{4.21}$$

The left and right factors of the RHS of the above equation are analytic at $z = q^{-n}$, whereas $(1-zq^n)^{-1}$ has a simple pole there. Therefore,

$$\operatorname*{Res}_{z=q^{-n}} \left(\frac{1}{(z;q)_\infty} \right) = \frac{1}{(z;q)_n}\bigg|_{z=q^{-n}} \left[\operatorname*{Res}_{z=q^{-n}} \left(\frac{1}{1-zq^k} \right) \right] \frac{1}{(zq^{n+1};q)_\infty}\bigg|_{z=q^{-n}}.$$

The proof is concluded by using that $\operatorname*{Res}_{z=q^{-n}} ((1-zq^n)^{-1}) = -q^{-n}$, and

$$\begin{aligned} \frac{1}{(z;q)_n}\bigg|_{z=q^{-n}} &= \frac{1}{(q^{-n};q)_n} = \prod_{k=0}^{n-1} \frac{1}{1-q^{-n+k}} = \prod_{k=0}^{n-1} \frac{q^{n-k}}{q^{n-k}-1} \\ &= \prod_{m=1}^{n} \frac{q^m}{q^m-1} = \left(\prod_{m=1}^{n} q^m \right) \left(\prod_{m=1}^{n} \frac{-1}{1-q^m} \right) = \frac{(-1)^n q^{\binom{n+1}{2}}}{(q;q)_n}. \end{aligned}$$

□

Lemma 4.5.1 can be used to prove the following result.

Lemma 4.5.2. *For complex $x \neq 0$ and $0 < q < 1$,*

$$\phi(x) = \lim_{N\to\infty} \frac{(q;q)_\infty}{2\pi i} \oint_{C_N} \frac{z^{\frac{1}{2}(\log_q(z)+1)-\log_q(x)}}{(z;q)_\infty} dz, \tag{4.22}$$

where, for $N \in \mathbb{N}$, the integration is performed once clockwise around the curve C_N defined in Eq. (4.23), with $0 < \rho < 1$ and $\psi, \varphi \in (0, \pi)$.

Proof. Assume that $x \neq 0$ and $0 < q < 1$. Define, for $N \in \mathbb{N}$, the contour $C_N : [-1, 2) \to \mathbb{C}$,

$$C_N(t) = \begin{cases} \rho - t(q^{-N+\frac{1}{2}} - \rho)e^{-i\psi} & \text{for } t \in [-1, 0), \\ \rho + t(q^{-N+\frac{1}{2}} - \rho)e^{i\varphi} & \text{for } t \in [0, 1), \\ \rho + (q^{-N+\frac{1}{2}} - \rho)e^{i[\varphi-(\psi+\varphi)(t-1)]} & \text{for } t \in [1, 2), \end{cases} \tag{4.23}$$

where $0 < \rho < 1$ and $\varphi, \psi \in (0, \pi)$. This contour surrounds exactly the N leftmost poles of $(z;q)_\infty^{-1}$, which are located at $z = q^{-n}$ with $n \in \mathbb{Z}_{\geq 0}$. See Fig. 4.3 for a sketch of C_1.

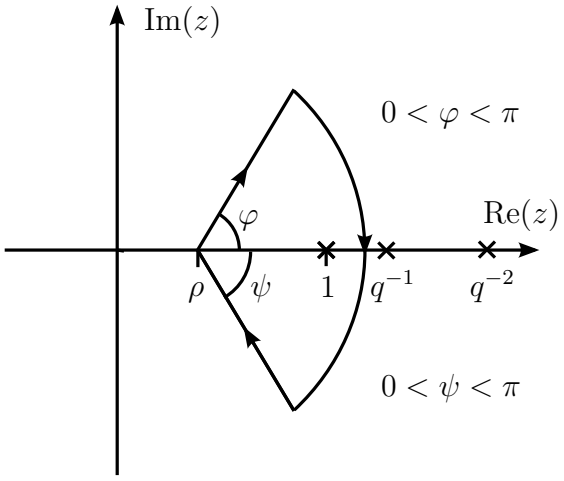

Figure 4.3: The contour C_1, surrounding the leftmost pole of $(z;q)_\infty^{-1}$. The arrows indicate the direction of integration used in Eq. (4.22).

The function $h(z) = z^{\frac{1}{2}(\log_q(z)+1)-\log_q(x)}$ is analytic in $\mathbb{C}\setminus(-\infty, 0]$. There-

fore,

$$\frac{1}{2\pi i}\oint_{C_N}\frac{h(z)}{(z;q)_\infty}dz=\sum_{n=0}^{N-1}h(q^{-n})\operatorname{Res}\left((z;q)_\infty^{-1}\,;\,z=q^{-n}\right). \tag{4.24}$$

Inserting Eq. (4.19), we obtain, for $N\in\mathbb{N}$,

$$\frac{(q;q)_\infty}{2\pi i}\oint_{C_N}\frac{z^{\frac{1}{2}(\log_q(z)+1)-\log_q(x)}}{(z;q)_\infty}dz=\sum_{n=0}^{N}\frac{(-x)^n}{(q;q)_n}q^{n^2-n}, \tag{4.25}$$

where the integration is performed once clockwise. This is accounted for by a factor of (-1). Taking the limit $N\to\infty$ in Eq. (4.25), we obtain Eq. (4.22).

□

In the limit $N\to\infty$, the contour C_N in Eq. (4.22) can be replaced by a contour C. This is stated in the following proposition.

Proposition 4.5.1. *For complex $x\neq 0$ and $0<q<1$,*

$$\phi(x)=\frac{(q;q)_\infty}{2\pi i}\int_{C}\frac{z^{\frac{1}{2}(\log_q(z)+1)-\log_q(x)}}{(z;q)_\infty}dz, \tag{4.26}$$

where the integration is performed once clockwise around the contour C defined in Eq. (4.27), with $0<\rho<1$ and $\psi,\varphi\in(0,\pi)$.

Proof. We need to show that in the limit $N\to\infty$, the contribution of the circle segment $C_N([1,2])$ to the contour integral (4.25) vanishes. In that case, in the limit $N\to\infty$, C_N can be replaced by the contour $C:(-\infty,\infty)\to\mathbb{C}$, where

$$C(t)=\begin{cases}\rho-te^{-i\psi} & \text{for } t<0,\\ \rho+te^{i\varphi} & \text{for } t\geq 0,\end{cases} \tag{4.27}$$

with $0 < \rho < 1$ and $\varphi, \psi \in (0, \pi)$ – see Fig. 4.4.

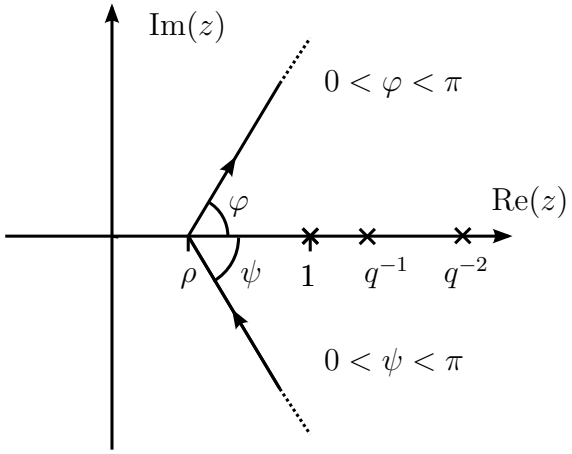

Figure 4.4: The contour of integration C used in Eq. (4.26).

Assume $0 < q < 1$; $x \in \mathbb{C} \setminus \{0\}$ and $z \in C_N([1,2))$. Hence, $z = \rho + (q^{-N+\frac{1}{2}} - \rho)e^{i\theta}$, where $\theta \in (-\psi, \varphi]$. For $N \to \infty$, $\log_q(z) = -N + \frac{1}{2} - \frac{i\theta}{\epsilon} + o(1)$, where $\epsilon = -\ln(q)$. Therefore,

$$\log_q\left(z^{(1+\log_q(z))/2-\log_q(x)}\right) = \frac{N^2}{2} + \left(\frac{i\theta - \ln(x)}{\epsilon} - 1\right)N + \mathcal{O}(1). \quad (4.28)$$

Moreover, we estimate for $N \geq 1$,

$$\left|(z,q)_\infty\right| = \left|\prod_{n=0}^{\infty}\left(1 - [\rho + (q^{-N+\frac{1}{2}} - \rho)e^{i\theta}]q^n\right)\right| \geq \left|\prod_{n=0}^{\infty}(1 - q^{-N+\frac{1}{2}+n})\right|,$$

where we use that for $v, w \in \mathbb{C}$, $|v - w| \geq ||v| - |w||$. Further,

$$\left|\prod_{n=0}^{\infty}(1 - q^{-N+\frac{1}{2}+n})\right| = \left|(q^{\frac{1}{2}}; q^{-1})_{N+1}(q^{\frac{3}{2}}; q)_\infty\right| \geq a\left|(q^{\frac{3}{2}}; q)_\infty\right| \prod_{k=0}^{N} q^{\frac{1}{2}-k},$$

where $a > 0$ is a constant independent of N and we used that for $p > 1$,

$\prod_{n=1}^{\infty} \frac{p^n}{p^n-1} < \infty$. From the last expression we obtain

$$(z;q)_\infty \geq a\big|(q^{\frac{3}{2}};q)_\infty\big|\, q^{-\frac{N^2-1}{2}}. \tag{4.29}$$

Using Eqs. (4.28) and (4.29), we get

$$\left|\frac{h(z)}{(z;q)_\infty}\right| \leq b\, q^{N^2-N}|x|^N,$$

where $b > 0$ is another constant independent of N. Taking the integral over $C_N([1,2))$ leads to a further factor of $(\psi+\varphi)q^{-N}$. We obtain the estimation

$$\frac{1}{2\pi i}\int_{C_N([1,2))} \left|\frac{h(z)}{(z;q)_\infty}\right| dz \leq b(\psi+\varphi)\, q^{N^2-2N}|x|^N. \tag{4.30}$$

For $N \to \infty$, the RHS of Eq. (4.30) tends to 0. With this we conclude that in the limit $N \to \infty$, the contour C_N in Eq. (4.25) can be replaced by the contour C. □

The principal branch of the Euler dilogarithm ([21, §25.2]), is defined for $z \in \mathbb{C}$ as

$$\mathrm{Li}_2(z) = -\int_0^z \frac{\ln(1-w)}{w} dw, \tag{4.31}$$

where the principal branch of the logarithm is taken in the integral and, for $x > 1$,

$$\mathrm{Li}_2(x) = \lim_{\delta \to 0^-} \mathrm{Li}_2(xe^{i\delta}). \tag{4.32}$$

By this definition, $\mathrm{Im}(\mathrm{Li}_2(x)) < 0$ for $x > 1$. This is consistent with the definition of the function $\mathrm{dilog}(1-x)$ in Maple 18.

In [52], the following result on the asymptotics of $(z;q)_\infty$ was derived by using the Euler-Maclaurin summation formula ([21, §2.4(i)]).

Lemma 4.5.3 (Prellberg [52]). *For complex z with $|\arg(1-z)| < \pi$, $0 < q < 1$ and $m \in \mathbb{N}$,*

$$\ln(z;q)_\infty = \frac{1}{\ln(q)}\operatorname{Li}_2(z) + \frac{1}{2}\ln(1-z) + \\ + \sum_{n=1}^{m-1} \frac{B_{2n}}{(2n)!}(\ln q)^{2n-1}\left(z\frac{d}{dz}\right)^{2n-2}\frac{z}{1-z} + (\ln q)^{2m-1}R_m(z,q), \tag{4.33}$$

where the Bernoulli numbers $(B_n)_{n=0}^\infty$ have the exponential generating function $\sum_{n=0}^\infty B_n \frac{t^n}{n!} = \frac{t}{e^t-1}$ and the remainder term satisfies, for $m \in \mathbb{N}$, the bound

$$\left|R_m(z,q)\right| \le \frac{2\left|B_{2m}\right|}{(2m!)}\int_0^1 \left|\left(u\frac{d}{du}\right)^{2m-1}\frac{zu}{1-zu}\right|\frac{du}{u}. \tag{4.34}$$

For $m = 1$, we get from Eq. (4.34) for $z \in \mathbb{C}\setminus\mathbb{R}$ with $\arg(z) = \varphi$,

$$\begin{aligned}\left|R_1(z,q)\right| &\le \frac{1}{6}\int_0^1 \left|\frac{z}{(1-zu)^2}\right| du = \frac{1}{6}\int_0^{|z|}\frac{1}{|v-e^{-i\varphi}|^2}dv \\ &= \frac{1}{6\sin(\varphi)^2}\int_0^{|z|}\frac{1}{1+\left(\frac{v-\cos(\varphi)}{\sin(\varphi)}\right)^2}dv \\ &= \frac{1}{6\,\sin(\varphi)}\left(\arctan\left(\frac{|z|-\cos(\varphi)}{\sin(\varphi)}\right)+\arctan\left(\frac{\cos(\varphi)}{\sin(\varphi)}\right)\right) \\ &= \frac{1}{6\,\sin(\varphi)}\left(\arctan\left(\frac{|z|-\cos(\varphi)}{\sin(\varphi)}\right)-\psi\right),\end{aligned} \tag{4.35}$$

where $\varphi = \arg(z)$, $\psi = \varphi \pm \frac{\pi}{2}$ for $\varphi \lessgtr 0$, and for $z < 1$,

$$\left|R_1(z,q)\right| \le \frac{|z|}{1-z}. \tag{4.36}$$

Since the RHS of Eq. (4.36) diverges for $z \to 1^-$, Eq. (4.33) does not yield an asymptotic expression for $(q;q)_\infty$. For this separate case, the following

formula is given in [52]. For $q = e^{-\epsilon} \to 1^-$,

$$\ln(q;q)_\infty = -\frac{\pi^2}{6\epsilon} + \ln\left(\sqrt{\frac{2\pi}{\epsilon}}\right) + \mathcal{O}(\epsilon). \tag{4.37}$$

The following lemma is the starting point of the asymptotic analysis of $\phi(x)$ by means of the saddle point method.

Lemma 4.5.4. *For complex $x \neq 0$, $k \in \mathbb{Z}$ and $0 < q = e^{-\epsilon} < 1$,*

$$\phi(q^k x) = \frac{(q;q)_\infty}{2\pi i} \int_C \exp\left(\frac{1}{\epsilon} f(z)\right) g_k(z,q) dz, \tag{4.38}$$

where the contour C is defined in Eq. (4.27) with $0 < \rho < 1$ and $\psi, \varphi \in (0, \pi)$,

$$f(z) = \ln(x)\ln(z) + \mathrm{Li}_2(z) - \frac{1}{2}\ln(z)^2, \tag{4.39}$$

$$g_k(z,q) = \frac{1}{z^k}\left(\frac{z}{1-z}\right)^{\frac{1}{2}} \exp\left(\epsilon R_1(z,q)\right), \tag{4.40}$$

and

$$R_1(z,q) = -\frac{1}{\epsilon}\left(\ln\left((z;q)_\infty\right) + \frac{1}{\epsilon}\mathrm{Li}_2(z) - \frac{1}{2}\ln(1-z)\right). \tag{4.41}$$

Proof. This follows immediately from inserting Eq. (4.33) with $m = 1$ into Eq. (4.26). □

Note that due to the bound (4.35), we have

$$\phi(q^k x) = \frac{(q;q)_\infty}{2\pi i} \int_C \exp\left(\frac{1}{\epsilon} f(z)\right) g_k(z,1) dz \left(1 + \mathcal{O}(\epsilon)\right). \tag{4.42}$$

The integral (4.38) can be analysed via the method of steepest descents. To this end, we first need to know more about the saddle point landscape of the function f, which is also called the kernel of the integrand. In particular, we are interested in the paths of steepest descent and ascent of the function $\mathcal{R}(z) = \mathrm{Re}(f(z))$.

4.6 Saddle point landscape of the kernel $f(z)$

The kernel f defined in Eq. (4.39) is an analytic function of z if $x \neq 0$ for $z \in \mathbb{C} \setminus ((-\infty, 0] \cup [1, \infty))$. For $x \in \mathbb{C} \setminus (-\infty, 0]$ it has the two saddle points

$$z_\pm = \frac{1}{2}\left(1 \pm \sqrt{1-4x}\right), \tag{4.43}$$

which are the zeros of the derivative

$$f'(z) = \frac{1}{z} \ln\left(\frac{x}{z(1-z)}\right). \tag{4.44}$$

They thus satisfy the equation

$$z_\pm(1 - z_\pm) - x = 0. \tag{4.45}$$

The saddle points $z_\pm$ are real for real $x < \frac{1}{4}$ and coalesce in the point $z_c = \frac{1}{2}$ for $x = x_c = \frac{1}{4}$. For $x > \frac{1}{4}$, $z_+ = z_-^*$ and $\mathrm{Re}(z_\pm) = \frac{1}{2}$. The saddle points are non-degenerate, i.e. $f''(z_\pm) \neq 0$ unless $x = \frac{1}{4}$, in which case $z_c = \frac{1}{2}$ is a double saddle point.

Now consider the surface defined by $\mathcal{R}(z) = \mathrm{Re}(f(z))$. It follows from the general theory of analytic functions that for $x \in \mathbb{C} \setminus (-\infty, 0]$, two paths of steepest descent and two paths of steepest ascent of $\mathcal{R}(z)$ originate

from each of the two ordinary saddle points of f if $x \neq \frac{1}{4}$; if $x = \frac{1}{4}$, then three paths of steepest descent and three paths of steepest ascent of $\mathcal{R}(z)$ originate from the double saddle point $z_c = \frac{1}{2}$ (see e.g. [29, Chapter 8]). On the paths of steepest descent and ascent of $\mathcal{R}(z)$, the function $\mathcal{I}(z) = \mathrm{Im}(f(z))$ is constant.

We aim to show that the integration contour C used in Eq. (4.38) can be deformed into a contour connecting z_+ with $\pm i\infty$ via paths of steepest descent of $\mathcal{R}(z)$ for $0 < x \leq \frac{1}{4}$, and a composite contour connecting z_+ and z_- with 0 and $\pm i\infty$, respectively, if $x > \frac{1}{4}$. To this purpose, we need to study the asymptotic behaviour of $f(z)$ when $|z| \to \infty$ and $|z| \to 0$. As a preliminary step, we state the following Lemma.

Lemma 4.6.1. *For $\lambda \to \infty$, and $0 < |\varphi| \leq \pi$,*

$$\mathrm{Li}_2(\lambda e^{i\varphi}) = -\frac{1}{2}\ln(\lambda)^2 - i\psi\ln(\lambda) - \frac{\pi^2 - 3\psi^2}{6} + \mathcal{O}\left(\frac{1}{\lambda}\right), \tag{4.46}$$

uniformly with respect to φ, where $\psi = \varphi \pm \pi$ for $\varphi \lessgtr 0$.

Proof. For $z \in \mathbb{C} \setminus [0, \infty)$, the dilogarithm satisfies the identity ([21, eq. 25.12.4])

$$\mathrm{Li}_2(z) = -\frac{\pi^2}{6} - \frac{1}{2}(\ln(-z))^2 - \mathrm{Li}_2\left(\frac{1}{z}\right). \tag{4.47}$$

Since for $|z| < 1$,

$$\mathrm{Li}_2(z) = \sum_{n=1}^{\infty} \frac{z^n}{n^2},$$

we have for $\varphi \in (-\pi, \pi]$ and $\lambda \to \infty$,

$$\mathrm{Li}_2\left(\frac{e^{-i\varphi}}{\lambda}\right) = \mathcal{O}\left(\frac{1}{\lambda}\right) \tag{4.48}$$

uniformly with respect to φ. Setting $z = \lambda e^{i\varphi}$ in Eq. (4.47) and substituting

Eq. (4.48), we arrive at Eq. (4.46).

□

From Eq. (4.46), we can derive the asymptotic behaviour of the function f in the limits $|z| \to \infty$ and $|z| \to 0$, stated in the following lemma.

Lemma 4.6.2. *For complex $x \neq 0$, we have the following.*

(i) *For $\lambda \to \infty$ and $0 < |\varphi| < \pi$,*

$$f(\lambda\, e^{i\varphi}) = -\ln(\lambda)^2 + (\ln(x) - i\gamma)\ln(\lambda) + \mathcal{O}(1), \tag{4.49}$$

uniformly with respect to φ, where $\gamma = 2\varphi \pm \pi$ for $\varphi \lessgtr 0$.

(ii) *For $\lambda \to 0$ and $0 \leq |\varphi| < \pi$*

$$f(\lambda\, e^{i\varphi}) = -\frac{1}{2}\ln(\lambda)^2 + (\ln(x) - i\varphi)\ln(\lambda) + \mathcal{O}(1), \tag{4.50}$$

uniformly with respect to φ.

Proof. Let $x \in \mathbb{C} \setminus \{0\}$.

For (i), assume $0 < |\varphi| < \pi$. Using Eq. (4.46), we have for $\varphi \lessgtr 0$,

$$\begin{aligned} f(\lambda e^{i\varphi}) &= -\frac{1}{2}\ln(\lambda e^{i\varphi})^2 + \ln(x)\ln(\lambda e^{i\varphi}) + \mathrm{Li}_2(\lambda e^{i\varphi}) \\ &= -\ln(\lambda)^2 + \Big(\ln(x) - i(2\varphi \pm \pi)\Big)\ln(\lambda) \\ &\quad + \varphi\,(i\ln(x) \pm \pi) - \frac{2\pi^2}{3} + \mathcal{O}\left(\frac{1}{\lambda}\right), \end{aligned}$$

uniformly with respect to φ. This proves (i).

For (ii), assume $0 \leq |\varphi| < \pi$. With Eq. (4.48), we have for $\lambda \to 0$,

$$\begin{aligned} f(\lambda e^{i\varphi}) &= -\frac{1}{2}\ln(\lambda e^{i\varphi})^2 + \ln(x)\ln(\lambda e^{i\varphi}) + \mathcal{O}(\lambda) \\ &= -\frac{1}{2}\ln(\lambda)^2 + (\ln(x) - i\varphi)\ln(\lambda) + \frac{1}{2}\varphi^2 + i\varphi\ln(x) + \mathcal{O}(\lambda), \end{aligned}$$

leading to Eq. (4.50).

□

Due to the branch cut of the logarithm, the function f is not analytic on the lines $(-\infty, 0]$ and $[1, \infty)$. For $x > 0$ and $z = \lambda e^{i\varphi}$, we have

$$\lim_{\varphi \to \pm\pi} \operatorname{Im}(f(\lambda e^{i\varphi})) = \pm\pi \ln(x/\lambda) \quad (\lambda > 0), \tag{4.51a}$$

$$\lim_{\varphi \to \pm 0} \operatorname{Im}(f(\lambda e^{i\varphi})) = \pm\pi \ln(\lambda) \qquad (\lambda > 1); \tag{4.51b}$$

and

$$\left.\begin{array}{ll} \lim_{\varphi\to\pm\pi} \operatorname{Im}(f'(\lambda e^{i\varphi})) & (\lambda > 0) \\ \lim_{\varphi\to\pm 0} \operatorname{Im}(f'(\lambda e^{i\varphi})) & (\lambda > 1) \end{array}\right\} = \pm\frac{\pi}{\lambda}. \tag{4.52}$$

Note also that for $x > 0$, the function f is real on the segment $z \in (0, 1)$, and therefore $f(z)^* = f(z^*)$ for $z \in \mathbb{C} \setminus ((-\infty, 0) \cup [1, \infty))$.

We now prove the main result of this section.

Lemma 4.6.3. *For $0 < x \leq x_c = \frac{1}{4}$, the two paths of steepest descent of the function $\mathcal{R}(z) = \operatorname{Re}(f(z))$, originating from the saddle point $z_+ = \frac{1}{2}\big(1 + \sqrt{1 - 4x}\big)$, end at $\pm i\infty$.*

Proof. For $0 < x < \frac{1}{4}$, z_- and z_+ are the local maximum and minimum of f on the segment $(0, 1)$, respectively, and $\mathcal{I}(z) = 0$ on this line. Hence, the paths of steepest descent of $\mathcal{R}(z)$ originating from z_- end at 0 and z_+, respectively. From this it follows that the paths of steepest ascent origin-

ating from z_- and the paths of steepest descent originating from z_+ meet the real line at an angle of $\frac{\pi}{2}$. According to Lemma 4.6.2, the imaginary part of f tends to $-\infty$ for $|z| \to 0$ and $|z| \to \infty$. Therefore, the paths of steepest ascent originating from z_- can only end on the lines $(-\infty, 0)$ or $[1, \infty)$, where f is not analytic. Since $\mathrm{Im}(f(z)) = \mathcal{I}(z)$ vanishes on these contours, according to Eq. (4.51) they can only end at $z = -x$. Since the paths of steepest descent originating from z_+ cannot intersect with the paths of steepest ascent originating from z_-, the paths of steepest descent originating from z_+ necessarily end at infinity. From the asymptotic behaviour of $\mathcal{I}(z)$ stated in Eq. (4.49), it follows that they end at $\pm i\infty$, since the angle γ in that equation is zero for $\varphi = \pm\frac{\pi}{2}$. The statement remains true for $x = x_c = \frac{1}{4}$, in which case z_- and z_+ coalesce in $z_c = \frac{1}{2}$.

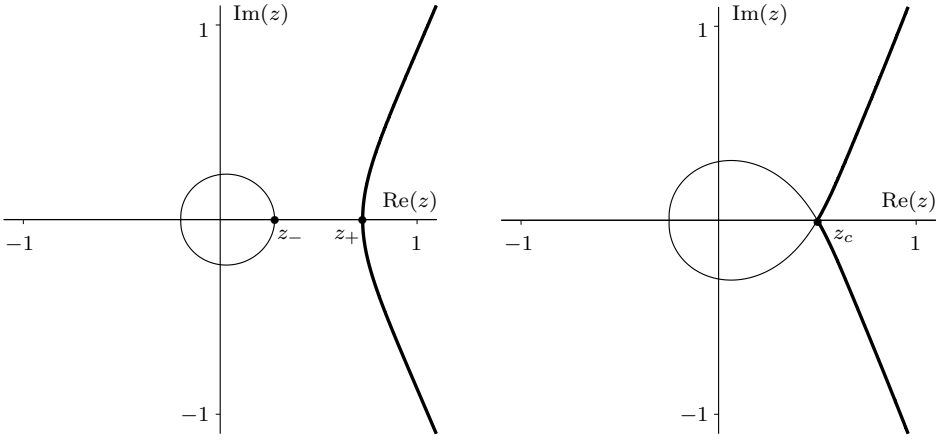

(a) $x = \frac{1}{5}$ (b) $x = \frac{1}{4}$

Figure 4.5: (a): The paths of steepest ascent of the function f connecting the saddle point z_- with the negative real line (thin) and the paths of steepest descent (thick) connecting z_+ with $\pm i\infty$ for $x = \frac{1}{5} < x_c$. (b): The paths of steepest ascent (thin) and the paths of steepest descent (thick) connecting the double saddle point $z_c = \frac{1}{2}$ of the function f with the negative real line and $\pm i\infty$, respectively, for $x = x_c = \frac{1}{4}$.

□

In Fig. 4.5, the relevant paths of steepest descent and ascent originating from the saddle points of f are plotted for $x < x_c$ and $x = x_c$. For $x > x_c$, one obtains a different picture. This is stated in the following lemma.

Lemma 4.6.4. *For $x > \frac{1}{4}$, the paths of steepest descent of the function $\mathcal{R}(z)$ defined in Eq. (4.39), originating from the saddle points $z_\pm = \frac{1}{2}\big(1 \pm \sqrt{1-4x}\big)$, end at 0 and $\pm i\infty$, respectively.*

Proof. For $x > \frac{1}{4}$, $z_+ = z_-^*$, and $\mathrm{Re}(z_\pm) = \frac{1}{2}$. According to Eq. (4.52), the imaginary part of $f'(z)$ is positive when the lines $z < 0$ or $z > 1$ are approached from the positive half plane and negative when approached from the negative half plane. From this it follows that no path of steepest descent can end on the negative real line or on the segment $[1, \infty)$. Therefore, the two paths of steepest descent originating from $z_\pm$ necessarily end at 0 and infinity, respectively. Again, the asymptotic behaviour of $\mathcal{I}(z)$, given by Eq. (4.49) determines that the end points at infinity are $\pm i\infty$. In Fig. 4.6, we show the paths of steepest descent and ascent of $\mathcal{R}(z)$ originating from the saddle points $z_\pm$ for $x = 0.3 > x_c$.

□

The arguments of the above proof can be extended to complex values of x. Here we only consider the case $x > 0$, since we are mainly interested in the asymptotic behaviour for real x around $x_c = \frac{1}{4}$.

4.7 Asymptotic analysis of $\phi(q^k x)$

From Lemma 4.6.3 it follows that for $0 < x \leq \frac{1}{4}$, the contour C used in the integral representation (4.38) can be deformed into a contour connecting the saddle point z_+ of f with $\pm i\infty$ via paths of steepest descent of

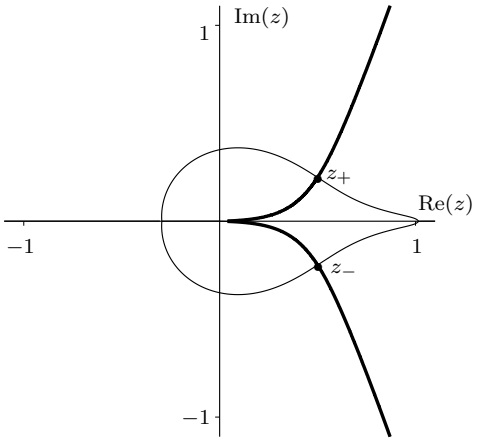

Figure 4.6: Paths of steepest descent (thick) and ascent (thin) originating from the saddle points $z_\pm$ of the function f for $x = 0.3 > x_c = \frac{1}{4}$.

$\mathcal{R}(z) = \mathrm{Re}(f(z))$; for $x > \frac{1}{4}$, C can be deformed into a composite contour connecting $z_\pm$ with 0 and $\pm i\infty$ via paths of steepest descent of $\mathcal{R}(z)$, respectively – see Figs. 4.5 and 4.6.

For $x > 0$ and $x \neq \frac{1}{4}$, the saddle points are separated and Theorem 2.2.1 can be applied. The result is stated in the following proposition.

Proposition 4.7.1. *Let $k \in \mathbb{Z}$, and define*

$$c_0^{(\pm)} = \frac{g_k(z_\pm, q)}{\sqrt{f''(z_\pm)}}, \tag{4.53}$$

and $h_\pm = f(z_\pm) - \frac{\pi^2}{6}$. We have the following.

(i) *For $q = e^{-\epsilon} \to 1^-$ and $x \in (0, \frac{1}{4})$,*

$$\phi(q^k x) \ = e^{\frac{h_\pm}{\epsilon}} c_0^{(+)} \left(1 + \mathcal{O}\big(\epsilon\big)\right), \tag{4.54a}$$

uniformly for $x \in [x_1, x_2]$ if $0 < x_1 < x_2 < \frac{1}{4}$.

(ii) *For* $q = e^{-\epsilon} \to 1^-$ *and* $x \in (\frac{1}{4}, \infty)$,

$$\phi(q^k x) \;=\; \left(c_0^{(+)} e^{\frac{h_+}{\epsilon}} + c_0^{(-)} e^{\frac{h_-}{\epsilon}}\right)\left(1 + \mathcal{O}(\epsilon)\right), \tag{4.54b}$$

uniformly for $x \in [x_3, x_4]$ *if* $\frac{1}{4} < x_3 < x_4 < \infty$.

Proof. Let $k \in \mathbb{Z}$ and suppose $x \in (0, \infty) \setminus \{\frac{1}{4}\}$. In this case, the saddle points of f in the integral (4.42) are separated and the ordinary method of steepest descents can be applied. We can also use Eq. (4.37) for $(q;q)_\infty$. We distinguish the two cases as in the statement of the proposition.

(i) If $0 < x < \frac{1}{4}$, then according to Lemma 4.6.3 the integration contour C in Eq. (4.22) can be chosen as the contour connecting the saddle point $z_+ = \frac{1}{2}(1+\sqrt{1-4x})$ with $\pm i\infty$ via paths of steepest descent of $\mathcal{R}(z)$. Therefore Theorem 2.2.1 can be applied to the integral where $\omega = \frac{\pi}{2}$ and therefore $\omega_0 = -\pi$. This leads to Eq. (4.54a).

(ii) For $x > \frac{1}{4}$, the saddle points $z_\pm$ are complex conjugates to each other, and according to Lemma 4.6.4, the integration contour C can be chosen as a contour containing both saddle points and connecting z_+ with $i\infty$ and 0 and z_- with $-i\infty$ and 0 via paths of steepest descent of $\mathcal{R}(z)$. The saddle point analysis proceeds exactly analogously to the case $x < \frac{1}{4}$, with the difference that now both saddle points contribute to the asymptotics. With this we obtain Eq. (4.54b).

□

Remark. Note that $\lim_{x\to 0^+} e^{\frac{h_+}{\epsilon}} c_0^{(+)} = 1 = \phi(0)$. Therefore, the validity of the asymptotic expression (4.54a) can be extended to $x = 0$.

Since for $x = \frac{1}{4}$, $f''(z_\pm) = f''(z_c) = 0$, the coefficients in Eq. (4.53) diverge in this case. To obtain an asymptotic expression which is valid in a region containing $x = \frac{1}{4}$, we apply the Chester-Friedman-Ursell method [19]. This leads us to the following theorem.

Theorem 4.7.1. *Let $k \in \mathbb{Z}$ and $0 < x_1 < \frac{1}{4}$. Then there exists a $x_2 > x_c$ such that for $q = e^{-\epsilon} \to 1^-$,*

$$\phi(q^k x) = (q;q)_\infty \, e^{\frac{\beta}{\epsilon}} \left(p_k \operatorname{Ai}\left(\frac{\alpha}{\epsilon^{\frac{2}{3}}}\right) \epsilon^{\frac{1}{3}} - q_k \operatorname{Ai}'\left(\frac{\alpha}{\epsilon^{\frac{2}{3}}}\right) \epsilon^{\frac{2}{3}} \right) (1+\mathcal{O}(\epsilon)), \quad (4.55)$$

uniformly for $x \in [x_1, x_2]$. Here,

$$\alpha = \left(\frac{3}{4}\left(f(z_-) - f(z_+)\right)\right)^{\frac{2}{3}} \text{ and } \beta = \frac{1}{2}\big(f(z_+) + f(z_-)\big), \quad (4.56)$$

where the root is chosen such that α is real; the coefficients p_k and q_k are given for $x \neq \frac{1}{4}$ by

$$p_k = \frac{\alpha^{\frac{1}{4}}}{\sqrt{2}} \left(\frac{g_k(z_+,1)}{\sqrt{f''(z_+)}} + \frac{g_k(z_-,1)}{\sqrt{-f''(z_-)}} \right), \quad (4.57a)$$

$$q_k = \frac{\alpha^{-\frac{1}{4}}}{\sqrt{2}} \left(\frac{g_k(z_+,1)}{\sqrt{f''(z_+)}} - \frac{g_k(z_-,1)}{\sqrt{-f''(z_-)}} \right), \quad (4.57b)$$

and $p_k = \lim_{x\to\frac{1}{4}} p_k$ and $q_k = \lim_{x\to\frac{1}{4}} q_k$ for $x = \frac{1}{4}$.

Proof. Let $k \in \mathbb{Z}$. For $x = \frac{1}{4}$, the two saddle points $z_\pm$ of the kernel f defined in Eq. (4.38) coalesce in the point $z_c = \frac{1}{2}$, and f and g_k are analytic around this point. Let α and β be defined as in Eq. (4.56), with the root being chosen such that α is real for positive values of x.

By using the relation

$$\operatorname{Li}_2(z) + \operatorname{Li}_2(1-z) = \frac{\pi^2}{6} - \ln(z)\ln(1-z) \quad (0 < z < 1), \quad (4.58)$$

the expression for β can be simplified for $0 < x < \frac{1}{4}$ to

$$\beta = \frac{\ln(x)^2}{4} + \frac{\pi^2}{12}. \tag{4.59}$$

Theorem 2.2.2 states that there exists a unique transformation $\mathrm{T} : z \mapsto u(z)$, such that

$$f(z) = \frac{u^3}{3} - \alpha u + \beta = p(u), \tag{4.60}$$

which is analytic and bijective if x and z lie in small regions around $x_c = \frac{1}{4}$ and $z_c = \frac{1}{2}$, respectively, and $u(z_\pm) = \pm\sqrt{\alpha}$.

Denote the part of C which lies in the region of analyticity of T by C_c. Since C_c contains the saddle points of f, the error from restricting the integration contour C to C_c in the integral (4.42) decays exponentially as $q = e^{-\epsilon} \to 1^-$. For $0 < x \leq \frac{1}{4}$, T maps C_c onto a segment D_c of the contour D in the u-plane connecting the point $+\sqrt{\alpha}$ with the points $\infty e^{\pm i\frac{\pi}{3}}$ via paths of steepest descent. For $x > \frac{1}{4}$, C_c is mapped onto a part D_c of the composite contour D connecting $\pm\sqrt{\alpha}$ with $-\infty$ and $\infty e^{\pm i\frac{\pi}{3}}$, respectively, via paths of steepest descent. The action of the mapping T is illustrated in Fig. 4.7. The error from extending D_c to the complete contour D decays exponentially in both cases when $q = e^{-\epsilon} \to 1^-$. We therefore have

$$\phi(q^k x) = \left(\frac{(q;q)_\infty}{2\pi i} \int_{\infty e^{-i\frac{\pi}{3}}}^{\infty e^{i\frac{\pi}{3}}} e^{\frac{p(u)}{\epsilon}} g_k(z(u), 1) \frac{dz}{du} du \right) (1 + \mathcal{O}(\epsilon)). \tag{4.61}$$

Now we insert the ansatz

$$g_k(z(u), 1) \frac{dz}{du} = p_k + u q_k + (u^2 - \alpha) H(u), \tag{4.62}$$

into Eq. (4.61), where $H(u)$ is some analytic function of u. Substituting $u = \pm\sqrt{\alpha}$ into the above formula, we get

$$g_k(z_\pm, 1) \left.\frac{dz}{du}\right|_{u=\pm\sqrt{\alpha}} = p_k \pm \sqrt{\alpha} q_k. \tag{4.63}$$

To obtain expressions for $\left.\frac{dz}{du}\right|_{u=\pm\sqrt{\alpha}}$, we take the second derivative of Eq. (4.60) with respect to u and substitute $u = \pm\sqrt{\alpha}$. This gives us

$$f''(z_\pm) \left(\left.\frac{dz}{du}\right|_{u=\pm\sqrt{\alpha}} \right)^2 = \pm 2\sqrt{\alpha}, \tag{4.64}$$

where we used that $f'(z_\pm) = 0$. With this we obtain

$$\left.\frac{dz}{du}\right|_{u=\pm\sqrt{\alpha}} = \sqrt{\frac{2\sqrt{\alpha}}{\pm f''(z_\pm)}} = \sqrt{\frac{2\sqrt{\alpha} z_\pm x}{\sqrt{1-4x}}}, \tag{4.65}$$

where the positive branch of the root has to be chosen. Here, we used that $f''(z_\pm) = (2z_\pm - 1)/(z_\pm x)$. Substituting Eq. (4.65) into Eq. (4.63) and solving for p_k and q_k, we obtain Eq. (4.57).

With Eq. (4.62), the integral in Eq. (4.61) becomes

$$\begin{aligned}
&\frac{1}{2\pi i} \int_{\infty e^{-i\frac{\pi}{3}}}^{\infty e^{i\frac{\pi}{3}}} e^{\frac{p(u)}{\epsilon}} g_k(z(u), 1) \frac{dz}{du} du \\
&= \frac{1}{2\pi i} \int_{\infty e^{-i\frac{\pi}{3}}}^{\infty e^{i\frac{\pi}{3}}} e^{\frac{p(u)}{\epsilon}} \big(p_k + u q_k + (u^2 - \alpha) H(u)\big) du \\
&= \epsilon^{\frac{1}{3}} p_k \operatorname{Ai}\left(\frac{\alpha}{\epsilon^{\frac{2}{3}}}\right) - \epsilon^{\frac{2}{3}} q_k \operatorname{Ai}'\left(\frac{\alpha}{\epsilon^{\frac{2}{3}}}\right) + \frac{\epsilon}{2\pi i} \int_{\infty e^{-i\frac{\pi}{3}}}^{\infty e^{i\frac{\pi}{3}}} e^{\frac{p(u)}{\epsilon}} H'(u) du,
\end{aligned}$$

where we integrated partially by using the fact that $p'(u) = u^2 - \alpha$. In the limit $q \to 1^-$, the asymptotic is dominated by the first two terms. Substituting the above expression into Eq. (4.42), we obtain Eq. (4.55) if x lies in a small neighbourhood of $x_c = \frac{1}{4}$.

To verify that Eq. (4.55) is valid uniformly in a bigger interval, we use the asymptotic expressions ([21, §9.7])

$$\mathrm{Ai}(z) = \frac{e^{-\zeta}}{2\sqrt{\pi} z^{\frac{1}{4}}} \left(1 + \mathcal{O}(\zeta^{-1})\right), \text{ and} \tag{4.66a}$$

$$\mathrm{Ai}'(z) = -\frac{e^{-\zeta} z^{\frac{1}{4}}}{2\sqrt{\pi}} \left(1 + \mathcal{O}(\zeta^{-1})\right), \tag{4.66b}$$

where $\zeta = \frac{2}{3} z^{\frac{3}{2}}$, valid uniformly for $|\arg(z)| \leq \pi - \delta$ with $\delta > 0$. Upon substituting the above expressions into Eq. (4.55) for $x < x_c$, we recover Eq. (4.54a). Hence, the asymptotic expression holds uniformly for $x \in [x_1, x_2]$, where $0 < x_1 < \frac{1}{4}$ and $x_2 > \frac{1}{4}$, if $x_2 - \frac{1}{4}$ is sufficiently small (we did not prove that α stays nonzero for $x > \frac{1}{4}$).

□

If Eq. (4.55) is valid in the interval $[\frac{1}{4}, x_2]$, then upon substituting asymptotic expressions for $\mathrm{Ai}(z)$ and $\mathrm{Ai}'(z)$ valid for $z \to -\infty$, Eq. (4.54b) needs to be recovered. With this argument, the region of validity of Theorem 4.7.1 can be extended further. This way of continuing uniform asymptotic expansions was examined in [72].

4.8 Uniform asymptotics and scaling function of $G(x,q)$

With Theorem 4.7.1 we obtain an asymptotic expression for $G(x,q)$.

Theorem 4.8.1. *For $0 < x \leq \frac{1}{4}$ and $q = e^{-\epsilon} \to 1^-$,*

$$G(x,q) = \left(\frac{z_+^{\frac{1}{2}} + z_-^{\frac{1}{2}}}{z_+^{\frac{3}{2}} + z_-^{\frac{3}{2}}}\right) \left(\frac{1 + \left(\frac{z_-^{\frac{1}{2}} - z_+^{\frac{1}{2}}}{z_-^{\frac{1}{2}} + z_+^{\frac{1}{2}}}\right) \epsilon^{\frac{1}{3}} \alpha^{-\frac{1}{2}} F\left(\alpha \epsilon^{-\frac{2}{3}}\right)}{1 + \left(\frac{z_-^{\frac{3}{2}} - z_+^{\frac{3}{2}}}{z_-^{\frac{3}{2}} + z_+^{\frac{3}{2}}}\right) \epsilon^{\frac{1}{3}} \alpha^{-\frac{1}{2}} F\left(\alpha \epsilon^{-\frac{2}{3}}\right)}\right) (1 + \mathcal{O}(\epsilon)) \tag{4.67}$$

uniformly for $x \in [x_1, x_c]$ if $0 < x_1 < x_c$, where α is defined in Eq. (4.56),

$$\left.\begin{aligned} z_+ &= \tfrac{1}{2}(1 + \sqrt{1-4x}) \\ z_- &= \tfrac{1}{2}(1 - \sqrt{1-4x}) \end{aligned}\right\},$$

and $F(s) = \frac{d}{ds} \ln(\mathrm{Ai}(s))$.

Proof. This follows directly from inserting Eq. (4.55) with $k = 0$ and $k = 1$ into Eq. (4.12) and simplifying the obtained expression.

□

In Fig. 4.8, the numerical approximation of $G(x,q)$ obtained from taking a finite convergent of the continued fraction Eq. (4.9) and the asymptotic expression (4.67) are plotted as functions of x for different values of ϵ. The picture shows the close agreement of the two curves.

From Theorem 4.8.1, we obtain the scaling behaviour of $G(x,q)$ around the tricritical point $(x,q) = (\frac{1}{4}, 1)$.

Corollary 4.8.1. *Let $s \in (s_1, \infty)$, where $s_1 \approx -2.34$ denotes the largest*

zero of the Airy function. Then for $x = \frac{1}{4}(1 - s\epsilon^{\frac{2}{3}})$ *and* $q = e^{-\epsilon} \to 1^-$,

$$G(x,q) = 2\left(1 + \frac{\mathrm{Ai}'(s)}{\mathrm{Ai}(s)}\epsilon^{\frac{1}{3}} + \left(\frac{3}{2}\left(\frac{\mathrm{Ai}'(s)}{\mathrm{Ai}(s)}\right)^2 - \frac{s}{2}\right)\epsilon^{\frac{2}{3}} + \mathcal{O}(\epsilon)\right). \quad (4.68)$$

Proof. This follows from substituting $x = \frac{1}{4}(1 - s\epsilon^{\frac{2}{3}})$ into Eq. (4.67) and using that $\alpha \sim 1 - 4x$ for $x \to \frac{1}{4}$. The asymptotic expression holds for all s for which $F(s) < \infty$, hence if $\mathrm{Ai}(s) \neq 0$. □

As mentioned before, in Chapter 3, a different parametrisation of Dyck paths was used, therefore different parameters of the scaling function were obtained there. The generating function considered here is related to the one considered in Chapter 3 by the relation $G(x,q) = G^{(\infty)}\big(\sqrt{x/q}, \sqrt{q}\big)$. One verifies that both expressions are equivalent by substituting $x \to qx^2$ and $q \to q^2$ into the result derived in Subsection 3.5.1. In this way, we validate the result from the heuristic scaling ansatz given in Section 3.3 for the case of Dyck paths.

In the following chapter, we will generalise our analysis of $\phi(q^k x)$ to a wider class of q-hypergeometric series which appear in the generating functions of other two-dimensional lattice models.

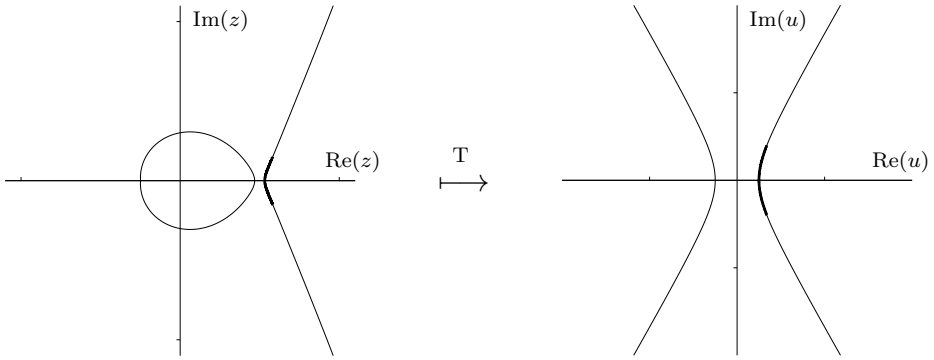

(a) $0 < x < \frac{1}{4}$

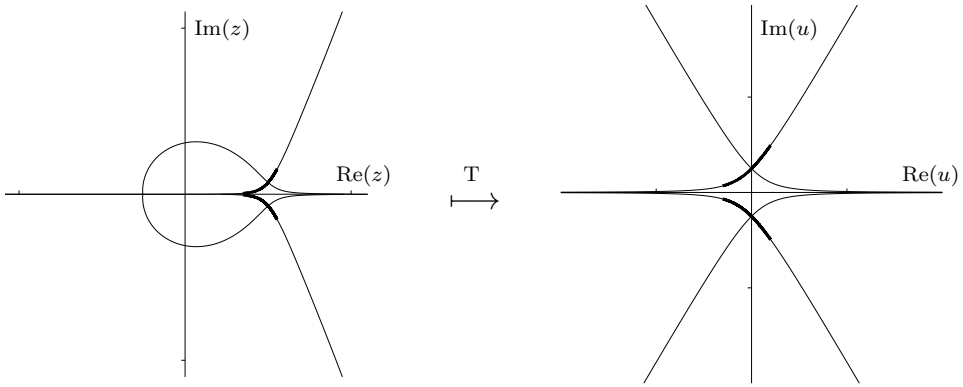

(b) $x > \frac{1}{4}$

Figure 4.7: Illustration of the mapping T defined by Eq. (4.60) in the subcritical case (a) and supercritical case (b). The bold segments of the integration contour C in the z-plane (left) are mapped onto the bold segments of the paths of steepest descents of $p(u) = \frac{u^3}{3} - \alpha u + \beta$.

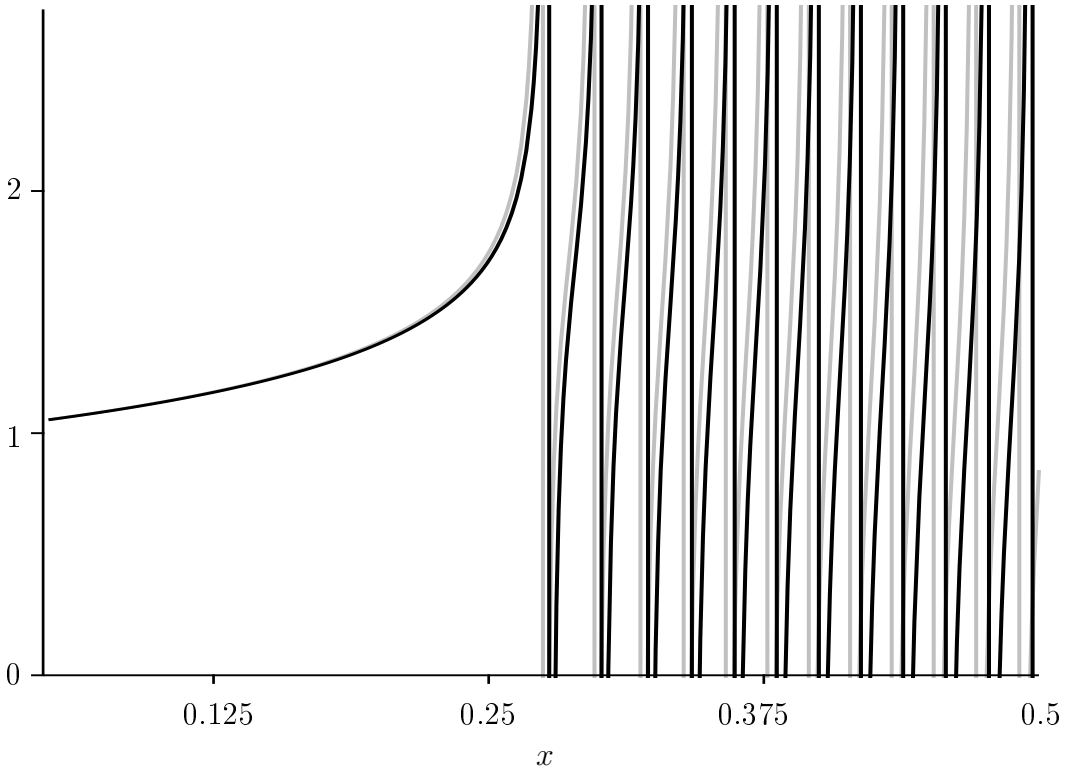

Figure 4.8: Plot of $G(x, q)$ (black) against the uniform asymptotic expression (4.67) (grey) for $\epsilon = 10^{-2}$ and x ranging between 0.05 and $\frac{1}{2}$.

5 General q-hypergeometric series

5.1 Introduction

In this chapter, which consists of joint work with Thomas Prellberg, we are going to derive general results on q-hypergeometric series, which will be used in the following chapters, and which generalise the results from Chapter 4. We will begin by giving the basic definitions, before deriving the functional equation satisfied by a q-hypergeometric series. For a certain range of parameters, we will then obtain a contour integral expression which will be the starting point for the asymptotic analysis carried out in the subsequent chapters.

In the following, we will write $(a_j)_{j=1}^n$ for a sequence of n values a_j. In the case $n = 0$, $(a_j)_{i=1}^n$ is the empty sequence, denoted by $-$. For a given set S, we write $(a_j)_{j=1}^n \in S$ if $a_j \in S$ for all $j \in [n]$. Here, $[n]$ denotes the set $\{1, 2, \ldots, n\}$.

5.2 Basic definitions and notation

Recall the definition (4.17) of the q-Pochhammer symbol. The general q-hypergeometric series is defined as follows.

Definition 5.2.1 ([31]). *For $r, s \in \mathbb{Z}_{\geq 0}$, complex $(a_k)_{k=1}^r$,$(b_k)_{k=1}^s$, $q \neq 0$, and such that for all $k \in [s]$ and $n \in \mathbb{Z}_{\geq 0}$, $b_k \neq q^{-n}$ and $q^n \neq 1$, the general*

q-hypergeometric series is defined as

$$ {}_r\phi_s\left(\begin{matrix}(a_k)_{k=1}^r\\(b_k)_{k=1}^s\end{matrix};q,x\right)=\sum_{n=0}^{\infty}\left(\frac{\prod_{i=1}^r(a_i;q)_n}{\prod_{j=1}^s(b_j;q)_n}\right)\frac{x^n\left((-1)^nq^{\binom{n}{2}}\right)^{1+s-r}}{(q;q)_n}. \quad (5.1) $$

Remark. The series defined in Eq. (5.1) is seen as a formal object and not necessarily convergent. For $|q|<1$, it converges absolutely for all $x\in\mathbb{C}$ if $r<s+1$ and for all $x\in\mathbb{C}$ with $|x|<1$ if $r=s+1$.

To save space we also occasionally write ${}_r\phi_s((a_k)_{k=1}^r;(b_k)_{k=1}^s;q,s)$ for the series defined in Eq. (5.1).

The fraction

$$ \Phi(x)=\frac{\phi(qx)}{\phi(x)}, \quad (5.2) $$

where

$$ \phi(x)={}_r\phi_s\left(\begin{matrix}(a_k)_{k=1}^r\\(b_k)_{k=1}^s\end{matrix};q,(-1)^{s-r}x\right) \quad (5.3) $$

occurs in the generating functions of many combinatorial lattice models; the case $r=0,s=1$ and $b_1=0$ was considered in Chapter 4.

In the next section, we will first derive the functional equation satisfied by $\phi(x)$, before discussing its asymptotic behaviour in the limit $q\to1^-$, if the parameters $(a_i)_{i=1}^r,(b_j)_{j=1}^s$ and x satisfy certain conditions.

5.3 Functional equation for $\phi(x)$ and $\Phi(x)$

For $q\in\mathbb{C}$, we define the operator $\sigma:\phi(x)\mapsto\phi(qx)$, and prove the following.

Lemma 5.3.1. *Assume that the parameters of $\phi(x)$ satisfy the condi-*

tions given in Definition 5.2.1. Then it satisfies the functional equation

$$\left[x\left(\prod_{i=1}^{r} 1-a_i\sigma\right)\sigma^{1+s-r}+\left(\prod_{j=1}^{s} 1-\frac{b_j}{q}\sigma\right)(1-\sigma)\right]\phi(x)=0. \tag{5.4}$$

Proof. We define, for $n \in \mathbb{Z}_{\geq 0}$,

$$c_n=(-1)^n\left(\frac{\prod_{i=1}^{r}(a_i;q)_n}{\prod_{j=1}^{s}(b_j;q)_n}\right)\frac{q^{\binom{n}{2}(1+s-r)}}{(q;q)_n}. \tag{5.5}$$

Thus,

$$\phi(x)=\sum_{n=0}^{\infty} c_n x^n=\sum_{n=1}^{\infty} c_{n-1}x^{n-1}. \tag{5.6}$$

From Eq. (5.5), we obtain that, for $n \in \mathbb{N}$,

$$c_n=-\left(\frac{\prod_{i=1}^{r}(1-a_iq^{n-1})}{\prod_{j=1}^{s}(1-b_jq^{n-1})}\right)\frac{q^{(n-1)(1+s-r)}}{1-q^n}c_{n-1}. \tag{5.7}$$

Inserting Eq. (5.7) into Eq. (5.6), we get

$$\begin{aligned}\phi(x)&=c_0+\sum_{n=1}^{\infty} c_n x^n\\&=c_0-\sum_{n=1}^{\infty}\left(\frac{\prod_{i=1}^{r}(1-a_iq^{n-1})}{\prod_{j=1}^{s}(1-b_jq^{n-1})}\right)\frac{q^{(n-1)(1+s-r)}}{1-q^n}c_{n-1}x^n.\end{aligned} \tag{5.8}$$

From Eq. (5.8) one verifies that

$$\begin{aligned}
&\left(\prod_{j=1}^{s} 1-\frac{b_j}{q}\sigma\right)(1-\sigma)\phi(x)\\
=&-\sum_{n=1}^{\infty}\left(\prod_{i=1}^{r} 1-a_iq^{n-1}\right)q^{(n-1)(1+s-r)}c_{n-1}x^n\\
=&-\sum_{n=1}^{\infty}x\left(\prod_{i=1}^{r} 1-a_iq^{n-1}\right)q^{(n-1)(1+s-r)}c_{n-1}x^{n-1}\\
=&-x\left(\prod_{i=1}^{r} 1-a_i\sigma\right)\sigma^{1+s-r}\phi(x).
\end{aligned}$$

Hence we obtain Eq. (5.4). □

Defining for given $(a_j)_{j=1}^r$ and $(b_j)_{j=1}^s$, $k\in[r]$ and $n\in[s]$,

$$\alpha_k=(-1)^k\sum_{S\in[r]^k}\prod_{j\in S}a_j \text{ and } \beta_k=\frac{(-1)^k}{q^k}\sum_{S\in[s]^k}\prod_{j\in S}b_j, \tag{5.9}$$

where, for $m,n\in\mathbb{Z}_{\geq 0}$, $[n]^m$ is the set of m-subsets of $[n]$, we can rewrite Eq. (5.4) as

$$\left[x\sum_{k=0}^{r}\alpha_k\sigma^{1+s-r+k}+\sum_{k=0}^{s}\beta_k\sigma^k(1-\sigma)\right]\phi(x)=0. \tag{5.10}$$

If we substitute

$$\phi(q^nx)=\phi(x)\prod_{j=0}^{n-1}\Phi(q^jx) \tag{5.11}$$

into Eq. (5.10), then we obtain the following Corollary.

Corollary 5.3.1. *The function $\Phi(x)$ satisfies the functional equation*

$$x\sum_{k=0}^{r}\left[\alpha_k\left(\prod_{j=0}^{s-r+k}\Phi(q^jx)\right)\right]+\sum_{k=0}^{s}\left[\beta_k\left(\prod_{j=0}^{k-1}\Phi(q^jx)\right)\left(1-\Phi(q^kx)\right)\right]=0. \tag{5.12}$$

In the limit $q \to 1^-$, Eq. (5.12) yields

$$x \sum_{k=0}^{r} \alpha_k \Phi(x)^{1+s-r+k} + \sum_{k=0}^{s} \beta_k \Phi(x)^k \big(1 - \Phi(x)\big) = 0. \tag{5.13}$$

Our aim is to analyse the function $\phi(x)$ asymptotically in the limit $q \to 1^-$. To this purpose, we will first derive a contour integral representation for $\phi(x)$.

5.4 Contour integral representation of $\phi(x)$

The following result is a generalisation of Lemma 4.5.2.

Lemma 5.4.1. *Let $r, s \in \mathbb{Z}_{\geq 0}$, $r \leq s+1$, $0 < q < 1$, $x \in \mathbb{C} \setminus \{0\}$, $|x| < 1$ if $r = s+1$, and $(a_i)_{i=1}^r \in (-\infty, 1)$. Then,*

$$\phi(x) = \lim_{N \to \infty} \frac{A}{2\pi i} \int_{C_N} \left(\frac{\prod_{j=1}^{s} (b_j/z; q)_\infty}{\prod_{i=1}^{r} (a_i/z; q)_\infty} \right) \frac{z^{\frac{s-r}{2}(\log_q(z)+1) - \log_q(x)}}{(z; q)_\infty} dz, \tag{5.14}$$

where for $N \in \mathbb{Z}_{\geq 0}$, the contour C_N is defined in Eq. (5.16), with $\max\left((a_i)_{i=1}^r, 0\right) < \rho < 1$, $\psi, \varphi \in (0, \pi)$, and

$$A = (q; q)_\infty \frac{\prod_{i=1}^{r} (a_i; q)_\infty}{\prod_{j=1}^{s} (b_j; q)_\infty}. \tag{5.15}$$

Proof. Let the parameters of $\phi(x)$ satisfy the conditions of the lemma. This ensures that the series converges.

Define for $N \in \mathbb{N}$ the contour $C_N : [-1, 2) \mapsto \mathbb{C}$,

$$C_N(t) = \begin{cases} \rho - t(q^{-N+\frac{1}{2}} - \rho)e^{-i\psi} & \text{for } t \in [-1, 0), \\ \rho + t(q^{-N+\frac{1}{2}} - \rho)e^{i\varphi} & \text{for } t \in [0, 1), \\ \rho + (q^{-N+\frac{1}{2}} - \rho)e^{i[\varphi-(\psi+\varphi)(t-1)]} & \text{for } t \in [1, 2), \end{cases} \tag{5.16}$$

where $\max\left((a_i)_{i=1}^r, 0\right) < \rho < 1$ and $\varphi, \psi \in (0, \pi)$. This contour surrounds exactly the N leftmost poles of $(z; q)_\infty^{-1}$, which are located at $z = q^{-n}$ with $n \in \mathbb{Z}_{\geq 0}$ – see Fig. 4.3 for the case $N = 1$.

Now we define the function

$$h(z) = A \left(\frac{\prod_{j=1}^s (b_j/z; q)_\infty}{\prod_{i=1}^r (a_i/z; q)_\infty} \right) z^{\frac{s-r}{2}(\log_q(z)+1)-\log_q(x)}, \tag{5.17}$$

where A is given by Eq. (5.15). Under the assumptions made, this function is analytic inside the region surrounded by C_N for arbitrary N. Therefore,

$$\frac{1}{2\pi i} \oint_{C_N} \frac{h(z)}{(z; q)_\infty} dz = \sum_{n=0}^{N-1} h(q^{-n}) \operatorname{Res}\left((z; q)_\infty^{-1} \, ; \, z = q^{-n} \right). \tag{5.18}$$

For $n \in \mathbb{Z}_{\geq 0}$, we have

$$\begin{aligned} h(q^{-n}) &= A \left(\frac{\prod_{j=1}^s (b_j q^n; q)_\infty}{\prod_{i=1}^r (a_i q^n; q)_\infty} \right) q^{\binom{n}{2}(s-r)} x^n \\ &= (q; q)_\infty \left(\frac{\prod_{i=1}^r (a_i; q)_n}{\prod_{j=1}^s (b_j; q)_n} \right) q^{\binom{n}{2}(s-r)} x^n, \end{aligned}$$

Together with Lemma 4.5.1, we obtain for $N \in \mathbb{N}$,

$$\frac{1}{2\pi i} \oint_{C_N} \frac{h(z)}{(z; q)_\infty} dz = \sum_{n=0}^{N-1} \left(\frac{\prod_{i=1}^r (a_i; q)_n}{\prod_{j=1}^s (b_j; q)_n} \right) \frac{(-x)^n}{(q; q)_n} q^{\binom{n}{2}(1+s-r)}, \tag{5.19}$$

where the integration on the LHS is performed once clockwise, which is to

be accounted for by a factor of -1. Taking the limit $N \to \infty$, we obtain Eq. (5.14).

□

Due to the limit occurring in Eq. (5.14), Lemma 5.4.1 does not yet give an integral representation which we can use to analyse $\phi(x)$ asymptotically. The following proposition states that there is a limiting contour C, such that C_N can be replaced by C in the limit $N \to \infty$. This generalises Prop. 4.5.1.

Proposition 5.4.1. *Assume the parameters of $\phi(x)$ satisfy the conditions of Lemma 5.4.1. Then,*

$$\phi(x) = \frac{A}{2\pi i} \int_C \left(\frac{\prod_{j=1}^{s} (b_j/z;q)_\infty}{\prod_{i=1}^{r} (a_i/z;q)_\infty} \right) \frac{z^{\frac{s-r}{2}(\log_q(z)+1)-\log_q(x)}}{(z;q)_\infty} dz, \tag{5.20}$$

where the contour C is defined in Eq. (5.21), with $\max\left((a_i)_{i=1}^r, 0\right) < \rho < 1$, $\psi, \varphi \in (0,\pi)$ and A is given by Eq. (5.15).

Proof. We need to show that in the limit $N \to \infty$, the contribution of the circle segment $C_N([1,2))$ to the contour integral (5.19) vanishes. If this is the case, then in the limit $N \to \infty$, C_N can be replaced by the contour C, defined as

$$C(t) = \begin{cases} \rho - te^{-i\psi} & \text{for } t < 0, \\ \rho + te^{i\varphi} & \text{for } t \geq 0, \end{cases} \tag{5.21}$$

where $\max\left((a_i)_{i=1}^r, 0\right) < \rho < 1$ and $\varphi, \psi \in (0,\pi)$ – see Fig. 4.4.

Assume $z \in C([1,2))$, hence, $z = \rho + (q^{-N+\frac{1}{2}} - \rho)e^{i\theta}$, where $\theta \in (-\psi, \varphi]$.

Then for $N \to \infty$,

$$\log_q(z) = -N + \frac{1}{2} - \frac{i\theta}{\epsilon} + o(1),$$

where $\epsilon = -\ln(q)$. Therefore in this limit,

$$\begin{aligned} & \log_q\left(z^{(s-r)(1+\log_q(z))/2-\log_q(x)}\right) \\ = & \left(-N + \frac{1}{2} - \frac{i\theta}{\epsilon}\right)\left(\frac{s-r}{2}\left(-N + \frac{3}{2} - \frac{i\theta}{\epsilon}\right) + \frac{\ln(x)}{\epsilon}\right) + o(1) \\ = & \left(\frac{s-r}{2}\right)N^2 - \left(s - r + \frac{\ln(x) + i\theta(r-s)}{\epsilon}\right)N + \mathcal{O}(1). \end{aligned} \tag{5.22}$$

Note that

$$\lim_{N\to\infty} \frac{\prod_{j=1}^{s}(b_j/z;q)_\infty}{\prod_{i=1}^{r}(a_i/z;q)_\infty} = 1. \tag{5.23}$$

Using Eqs. (5.22) and (5.23) together with Eq. (4.29), we get

$$\left|\frac{h(z)}{(z;q)_\infty}\right| \leq b\, q^{\frac{1+s-r}{2}N^2-(s-r)N}|x|^N,$$

with an N-independent constant $b > 0$. Taking the integral over $C_N([1,2))$ leads to a further factor of q^{-N}. We obtain the estimation

$$\frac{1}{2\pi i}\int_{C_N([1,2))}\left|\frac{h(z)}{(z;q)_\infty}\right| dz \leq b(\varphi+\psi)\, q^{\frac{1+s-r}{2}N^2-(1+s-r)N}|x|^N, \tag{5.24}$$

For $N \to \infty$, the RHS of Eq. (5.24) tends to 0 for all complex x if $r < s+1$ and for $|x| < 1$ if $r = s+1$. With this we conclude that in the limit $N \to \infty$, the contour C_N can be replaced by C. □

Now we are ready to prove the following lemma, which is the starting point of the asymptotic analysis of $\phi(x)$ by means of the saddle point method.

Lemma 5.4.2. *Assume* $r \leq s+1$, $0 < q = e^{-\epsilon} < 1$, $k \in \mathbb{Z}$, $x \in \mathbb{C}$, $(a_i)_{i=1}^r, (b_j)_{j=1}^s \in (-\infty, 1)$, *and* $|x| < |q^{-k}|$ *if* $r = s+1$. *Then,*

$$\phi(q^k x) = \frac{A}{2\pi i}\left(\int_C \exp\left(\frac{1}{\epsilon}f(z)\right) g_k(z,q)dz\right), \tag{5.25}$$

where the contour C *is defined in Eq. (5.21) with* $\max((a_i)_{i=1}^r, (b_j)_{j=1}^s, 0) < \rho < 1$ *and* $\psi, \varphi \in (0, \pi)$, A *is defined in Eq. (5.15),*

$$\begin{aligned} f(z) &= \ln(x)\ln(z) + \mathrm{Li}_2(z) - \frac{s-r}{2}\ln(z)^2 + \\ &\quad + \sum_{i=1}^r \mathrm{Li}_2\left(\frac{a_i}{z}\right) - \sum_{j=1}^s \mathrm{Li}_2\left(\frac{b_j}{z}\right), \end{aligned} \tag{5.26}$$

$$g_k(z,q) = \frac{1}{z^k}\left(\frac{1}{1-z}\frac{\prod_{j=1}^s (z-b_j)}{\prod_{i=1}^r (z-a_i)}\right)^{\frac{1}{2}} \exp\big(\epsilon S(z,q)\big), \tag{5.27}$$

and

$$S(z,q) = R_1(z,q) + \sum_{i=1}^r R_1\Big(\frac{a_i}{z}, q\Big) - \sum_{j=1}^s R_1\Big(\frac{b_j}{z}, q\Big), \tag{5.28}$$

with R_1 *defined in Eq. (4.41).*

Proof. With the definitions of the functions f and g_k in Eqs. (5.26) and (5.27), this follows directly from Prop. 5.4.1. □

5.5 Saddle point landscape of the kernel $f(z)$

We will begin this section with a discussion of the asymptotic properties of the function f defined in Eq. (5.26), thereby generalising Lemma 4.6.2. The results from this discussion will be used to gain insights into how the contours of steepest descent of the function $\mathcal{R}(z) = \mathrm{Re}(f(z))$ originating from the saddle points of f lie in the complex plane.

Lemma 5.5.1. *Assume* $r, s \in \mathbb{Z}_{\geq 0}$, $x \in \mathbb{C} \setminus \{0\}$, $(a_i)_{i=0}^r, (b_j)_{j=0}^s \in \mathbb{C}$ *and*

$\varphi \in (-\pi, \pi)$. *Then we have the following:*

(i) *For* $\lambda \to \infty$,

$$f(\lambda e^{i\varphi}) = -\frac{\ell}{2}\ln(\lambda)^2 + (\ln(x) - i\gamma)\ln(\lambda) + \mathcal{O}(1), \tag{5.29}$$

uniformly with respect to φ, *where* $\ell = s - r + 1$ *and* $\gamma = \ell\varphi \pm \pi$ *for* $\varphi \lessgtr 0$.

(ii) *For* $\lambda \to 0$,

$$f(\lambda e^{i\varphi}) = -\frac{s_0 - r_0}{2}\ln(\lambda)^2 + \left[\ln\left(x\left|\frac{\prod_{a_i\neq 0} a_i}{\prod_{b_j\neq 0} b_j}\right|\right) + \right.$$
$$\left. + i\left(\sum_{a_i\neq 0}\alpha_i - \sum_{b_j\neq 0}\beta_j - (s-r)\varphi\right)\right]\ln(\lambda) + \mathcal{O}(1), \tag{5.30}$$

uniformly with respect to φ, *where* $\alpha_i = \arg(-a_i e^{-i\varphi})$ *for* $i \in [r]$, $\beta_j = \arg(-b_j e^{-i\varphi})$ *for* $j \in [s]$, *and* r_0 *and* s_0 *are the number of zeros in* $(a_i)_{i=0}^{\infty}$ *and* $(b_j)_{j=0}^{\infty}$, *respectively.*

Proof. We assume $(a_i)_{i=0}^{r}, (b_j)_{j=0}^{s} \in \mathbb{C}$, $x \in \mathbb{C}\setminus\{0\}$ and $\varphi \in (-\pi, \pi)$.

(i) Let $z = \lambda e^{i\varphi}$, where $\lambda > 0$ and $0 < |\varphi| < \pi$. First note that it follows from Eq. (4.48) that for $\lambda \to \infty$,

$$\sum_{i=1}^{r}\mathrm{Li}_2\left(\frac{a_i}{\lambda}e^{-i\varphi}\right) - \sum_{j=1}^{s}\mathrm{Li}_2\left(\frac{b_j}{\lambda}e^{-i\varphi}\right) = \mathcal{O}\left(\frac{1}{\lambda}\right), \tag{5.31}$$

where the convergence is uniform for all $\varphi \in (-\pi, \pi)$. Inserting the above equation and Eq. (4.46) into Eq. (5.26), we get in the same

limit,

$$\begin{aligned} f\left(\lambda e^{i\varphi}\right) = & -\frac{s-r}{2}\ln(\lambda e^{i\varphi})^2 + \ln(x)\ln(\lambda e^{i\varphi}) - \frac{1}{2}\ln(\lambda)^2 - \\ & - i\psi\ln(\lambda) - \frac{\pi^2 - 3\psi^2}{6} + \mathcal{O}\left(\frac{1}{\lambda}\right) \\ = & -\frac{s-r+1}{2}\ln(\lambda)^2 + \\ & + \left(\ln(x) - i((s-r)\varphi + \psi)\right)\ln(\lambda) + \mathcal{O}(1). \end{aligned}$$

with $\psi = \varphi \pm \pi$ for $\varphi \lessgtr 0$ and where $R(\lambda, \varphi) \to 0$ uniformly for all $\varphi \in (-\pi, \pi)$. This concludes the proof of the first part.

(ii) From Lemma 4.6.1 we have for $a \in \mathbb{C} \setminus \{0\}$, $\lambda \to 0$ and $\varphi \in (-\pi, \pi)$,

$$\mathrm{Li}_2\left(\frac{a}{\lambda}e^{-i\varphi}\right) = -\frac{1}{2}\ln(\lambda)^2 + (\ln(|a|) + i\alpha)\ln(\lambda) + \mathcal{O}(1), \quad (5.32)$$

uniformly with respect to φ, where $\alpha = \arg(-ae^{-i\varphi})$. Inserting the above expression into Eq. (5.26), we obtain

$$\begin{aligned} f(\lambda e^{i\varphi}) = & -\frac{s-r}{2}\ln(\lambda e^{i\varphi})^2 + \ln(x)\ln(\lambda e^{i\varphi}) + \\ & + \sum_{a_i \neq 0}\left(-\frac{1}{2}\ln(\lambda)^2 + (\ln(|a_i|) + i\alpha_i)\ln(\lambda)\right) - \\ & - \sum_{b_j \neq 0}\left(-\frac{1}{2}\ln(\lambda)^2 + (\ln(|b_j|) + i\beta_j)\ln(\lambda)\right) + \mathcal{O}(1) \\ = & -\frac{s_0 - r_0}{2}\ln(\lambda)^2 + \left[\ln\left(x\left|\frac{\prod_{a_i\neq 0} a_i}{\prod_{b_j \neq 0} b_j}\right|\right) + \right. \\ & \left. + i\left(\sum_{\alpha_i \neq 0}\alpha_i - \sum_{\beta_j \neq 0}\beta_j\right)\right]\ln(\lambda) + \mathcal{O}(1), \end{aligned}$$

where $\alpha_i = \arg(-a_i e^{-i\varphi})$ for $i \in [r]$ and $\beta_j = \arg(-b_j e^{-i\varphi})$ for $j \in [s]$, and r_0 and s_0 are the numbers of zeros in $(a_i)_{i=0}^r$ and $(b_j)_{j=0}^s$,

respectively. This leads to the assertion.

□

Concerning the location of the saddle points, we have the following two lemmas. Note that in the following, the function h is not the one used above.

Lemma 5.5.2. *Let* $r, s \in \mathbb{Z}_{\geq 0}$, $(a_i)_{i=1}^r, (b_j)_{j=1}^s \in \mathbb{C}$, $x \in \mathbb{C} \setminus \{0\}$ *and* $z \in \mathbb{C} \setminus \left(\{0\} \cup_{i=1}^r \{a_i\} \cup_{j=1}^s \{b_j\}\right)$. *If* $f'(z) = 0$, *then*

$$\chi(z) = x \left(\prod_{i=1}^{r} z - a_i \right) - \left(\prod_{j=1}^{s} z - b_j \right) (1 - z) = 0. \tag{5.33}$$

Proof. It can be assumed without loss of generality that $a_i \neq b_j$ for all $(i, j) \in [r] \times [s]$. Taking the derivative of Eq. (5.26), we get

$$\begin{aligned} f'(z) \ &= \frac{1}{z} \Bigg(\ln(x) + \sum_{i=1}^{r} \ln\left(1 - \frac{a_i}{z}\right) - \sum_{j=1}^{s} \ln\left(1 - \frac{b_j}{z}\right) \\ &\quad - (s - r)\ln(z) - \ln(1 - z) \Bigg). \end{aligned} \tag{5.34}$$

The RHS of the last expression evaluates to zero if

$$\frac{1}{z} \ln\left(\frac{x}{z^{s-r}(1-z)} \frac{\prod_{i=1}^{r}(1 - \frac{a_i}{z})}{\prod_{j=1}^{s}(1 - \frac{b_j}{z})} \right) = \frac{1}{z} \ln\left(\frac{x}{1-z} \frac{\prod_{i=1}^{r}(z - a_i)}{\prod_{j=1}^{s}(z - b_j)} \right) = 0,$$

and this is the case if and only if the argument of the logarithm equals one, which is when Eq. (5.33) is satisfied. □

For $z \neq 0$, Eq. (5.33) can be rewritten as

$$x \sum_{k=0}^{r} \frac{\alpha_k}{z^{1+s-r+k}} + \sum_{k=0}^{s} \frac{\beta_k}{z^k} \left(1 - \frac{1}{z}\right) = 0, \tag{5.35}$$

where the $(\alpha_j)_{j=0}^r$ and $(\beta_j)_{j=0}^s$ are defined in Eq. (5.9) with $q = 1$. Comparing this equation with Eq. (5.13), we see that for $q = 1$, $\Phi(x)$ is equal to the inverse of a saddle point of $f(z)$.

Lemma 5.5.3. *Let $r, s \in \mathbb{Z}_{\geq 0}$, $(a_i)_{i=1}^r, (b_j)_{j=1}^s \in (-\infty, 1)$, and define $\mu = \max((a_i)_{i=1}^r, (b_j)_{j=1}^s, 0)$, with $\max(-) = -\infty$. Then we have the following:*

(i) *If $\mu = \max((a_i)_{i=1}^r)$, then for all $x > 0$, there exists a point $z_1 \in (\mu, 1)$ with $f'(z_1) = 0$ and this point is a local minimum of $f(z)$ on the real line.*

(ii) *If $\mu = \max((b_j)_{j=1}^s, 0)$, then there exists a value $x_c > 0$ such that for all $0 < x < x_c$, there exist two points $z_1, z_2 \in (\mu, 1)$ with $z_1 < z_2$, $f'(z_1) = f'(z_2) = 0$, and where z_1 is a local maximum and z_2 is a local minimum of f on the real line. For $x = x_c$, there exists a point z_c with $f'(z_c) = f''(z_c) = 0$ and for all $x > x_c$, $f'(z) \neq 0$ for all $z \in (\mu, 1)$.*

Proof. Assume the parameters satisfy the conditions stated in the lemma. Note that it follows from the definition of f that one can assume without loss of generality that $a_i \neq b_j$ for all $i \in [r]$ and $j \in [s]$. Define the value μ as in the statement of the lemma. For $z \in (\mu, 1)$, $f'(z)$ is real and $f'(z) = 0$ if and only if Eq. (5.33) is satisfied. For $x = 0$, we have

$$\chi(z) = \left(\prod_{j=1}^{s} z - b_j \right) (z - 1) \,, \tag{5.36}$$

thus in that case $\chi(z)$ has zeros at $z = 1$ and $z = b_j < 1$, where $j \in [s]$. Since $z = 1$ is a simple zero and the leading coefficient of $\chi(z)$ is positive, $\chi(z)$ changes from negative to positive at $z = 1$ and is negative for $z \in$

$(\max((b_j)_{j=1}^s, 1)$. For arbitrary x, the derivative of $\chi(z)$ with respect to x is

$$\frac{\partial}{\partial x}\chi(z) = \prod_{i=1}^{r}(z - a_i). \tag{5.37}$$

Now we distinguish the cases $\mu = \max((a_i)_{i=1}^r)$ and $\mu = \max((b_j)_{j=1}^s, 0)$.

(i) If $\mu = \max((a_i)_{i=1}^r)$ (implying that $r > 0$), then according to Eq. (5.34),

$$\lim_{z\to\mu^+} f'(z) = -\infty \text{ and } \lim_{z\to 1^-} f'(z) = \infty.$$

Since $f'(z)$ is continuous in $(\mu, 1)$, we conclude that there exists a z_1 in $(\mu, 1)$ with $f'(z_1) = 0$, at which $f'(z_1)$ changes from negative to positive. Hence z_1 is a local minimum of f on the real line.

(ii) If $\mu = \max((b_j)_{j=1}^s, 0)$, then the RHS of Eq. (5.37) is positive for $z \in (\mu, 1)$, hence there is a $c_1 > 0$ such that $\frac{\partial}{\partial x}\chi(z) > c_1$ for all $z \in (\mu, 1)$. If we choose a $c_2 > 0$ such that $\max\left\{(1 - z)\prod_{j=1}^s(z - b_j) \,|\, z \in (\mu, 1)\right\} < c_2$, then

$$\chi(z) \geq xc_1 - c_2. \tag{5.38}$$

Now we define

$$m(x) = \inf\left\{\chi(z) \,\middle|\, z \in (\mu, 1)\right\}.$$

From Eq. (5.38) we know that $\chi(z) \geq 0$ for all $z \in (\mu, 1)$ if $x > c_2/c_1$, hence the set $\left\{x > 0 \,\middle|\, m(x) \leq 0\right\}$ has a supremum. Since for all $x > 0$, $\chi(\mu) > 0$ and $\chi(1) > 0$, it follows from the intermediate value theorem that if $m(x) < 0$, then there are at least two values z_1, z_2

with $\chi(z_1) = \chi(z_2) = 0$ and hence $f'(z_1) = f'(z_2) = 0$. Since

$$\lim_{z\to\mu^+} f'(z) = \infty \text{ and } \lim_{z\to 1^-} f'(z) = \infty,$$

the points z_1 and z_2 can be chosen such that z_1 is a local maximum and z_2 is a local minimum of f, respectively, and $z_1 < z_2$. If $m(x) = 0$, then there exists at least one point z_c with $f'(z_c) = f''(z_c) = 0$, which is a local minimum of f on the real line. The assertion thus follows with $x_c = \sup\big\{x > 0 \,\big|\, m(x) \le 0\big\}$.

□

To analyse $\phi(x)$ asymptotically, we need to know how the paths of steepest descent and ascent of the function $\mathcal{R}(z) = \mathrm{Re}(f(z))$, originating from the saddle points of f, lie in the complex plane. We begin by observing the following.

Lemma 5.5.4. *Let $r, s \in \mathbb{Z}_{\ge 0}$, $(a_i)_{i=1}^r, (b_j)_{j=1}^s \in (-\infty, 1)$ and $x > 0$, and define the value of $f(z)$ on the real line by its limit value when the real line is approached from the upper half plane. Then we have*

$$\mathrm{Im}\big(f(z)\big) = \begin{cases} \pi\left(\sum_{b_j<z} \ln\left(\frac{b_j}{z}\right) - \sum_{a_i<z} \ln\left(\frac{a_i}{z}\right) + \ln\left(\frac{x}{|z|^{s-r}}\right)\right) & (z < 0), \\ \pi\left(\sum_{b_j>z} \ln\left(\frac{b_j}{z}\right) - \sum_{a_i>z} \ln\left(\frac{a_i}{z}\right)\right) & (0 < z < 1), \\ \pi \ln(z) & (z \ge 1). \end{cases}$$

Proof. This follows from the fact that for $z = |z|e^{i\varphi}$, $|z| > 1$ and $\varphi \to 0^+$, $\mathrm{Im}\big(\mathrm{Li}_2(z)\big) = \pi \ln(z)$. □

Using Lemma 5.5.4, we can now prove the following result.

Lemma 5.5.5. *For $r \in \mathbb{Z}_{\geq 0}, s \in \mathbb{N}$, $r < s+1$, $(a_i)_{i=1}^r \in (-\infty, 0]$ and $(b_j)_{j=1}^s \in [0,1)$, there exists a $x_c > 0$ such that for $0 < x \leq x_c$, there is a continuous and piecewise differentiable curve $C : \mathbb{R} \to \mathbb{C} \setminus \big((-\infty, \mu] \cup [1, \infty)\big)$, where $\mu = \max((b_j)_{j=1}^s)$, with $\operatorname{Im}\big(f(C(t))\big) = 0$ for all $t \in \mathbb{R}$, and*

$$\lim_{t \to \pm\infty} |C(t)| = \infty, \text{ and } \lim_{t \to \pm\infty} \arg(C(t)) = \pm\frac{\pi}{\ell},$$

where $\ell = 1 + s - r$, and $C(0) = z_0$, with $z_0 \in \big(\mu, 1\big)$ and $f'(z_0) = 0$. Moreover, for all $t \neq 0$, $\operatorname{Re}\big(f(C(t))\big) < \operatorname{Re}\big(f(z_0)\big)$, and for $t \to \pm\infty$,

$$\operatorname{Re}\big(f(C(t))\big) \sim -\frac{\ell}{2} \ln(|C(t)|)^2.$$

Proof. Assume the conditions of the lemma are satisfied and define $\mu = \max((b_j)_{j=1}^s)$. Note that for this choice of parameters, one obtains from Eq. (5.34) for $\lambda > 0$,

$$\lim_{\varphi \to \pm\pi} \operatorname{Im}\big(f'(\lambda e^{i\varphi})\big) = \pm\frac{\pi}{\lambda}\left((s-r) + \sum_{|a_i| > \lambda} 1\right). \tag{5.39}$$

From Lemma 5.5.3 it follows that there exists a $x_c > 0$ such that for $0 < x < x_c$, there are two points $z_1, z_2 \in \max(\mu, 1)$, $z_1 < z_2$, with $f'(z_1) = f'(z_2) = 0$, which are the local maximum and minimum of f on the real line, respectively, and for $x = x_c$, there is one point $z_c \in \max(\mu, 1)$ with $f'(z_c) = f''(z_c) = 0$, which is a local minimum of $f(z)$ on the real line. Because $f(z)$ is real for $z \in (\mu, 1)$ if $x > 0$, it follows that $f(z^*) = f(z)^*$, where the * denotes complex conjugation. Therefore, it is sufficient to consider the upper half plane.

Since z_1 is a local maximum of $f(z)$ on the real line, it follows from the general theory of analytic functions that there exists a path of steepest ascent of $\mathcal{R}(z) = \mathrm{Re}(f(z))$ originating from z_1 and leading into the upper half plane. We call this path P_1 in the following. On P_1, the imaginary part of f, denoted by $\mathcal{I}(z)$, is zero. Since $r < s + 1$, we see from Lemma 5.5.1 that $\mathcal{R}(z)$ tends to $-\infty$ as $|z|$ tends to ∞, and therefore P_1 cannot end at infinity. Since f is analytic for $z \notin (-\infty, \mu] \cup [1, \infty)$, it therefore necessarily ends in a point of the set $(-\infty, \mu] \cup [1, \infty)$ where f is not analytic. Since the paths of steepest ascent and descent are paths on which the imaginary part of f is constant, it follows from the fact that $\mathcal{I}(z_1) = \mathcal{I}(z_2) = 0$ for $0 < x \leq x_c$ that the imaginary part of f needs to vanish at this end point if f can be defined there as a limit value, or there needs to be a contour of vanishing imaginary part leading into the end point, in case f diverges there. The only point where f diverges is the origin $z = 0$. From Lemma 5.5.4 we see that $\mathcal{I}(z) > 0$ for $z > 1$. Therefore the possible end points of P_1 are on the line $(-\infty, 0]$ and $z = 1$.

The point z_2 is a local minimum of f on the real line and therefore for $0 < x < x_c$, there exists a path of steepest descent of $\mathcal{R}(z)$ originating from z_2, leading into the upper half plane, the tangent of which is orthogonal to the real axis at z_2. We call this path P_2. Now P_2 can either end at infinity, at 0 or on the negative real line, but not at $z = 1$, since there is a path of steepest ascent from z_2 to 1, hence $f(1) > f(z_2)$, and therefore there can be no path of steepest descent from z_2 to 1. This also implies that P_1 cannot end at $z = 1$, since this would result in an intersection with P_2, leading to a contradiction (at the point of intersection, the real part of f would have to be both smaller and greater than $\mathcal{R}(z_1)$). To determine the end point of P_2 uniquely, we distinguish the following two cases.

$\underline{r < s}$. In this case, we see from Eq. (5.39) that the imaginary part of $f'(z)$ is positive for all z slightly above the negative real axis. From this it follows that the direction of steepest descent on a point slightly above the negative real axis points away from the real axis. Therefore, a path of steepest descent cannot end on the negative real axis, and according to the discussion above, P_2 either ends at 0 or infinity, and P_1 either ends on the negative real axis or at 0. In both cases, the path P_2 then necessarily ends at infinity, since P_1 cannot intersect P_2 and because 0 cannot be the end point of both paths. An example for this case is shown in Fig. 4.5.

$\underline{r = s}$. From Eq. (5.34) we see that again, $f'(z)$ has a positive imaginary part slightly above the negative real axis if z lies between the minimum of $(a_i)_{i=1}^r$ and 0. Therefore, the path of steepest descent P_2 cannot end on that segment. If z is smaller than the minimal value of $(a_i)_{i=1}^r$, then according to Lemma 5.5.4, we have

$$\operatorname{Im}\big(f(z)\big) = \pi \ln(x).$$

From this it follows that neither P_1 nor P_2 can end at a point on the segment $z < \min(a_i)_{i=1}^r$, unless $x = 1$ and unless the end point is a saddle point, i.e. the real part of $f'(z)$ also vanishes at that point. However, we see from Eq. (5.34) that for $x = 1$,

$$\begin{aligned}\operatorname{Re}\big(f'(z)\big) =& \frac{1}{|z|}\left(\sum_{j=1}^{s} \ln\left(1+\frac{b_j}{|z|}\right)\right. \\ &\left. - \sum_{i=1}^{r} \ln\left(1+\frac{a_i}{|z|}\right) + \ln(1+|z|)\right) \quad \big(z < \min(a_i)_{i=1}^r\big).\end{aligned}$$

Since this expression is strictly positive, it necessarily follows that P_1 ends at 0 and P_2 ends at infinity. An example for this case is shown in Fig. 5.1.

In both cases, P_2 can be parametrised by a curve C as stated in the lemma, and the asymptotic properties of C follow from the asymptotic behaviour of $\mathcal{R}(z) = \mathrm{Re}(f(z))$, described in Lemma 5.5.1. Since P_2 can possibly contain further saddle points of f, the contour C may not be smooth everywhere.

□

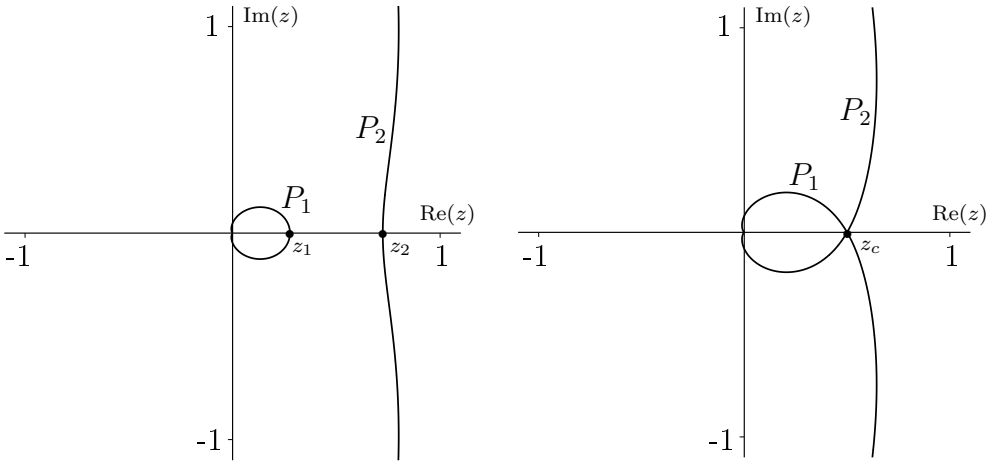

(a) $(a_j)_{j=1}^r = 0, (b_j)_{j=1}^s = \frac{1}{5}$, $x = \frac{1}{5}$ (b) $(a_j)_{j=1}^r = 0, (b_j)_{j=1}^s = \frac{1}{4}$, $x = \frac{1}{4}$

Figure 5.1: Paths of steepest descent and ascent if f satisfies the conditions with $r = s$.

Lemma 5.5.5 ensures that the integration contour C used in Eq. (5.25) can be deformed into a path of steepest descents of $\mathcal{R}(z)$, passing through a saddle point of f on the real line, if the parameters satisfy certain conditions. This makes it possible to apply the method of steepest descents to obtain the asymptotic behaviour of $\phi(q^k x)$. The case $r = s + 1$ is not included in Lemma 5.5.5. In fact, there is no path of steepest descent connecting a saddle point on the segment of the real line where f is analytic

with a point at infinity in that case. However, it is still possible to apply the method of steepest descents, since there does exist a suitable path of descent. This fact is stated in the following lemma.

Lemma 5.5.6. *For $s \in \mathbb{N}$, $r = s + 1$, $a_i = 0$ for $i \in [r]$ and $(b_j)_{j=1}^s \in [0, 1)$, there exists a $x_c > 0$ such that for $0 < x \leq x_c$ and $x < 1$, there is a continuous and piecewise differentiable curve $C : \mathbb{R} \to \mathbb{C} \setminus \big((-\infty, \mu] \cup [1, \infty)\big)$, where $\mu = \max((b_j)_{j=1}^s)$, such that*

$$\lim_{t \to \pm\infty} |C(t)| = \infty, \text{ and } \lim_{t \to \pm\infty} \arg(C(t)) = \pm\pi,$$

with $C(0) = z_0$, with $z_0 \in \big(\mu, 1\big)$ and $f'(z_0) = 0$. Moreover, for all $t \neq 0$, $\operatorname{Re}\big(f(C(t))\big) < \operatorname{Re}\big(f(z_0)\big)$, and for $t \to \pm\infty$,

$$\operatorname{Re}\big(f(C(t))\big) \sim \ln(x) \ln(|C(t)|).$$

Proof. If the parameters satisfy the named conditions, then as in the case considered in the previous lemma there is a $x_c > 0$ such that for $0 < x < x_c$, there are two saddle points $z_1, z_2 \in (\mu, 1)$, where $\mu = \max((b_j)_{j=1}^s)$, with z_1 and z_2 being the local maximum and minimum of $f(z)$ on the real line, respectively, and $z_1 < z_2$, which coalesce in one saddle point of order greater than one for $x = x_c$. The path of steepest ascent of $\mathcal{R}(z) = \operatorname{Re}(f(z))$ originating from z_1 and the path of steepest descent originating from z_2 and lying in the upper half plane are again called P_1 and P_2, respectively.

It follows from Lemma 5.5.1 that neither P_1 nor P_2 can end at a point at infinity, since $\operatorname{Im}(f(z)) \neq 0$ for $|z| \to \infty$. Since $r_0 > s_0$, P_1 can end at 0.

The only possible end point of P_2 is $z = -\frac{1}{x}$, the point on the negative real line at which, according to Lemma 5.5.4, the imaginary part of f vanishes – see Figures 5.2(a) and (b) for the case $r = 2, s = 1, b_1 = \frac{1}{5}$ and $x = \frac{3}{4}$ and $x = x_c = \frac{4}{5}$, respectively. This means that there exists a curve $\widetilde{C} : (-1, 1) \to \mathbb{C} \setminus \big((-\infty, \mu) \cup [1, \infty)\big)$ with $\widetilde{C}(0) = z_2$ and $\lim_{t\to\pm 1} \widetilde{C}(t) = -\frac{1}{x}$, and $\mathrm{Im}(f(\widetilde{C}(t)) = 0$ for all $t \in (-1, 1)$.

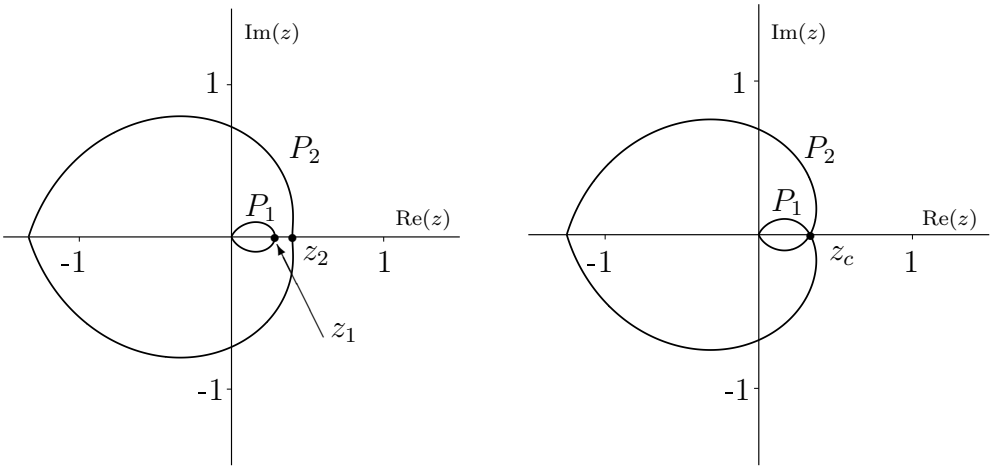

(a) $x = \frac{3}{4}$ (b) $x = \frac{4}{5}$

Figure 5.2: Paths of steepest descent and ascent of f if $r = 2, s = 1, a_1 = a_2 = 0, b_1 = \frac{1}{5}$ and $x = \frac{3}{4}(a)$ and $x = x_c = \frac{4}{5}$ (b). The latter value is the critical value of x, for which the two saddle points z_1 and z_2 coalesce in the point z_c.

Now we define for a small $\delta > 0$ the point

$$w_\delta = \min_{z\in P_2} \big(\mathrm{Re}(z) \,\big|\, \mathrm{Im}(z) = i\delta\big) + i\delta,$$

which exists if δ is chosen to be sufficiently small, the value

$$t_\delta = \max\big(0 < t < 1 \,\big|\, \widetilde{C}(t) = w_\delta\big),$$

and the contour $C : \mathbb{R} \to \mathbb{C} \setminus \big((-\infty, \mu) \cup [1, \infty)\big)$,

$$C(t) = \begin{cases} w_\delta^* + t + t_\delta & \text{for} \quad t \in (-\infty, -t_\delta), \\ \widetilde{C}(t) & \text{for} \quad t \in [-t_\delta, t_\delta], \\ w_\delta + t_\delta - t & \text{for} \quad t \in (t_\delta, \infty). \end{cases} \tag{5.40}$$

In Fig. 5.3, an example of C is shown, if the parameters of f are the same as in Fig. 5.2(a) and $\delta \approx 0.04$. To see that C has the properties stated, note that we have from Eq. (5.34) for $z < 0$,

$$\operatorname{Re}\big(f'(z)\big) = \frac{1}{z}\left(\ln(x) - \sum_{j=1}^{s} \ln\left(1 - \frac{b_j}{z}\right) + \ln\left(\frac{|z|}{1+|z|}\right)\right). \tag{5.41}$$

This expression is positive for $z < 0$ if $x < 1$ and $(b_j)_{j=1}^s \geq 0$. Therefore, if $0 < x \leq x_c$ and $x < 1$, the curve C is a path of descent connecting z_2 with infinity.

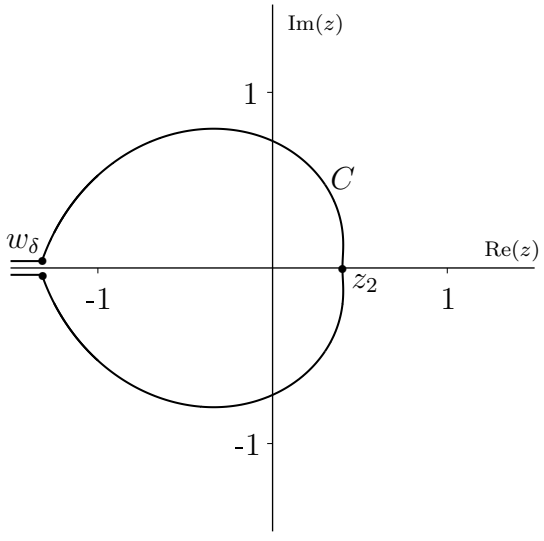

Figure 5.3: The curve C defined in Eq. (5.40) for $r = 2, s = 1, a_1 = a_2 = 0, b_1 = \frac{1}{5}, x = \frac{3}{4}$ and $\delta = 0.04$.

□

It is found that many q-hypergeometric series occurring in the combinatorics of lattice polygons satisfy the conditions of Lemmas 5.5.5 and 5.5.6. In this case, $\phi(q^k x)$ can be analysed by using the method of steepest descents.

5.6 Asymptotic analysis of $\phi(q^k x)$

The next proposition generalises Prop. 4.7.1. We formulate the following condition. Recall that $\mathcal{R}(z) = \mathrm{Re}(f(z))$.

Condition 5.6.1. *The contour C in Eq. (5.25) can be chosen such that it passes through an ordinary saddle point z_0 of f, which is a local minimum of f on the real line, and $\mathcal{R}(z_0) > \mathcal{R}(z)$ for all $z \neq z_0$ on C.*

Subject to the above condition, the following proposition holds.

Proposition 5.6.1. *Assume that the parameters of $\phi(q^k x)$ are such that there exists a $x_c > 0$ such that for $0 < x < x_c$, Condition 5.6.1 is satisfied. Then for $0 < x < x_c$ and $q = e^{-\epsilon} \to 1^-$,*

$$\phi(q^k x) = e^{\frac{h_0}{\epsilon}} \big(c_0 + \mathcal{O}(\epsilon)\big), \tag{5.42}$$

uniformly for $x \in [x_1, x_2]$ if $0 < x_1 < x_2 < x_c$, with

$$c_0 = \frac{g_k(z_0, 1)}{\sqrt{f''(z_0)}}, \tag{5.43}$$

and

$$h_0 = f(z_0) - \frac{\pi^2}{6} - \sum_{j=1}^{r} \mathrm{Li}_2(a_j) + \sum_{j=1}^{s} \mathrm{Li}_2(b_j). \tag{5.44}$$

Proof. If Condition 5.6.1 is satisfied, then Theorem 2.2.1 can be applied to the integral representation (5.25). Substituting the asymptotic forms given by Eqs. (4.33) and (4.37) into the prefactor A, this leads to the result. □

If the saddle point z_0 ceases to be a saddle point of order one for $x = x_c$, then Prop. 5.6.1 breaks down at this point, as can be seen from the fact that the coefficient c_0 diverges. If the following condition is satisfied, then an asymptotic expression which is valid uniformly for a range of parameters including x_c can be obtained in terms of generalised Airy integrals.

Condition 5.6.2. *The function f is real for $z \in (\mu, 1)$, where $0 < \mu < 1$ and z_0 is a local minimum of f on the real line. For $x = x_c$, the saddle z_0 coalesces with other saddle points of f to form a saddle point z_c of order $n \geq 2$, and the contour C in Eq. (4.38) can be chosen to pass through z_c such that on C, $\mathcal{R}(z) < \mathcal{R}(z_c)$ for $z \neq z_c$.*

Theorem 5.6.1. *Let the parameters of $\phi(q^k x)$ be such that conditions 5.6.1 and 5.6.2 with $n = 2$ are satisfied, and relabel $z_0 = z_2$. Let the saddle point z_1 with which z_2 coalesces for $x = x_c$ be real and $z_1 < z_2$ for $0 < x < x_c$. Then for $0 < x \leq x_c$ and $q = e^{-\epsilon} \to 1^-$,*

$$\phi(q^k x) = A e^{\frac{\beta}{\epsilon}} \left(p_k \operatorname{Ai}\left(\frac{\alpha}{\epsilon^{\frac{2}{3}}}\right) \epsilon^{\frac{1}{3}} - q_k \operatorname{Ai}'\left(\frac{\alpha}{\epsilon^{\frac{2}{3}}}\right) \epsilon^{\frac{2}{3}} \right) \big(1 + \mathcal{O}(\epsilon)\big), \tag{5.45}$$

uniformly for $x \in [x_1, x_c]$ if $0 < x_1 < x_c$, where A is defined in Eq. (5.15),

$$\alpha = \left(\frac{3}{4} \big(f(z_1) - f(z_2)\big) \right)^{\frac{2}{3}} \text{ and } \beta = \frac{1}{2}\big(f(z_1) + f(z_2)\big), \tag{5.46}$$

and p_k *and* q_k *are given for* $x < x_c$ *by*

$$p_k = \frac{\alpha^{\frac{1}{4}}}{\sqrt{2}} \left(\frac{g_k(z_1,1)}{\sqrt{f''(z_1)}} + \frac{g_k(z_2,1)}{\sqrt{-f''(z_2)}} \right), \tag{5.47a}$$

$$q_k = \frac{\alpha^{-\frac{1}{4}}}{\sqrt{2}} \left(\frac{g_k(z_2,1)}{\sqrt{f''(z_2)}} - \frac{g_k(z_1,1)}{\sqrt{-f''(z_1)}} \right), \tag{5.47b}$$

and $p_k = \lim_{x \to x_c^-} p_k$ *and* $q_k = \lim_{x \to x_c^-} q_k$ *for* $x = x_c$.

Proof. Let the assumptions of the statement of the theorem be satisfied. Thus for $x = x_c$, the ordinary saddle points z_1 and z_2 coalesce in the point $z = z_c$. Theorem 2.2.2 states that for x close to x_c, there exists a transformation $\mathrm{T} : z \mapsto z(u)$, such that

$$f(z(u)) = \frac{u^3}{3} - \alpha u + \beta = p(u), \tag{5.48}$$

which is analytic and bijective if z lies in a small region containing z_c, and where the coefficients are given by Eq. (5.46). Since z_2 is assumed to be a local minimum of f on the real line, z_1 is a local maximum. We can therefore choose a root for α which is positive for $0 < x \leq x_c$. Under the transformation T, z_1 and z_2 are mapped onto the points $-|\sqrt{\alpha}|$ and $|\sqrt{\alpha}|$ in the u-plane, respectively. The part C_c of the contour C which lies in the domain in which T is regular and bijective is mapped onto a segment D_c of the contour D connecting the point $|\sqrt{\alpha}|$ with $\infty e^{\pm \frac{i\pi}{3}}$ via paths of steepest descent of $\mathrm{Re}(p(u))$ – see Fig. 4.7. Since $f(z)$ and $p(u)$ are maximal inside C_c and D_c, respectively, the relative error from extending the integration to the complete contours decays exponentially in the limit $q = e^{-\epsilon} \to 1^-$.

We therefore have

$$\phi(q^k x) = \left(\frac{A}{2\pi i} \int_{\infty e^{-i\frac{\pi}{3}}}^{\infty e^{i\frac{\pi}{3}}} e^{\frac{p(u)}{\epsilon}} g_k(z(u), 1) \frac{dz}{du} du \right) (1 + \mathcal{O}(\epsilon)) \,. \tag{5.49}$$

Now we proceed analogously as in Chapter 4. Inserting the ansatz

$$g_k(z(u), 1) \frac{dz}{du} = p_k + u q_k + (u^2 - \alpha) H(u), \tag{5.50}$$

into Eq. (4.61), where $H(u)$ is some analytic function of u, and substituting $u = \pm\sqrt{\alpha}$ into the above formula, we get

$$g_k(z_{1,2}, 1) \left. \frac{dz}{du} \right|_{u=\pm|\sqrt{\alpha}|} = p_k \pm |\sqrt{\alpha}| q_k, \tag{5.51}$$

with the $+$ sign for z_2 and the $-$ sign for z_1. From taking the second derivative of Eq. (5.48) with respect to u, we get

$$\left. \frac{dz}{du} \right|_{u=\pm|\sqrt{\alpha}|} = \sqrt{\frac{2|\sqrt{\alpha}|}{\pm f''(z_{1,2})}}, \tag{5.52}$$

where the positive branch of the root has to be chosen, again with the $+$ sign for z_2 and the $-$ sign for z_1. Substituting this into Eq. (5.51) and solving for p_k and q_k, we obtain Eq. (5.47). The integral Eq. (5.49) can then be evaluated, giving Eq. (5.45) for x sufficiently close to x_c.

To show that the expression holds for all $0 < x \leq x_c$, one proceeds as in Chapter 4. For $0 < x < x_c$, the coefficient α is strictly positive, therefore the asymptotic expressions given in Eq. (4.66) can be inserted into Eq. (5.45). Upon also inserting Eqs. (4.33) and (4.37) into the prefactor A, we recover the result given in Prop. 5.6.1. This shows that Eq. (5.45) holds uniformly in the stated region. □

6 Uniform asymptotics of further models

In this chapter, we are going to consider three further models of lattice polygons and paths, whose area-width, area-perimeter or interaction-length generating functions can be expressed in terms of q-hypergeometric series, satisfying the conditions of Theorem 5.6.1. Asymptotic expressions for these series in the limit $q \to 1^-$ are therefore provided by this theorem. The three models we analyse are Schröder paths, directed column-convex polygons (DCCP) and partially directed self-avoiding walks (PDSAW).

Schröder paths are included in the family of generalised Motzkin paths which were considered in Chapter 3, where their area-width scaling behaviour was investigated heuristically. With the asymptotic result derived in the following, we are going to rigorously validate Conjecture 3.3.1 for the case $\ell = 2$. To this end, we will first give a straightforward exact solution for the area-width generating function of the model in terms of q-hypergeometric series, which was derived in [47] via a different method.

Partially directed self-avoiding walks (PDSAW) are self-avoiding random walks on $\mathbb{Z}^2$ where the walker is not allowed to step in one direction. This model slightly stands out from the other models considered in this thesis, as here we do not consider a notion of area, but the number of adjacent sites of the trajectory of the walker which are not visited directly after

one another. The mathematical methodology, however, is in line with the one employed for area-weighted polygon models. We will see that the scaling function of PDSAW, weighted with respect to the length of the walk and the number of interactions, is given by the inverse of the logarithmic derivative of the Airy function.

Directed column-convex polygons (DCCP) are self-avoiding polygons whose upper perimeter consists of a PDSAW and the lower perimeter consists of a fully directed random walk, where a fully directed random walk is a self-avoiding walk where the walker cannot step in two non-opposite directions. This model is a generalisation of the model of staircase polygons, in that it contains staircase polygons as a subset. The model is exactly solvable and a uniform asymptotic approximation of the area-width generating function is obtainable by using the general results of Chapter 5.

6.1 Schröder paths

6.1.1 Model definition and functional equation

As mentioned before, Schröder paths are included in the class of models called generalised Motzkin paths which we considered in Chapter 3, where they corresponded to the case $\ell = 2$. Below we define them once again explicitly.

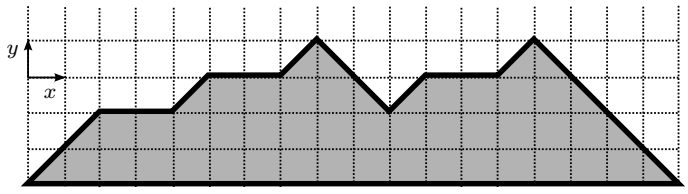

Figure 6.1: A Schröder path with 3 horizontal steps, width 18 and area 44.

Definition 6.1.1 (Schröder path)**.** *For $m \in \mathbb{Z}_{\geq 0}$, a Schröder path (SP)*

is a lattice walk $(x_k, y_k)_{k=0}^m$ *on* $\mathbb{Z}^2$ *such that* $x_0 = y_0 = y_m = 0$, *and* $y_k \geq 0$ *for all* $k \in [m]$. *Moreover, for* $0 \leq k < m$, (x_k, y_k) *is either* (x_k+1, y_k+1), $(x_k + 1, y_k - 1)$, *or* $(x_k + 2, y_k)$, *which corresponds to an up-, down- or horizontal step, respectively.*

Figure 6.1 shows an example for a Schröder path. The *width* of a SP is the x-coordinate of its final position, and the *area* of a SP is defined as in Chapter 3 as the total area between the trajectory and the line $y = 0$, measured in unit cells of $\mathbb{Z}^2$. Thus the example shown in Fig. 6.1 has width 18 and area 44.

We consider the generating function

$$S(a, x, q) = \sum_{k=0}^{\infty} \sum_{m=0}^{\infty} \sum_{n=0}^{\infty} s_{k,m,n} a^k x^m q^n, \tag{6.1}$$

where $s_{k,m,n}$ is the number of Schröder paths with k pairs of up- and down-steps, width m and area n. Substituting $\ell = 2$ into Eq. (3.9), we obtain the functional equation

$$1 + (x^2 - 1)S(x) + aqx^2 S(qx)S(x) = 0, \tag{6.2}$$

where we abbreviate $S(a, x, q) = S(x)$. Thus, the parameter a controls the relative weight between diagonal and horizontal steps of the walk, and x and q are the weights conjugate to the width and area of the trajectory, respectively.

In the next subsection, we will provide a straightforward derivation of the exact solution for $S(x)$ in terms of q-hypergeometric series.

6.1.2 Solution of the functional equation

Analogous to the solution for the functional equation for Dyck paths, a solution for $S(a, x, q) = S(x)$ can be obtained by using the ansatz

$$S(x) = \frac{\phi(qt)}{\phi(t)}, \tag{6.3}$$

where $t = x^2$. This leads to the linear equation

$$\big[t(1 + aq\sigma)\sigma + (1 - \sigma)\big]\phi(t) = 0, \tag{6.4}$$

with $\sigma\phi(t) = \phi(qt)$. Comparing the above equation with Eq. (5.4), we see that it is solved by the q-hypergeometric series

$$\phi(aq, t, q) = \phi(t) = {}_1\phi_1\left(\begin{matrix} -aq \\ 0 \end{matrix}; q, t\right). \tag{6.5}$$

6.1.3 Uniform asymptotics and scaling properties

For $a > 0$, Lemma 5.4.2, provides the integral representation

$$\phi(a, q^k t, q) = \frac{A}{2\pi i}\int_C \exp\left(\frac{f(z)}{\epsilon}\right) g_k(z, q)dz \tag{6.6}$$

with the contour C being defined in Eq. (5.21) with $0 < \rho < 1$, $\psi, \varphi \in (0, \pi)$, $A = (-a; q)_\infty (q; q)_\infty$,

$$f(z) \;=\; \ln(t)\ln(z) + \mathrm{Li}_2(z) + \mathrm{Li}_2(-a/z), \text{ and} \tag{6.7}$$

$$g_k(z, q) \;=\; \frac{1}{z^k}\left(\frac{z}{(1 - z)(z + a)}\right)^{\frac{1}{2}} \exp\left(\epsilon R(z, q)\right). \tag{6.8}$$

Here, $R(z,q) = R_1(z,q)+R_1(-a/z,q)$, where $R_1(z,q)$ is defined in Eq. (4.41). This remainder is bounded by a constant independent of q for all z on C. From the first derivative

$$f'(z) = \frac{1}{z}\ln\left(\frac{t(z+a)}{z(1-z)}\right), \tag{6.9}$$

we get the two saddle points

$$z_1 = \frac{1}{2}\left(1-t-\sqrt{d}\right) \text{ and } z_2 = \frac{1}{2}\left(1-t+\sqrt{d}\right), \tag{6.10}$$

where $d = (1-t)^2 - 4at$. The points z_1 and z_2 are the local maximum and minimum of the function f on the real line, respectively. For $0 < t < t_c = 1 + 2a - 2\sqrt{a^2+a}$, both saddle points are real and $0 < z_1 < z_2 < 1$, and they coalesce in the point $z_c = \sqrt{a^2+a} - a$ for $t = t_c$. Since for $a > 0$, the parameters of f satisfy the conditions of Lemma 5.5.5, the contour C can be chosen to connect the saddle point z_2 with the points $\infty\exp(\pm i\pi)$ via paths of steepest descent of $\mathcal{R}(z) = \mathrm{Re}(f(z))$. The conditions of Theorem 5.6.1 are therefore satisfied and hence this theorem provides the asymptotic expression (5.45) for $\phi(a, q^k t, q)$ for $0 < t \leq t_c$. Since the asymptotics is uniform for $a \in [a_1, a_2]$ if $0 < a_1 < a_2 < \infty$ and $t \in [t_1, t_c]$ if $0 < t_1 < t_c$, it also holds when a is replaced by aq. From substituting the asymptotic expressions for $\phi(aq, qx, q)$ and $\phi(aq, x, q)$ into Eq. (6.3), we obtain an asymptotic expression for $S(a, x, q)$ which is uniform in the same range of parameters.

The coefficient α is a regular function of $x = \sqrt{t}$ around $x = x_c = \sqrt{t_c}$ with a non-vanishing first derivative α'. Setting $x = x_c - s\epsilon^{\frac{2}{3}}$, we obtain

for $s \geq 0$ in the limit $q = e^{-\epsilon} \to 1^-$,

$$S(a,x,q) = \frac{1}{z_c}\left(1 + \left(\frac{q^{(0)}}{p^{(0)}} - \frac{q^{(1)}}{p^{(1)}}\right)\frac{\mathrm{Ai}'(\alpha'(x_c)s)}{\mathrm{Ai}(\alpha'(x_c)s)}\,\epsilon^{\frac{1}{3}} + \mathcal{O}\left(\epsilon^{\frac{2}{3}}\right)\right), \quad (6.11)$$

where the coefficients are given by Eq. (5.47). This result is equivalent to the one obtained in Chapter 3 for $\ell = 2$, thereby proving Conjecture 3.3.1 in this case. Equation (6.11) can be extended to negative values of s as long as $\mathrm{Ai}(\alpha'(x_c)s) \neq 0$.

6.2 Interacting partially directed self-avoiding walks

6.2.1 Model definition and generating function

Partially directed self-avoiding walks (PDSAW) form a subset of the model of self-avoiding walks (SAW) in that a PDSAW is an SAW, where the random walker is not allowed to step in one direction. The precise definition is the following.

Definition 6.2.1. *A partially directed self-avoiding walk (PDSAW) of length m is a lattice walk $(x_k, y_k)_{k=0}^m$ on $\mathbb{Z}^2$, such that $(x_0, y_0) = (0,0)$, $(x_i, y_i) \neq (x_j, y_j)$ for $i \neq j$, and such that for $0 \leq k < m$, (x_{k+1}, y_{k+1}) is either $(x_k + 1, y_k)$, $(x_k, y_k + 1)$ or $(x_k, y_k - 1)$.*

For a PDSAW $(x_k, y_k)_{k=0}^m$, we define as an *interaction* any pair of points $\mathbf{r}_i = (x_i, y_i)$ and $\mathbf{r}_j = (x_j, y_j)$ on the trajectory such that $|i - j| > 1$, and $|\mathbf{r}_i - \mathbf{r}_j| = 1$. This terminology stems from the use of self-avoiding walks as physical models of chain molecules. In these models, the points on the trajectory of an SAW represent small molecular units, called monomers, which are linked together to form a chain. If two non-neighbouring parts of the chain are spatially close to each other, they interact physically, and this

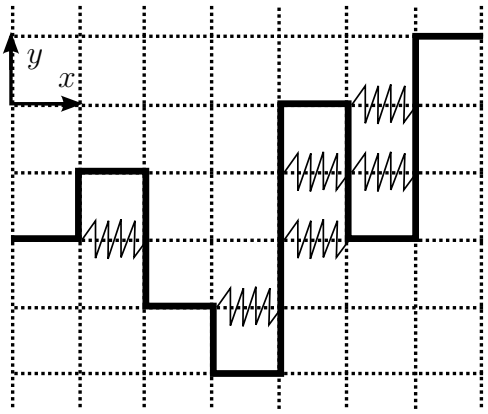

Figure 6.2: A partially directed self-avoiding walk (PDSAW) of length 20 with the underlying lattice (dotted) and arrows indicating the directions of the coordinate axes. The springs mark the self-interactions of the chain. Thus, there are 6 interactions in this example.

is taken into account by including an interaction energy in the partition function describing the system. In Fig. 6.2, we show an example PDSAW of length 20 with 4 interactions. The critical behaviour and the scaling behaviour of interacting PDSAW was studied in [49, 55] and again in the recent works [43, 16, 17].

The interaction-length generating function of PDSAW is defined as

$$P(x,y,\omega) = \sum_{m_x=0}^{\infty} \sum_{m_y=0}^{\infty} \sum_{n=0}^{\infty} c_{m_x,m_y,n} x^{m_x} y^{m_y} \omega^n, \tag{6.12}$$

where $c_{m_x,m_y,n}$ is the number of PDSAW trajectories with m_x horizontal and m_y vertical steps and n interactions. In [49], the solution

$$P\left(x,y,\omega\right) = \frac{y-q}{2y(\Phi(x(q-y))-1)+(y-q)(1-x)} \tag{6.13}$$

was derived, where $q = y\omega$, and

$$\Phi(x) = \frac{\phi(qx)}{\phi(x)} \tag{6.14}$$

with

$$\phi(x) = \sum_{n=0}^{\infty} \frac{q^{n(n-1)/2}(-x)^n}{(y;q)_n (q;q)_n} = {}_1\phi_1 \left(\begin{matrix} 0 \\ y \end{matrix} ; q\,,\, x \right). \tag{6.15}$$

This q-hypergeometric series is in the class satisfying the conditions of Theorem 5.6.1, but its asymptotics were also analysed in [52], since it also appears in the exact solution for the area-perimeter generating function of staircase polygons, which is given by

$$S(x,y,q) = y \left(\frac{{}_1\phi_1(0;qy;q;q^2x)}{{}_1\phi_1(0;qy;q;qx)} - 1 \right). \tag{6.16}$$

6.2.2 Uniform asymptotics and scaling properties

Theorem 5.3 of [52] states that for $0 < x, y < 1$ and $q = e^{-\epsilon} \to 1^-$,

$$S(x,y,q) = \frac{1}{2} \left(1 - x - y + \frac{2\epsilon^{\frac{1}{3}} \operatorname{Ai}'(\alpha\epsilon^{-\frac{2}{3}})}{\alpha^{\frac{1}{2}} \operatorname{Ai}(\alpha\epsilon^{-\frac{2}{3}})} d^{\frac{1}{2}} \right) (1 + \mathcal{O}(\epsilon)), \tag{6.17}$$

where $d = d(x,y) = \frac{1}{4}\left((1-x-y)^2 - 4xy\right)$ and $\alpha = \alpha(x,y)$ is given by

$$\begin{aligned} \frac{4}{3}\alpha^{\frac{3}{2}} = {} & \ln(z_m + \sqrt{d}) \ln(1 - z_m + \sqrt{d}) \\ & - \ln(z_m - \sqrt{d}) \ln(1 - z_m - \sqrt{d}) + \operatorname{Li}_2(z_m - \sqrt{d}) + \\ & + \operatorname{Li}_2(1 - z_m - \sqrt{d}) - \operatorname{Li}_2(z_m + \sqrt{d}) - \operatorname{Li}_2(1 - z_m + \sqrt{d}), \end{aligned} \tag{6.18}$$

with $z_m = \frac{1}{2}(1-x-y)$, and for $d \to 0$,

$$\alpha \sim \left(\frac{4}{1-(x-y)^2} \right)^{\frac{4}{3}} \left\{ \left(\frac{1-x-y}{2} \right)^2 - xy \right\}. \tag{6.19}$$

The asymptotic expression (6.17) is uniform for x and y lying in compact subsets of $(0,\infty)$ and $(-\infty,1)$, respectively. Therefore, it also holds upon

substituting $q^{-1}x(q-y)$ for x and $q^{-1}y$ for y. By using the relation

$$\Phi(x(q-y)) = \frac{q}{y} S\big(q^{-1}x(q-y), q^{-1}y, q\big) + 1, \tag{6.20}$$

we obtain for $\widetilde{d} = d(q^{-1}x(q-y), q^{-1}y) \geq 0$ and $q = e^{-\epsilon} = y\omega \to 1^-$,

$$P(x,y,\omega) = \frac{(y-1)\widetilde{\alpha}^{\frac{1}{2}}}{2\epsilon^{\frac{1}{3}}\widetilde{d}^{\frac{1}{2}}} \frac{\mathrm{Ai}(\widetilde{\alpha}\epsilon^{-\frac{2}{3}})}{\mathrm{Ai}'(\widetilde{\alpha}\epsilon^{-\frac{2}{3}})} \left(1 + \mathcal{O}(\epsilon)\right), \tag{6.21}$$

with $\widetilde{\alpha} = \alpha(q^{-1}x(q-y), q^{-1}y))$. This expression is valid in particular in the scaling limit where $\widetilde{d} \to 0$ and $q = e^{-\epsilon} \to 1^-$ such that $\widetilde{\alpha}\epsilon^{\frac{2}{3}}$ is held constant.

6.3 Directed column-convex polygons

6.3.1 Model definition and generating function

As already mentioned in the introduction, directed column-convex polygons (DCCP) form a subset of self-avoiding polygons which includes the set of staircase polygons. To define them, recall the definition of a partially directed walk (PDSAW) from the last section. Fully directed walks (FDW) are defined analogously, with the difference that from a point (x, y) on the trajectory of a FDW, the walker can only step towards $(x+1, y)$ or $(x, y+1)$. Thus, an FDW is an SAW where steps in two non-opposite directions are forbidden. Now DCCP are defined as follows.

Definition 6.3.1. *A directed column-convex polygon (DCCP) is a polygon on the square lattice $\mathbb{Z}^2$ with a fully directed walk as lower perimeter and a partially directed walk as upper perimeter, which only meet at their start and end points.*

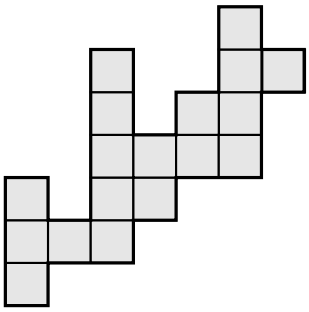

Figure 6.3: A directed column-convex polygon of area 18, horizontal perimeter 14, vertical perimeter 20 and thus total perimeter 34.

The *horizontal (vertical) perimeter* of a DCCP is the number of steps in x-direction (y-direction) which one needs to take to travel around the polygon once, and the *area* of a DCCP is the number of unit cells of $\mathbb{Z}^2$ enclosed by its perimeter – Fig. 6.3 shows an example.

The area-perimeter generating function of DCCP is defined as

$$C(x,y,q) = \sum_{m_x=0}^{\infty} \sum_{m_y=0}^{\infty} \sum_{n=0}^{\infty} c_{m_x,m_y,n} x^{m_x} y^{m_y} q^n, \tag{6.22}$$

where $c_{m_x,m_y,n}$ is the number of DCCP with horizontal perimeter $2m_x$, vertical perimeter $2m_y$ and area n.

In [53], the functional equation

$$\begin{aligned} 0 = {} & C(q^2x)C(qx)C(x) + yC(q^2x)C(qx) + yC(q^2x)C(x) \\ & - (1+q)C(qx)C(x) + y^2C(q^2x) - y(1+q)C(qx) \\ & + q(1+qx(y-1))C(x) + yq^2x(y-1), \end{aligned} \tag{6.23}$$

was derived, where $C(x,y,q)$ is abbreviated as $C(x)$. For $q=1$, one gets from Eq. (6.23) the cubic algebraic equation

$$C(x)^3 + 2(y-1)C(x)^2 + (y-1)(y+x-1)C(x) + yx(y-1) = 0.$$

In the same reference, a solution for $C(x)$ was derived as

$$C(x) = y\left(\frac{H(qx)}{H(x)} - 1\right), \tag{6.24}$$

where

$$H(x) = \sum_{n=0}^{\infty} \frac{q^{\binom{n}{2}}(-qx(1-y))^n}{(y;q)_n(qy;q)_n(q;q)_n} = {}_2\phi_2\left(\begin{matrix}0,0\\ y,qy\end{matrix};q,qx(1-y)\right). \tag{6.25}$$

The asymptotic behaviour of $C(x,y,q)$ in the limit $q \to 1^-$ will be studied in the next subsection.

6.3.2 Uniform asymptotics and scaling properties

Using that $(qy;q)_n = \frac{(1-yq^n)(y;q)_n}{1-y}$ in Prop. 5.4.1 and applying Lemma 5.4.2, we get for $\xi > 0, y < 1$ and $0 < q = e^{-\epsilon} < 1$ the integral representation

$${}_2\phi_2(0,0;y,qy;q,q^k\xi) = \frac{(1-y)(q;q)_\infty}{2\pi i(y;q)_\infty^2}\int_C \exp\left(\frac{1}{\epsilon}f(z)\right)\frac{g_k(z,q)}{1-\frac{y}{z}}dz, \tag{6.26}$$

where the functions f and g_k are given by Eqs. (5.26) and (5.27) with $r = s = 2, a_1 = a_2 = 0$ and $b_1 = b_2 = y$, and the contour C is defined in Eq. (5.21) with $(\psi,\varphi) \in (0,\pi)$ and $y < \rho < 1$. For $0 < y < 1$, the parameters of f satisfy the conditions of Lemma 5.5.5, hence there is a value $\xi_c > 0$ such that C can be chosen as a contour connecting a saddle point of f lying on the segment $(y,1)$ with two points at infinity via paths of steepest descents of the function $\mathcal{R}(z) = \mathrm{Re}(f(z))$. The saddle points of f are the zeros of the polynomial

$$s(z) = \xi z^2 - (z-y)^2(1-z). \tag{6.27}$$

For $0 < y < 1$ and $0 < \xi < \xi_c$, the function f has three real saddle points $0 < z_3 < y < z_1 < z_2 < 1$, and z_1 and z_2 coalesce for $\xi = \xi_c$. The asymptotic behaviour of ${}_2\phi_2(0,0;y,qy;q,qx(1-y))$ for $0 < x \leq x_c = \xi_c/(1-y)$ is therefore given by Theorem 5.6.1, with the function $g_k(z,q)$ replaced by $g_k(z,q)/(1-\frac{y}{z})$.

For example, in the symmetric case $x = y$, the saddle points z_1 and z_2 coalesce for $x = x_c = (10^{\frac{2}{3}} - 4)/3$ in the point

$$z_c = \frac{10^{\frac{2}{3}} - 4}{10^{\frac{1}{3}} - 1} \tag{6.28}$$

For $s \geq 0$ and $q = e^{-\epsilon} \to 1^-$,

$$C(x_c - s\epsilon^{\frac{2}{3}}, x_c - s\epsilon^{\frac{2}{3}}, q) = x_c \left(\frac{1}{z_c} - 1\right) + b_0 \frac{\mathrm{Ai}'(b_1 s)}{\mathrm{Ai}(b_1 s)} \epsilon^{\frac{1}{3}} + \mathcal{O}(\epsilon^{\frac{2}{3}}), \tag{6.29}$$

where $b_0 \approx 0.29$ and $b_1 = \alpha'(x_c) \approx 6.89$. From considering the imaginary part of the function f at the saddle point z_2, it is possible to extend the region of validity of the above equation to negative values of s, as long as $\mathrm{Ai}(b_1 s) \neq 0$.

7 Area-length scaling of Bernoulli meanders

7.1 Introduction

Bernoulli meanders (or ballot paths) are lattice walks defined similarly to Dyck paths, the only difference being that a Bernoulli meander need not end on the line $y = 0$. Thus, the model contains Dyck paths as a special case, and an expression for the area-length generating function of Bernoulli meanders in terms of the area-width generating function of Dyck paths can be obtained via a construction explained below. Using this expression, asymptotic results for the meander generating function can be obtained from the results for Dyck paths which were derived in Chapter 4.

The probability distribution of the area under a Bernoulli meander in the limit of the length of the walk tending towards infinity was derived by Takács in [69].

The reason for choosing the word length in this section rather than width is due to the fact that, contrary to the generalised Motzkin paths considered in Chapter 3, for Bernoulli meanders no confusion is possible between the number of steps of the trajectory and the horizontal distance between its end points.

We begin by defining the model precisely and derive an expression for

the generating function which we consider. Then we will state the final result of our computations, and the rest of the chapter contains the steps leading to this result.

The results in this chapter were obtained with Christoph Richard.

7.2 The model

Bernoulli meanders are defined as follows.

Definition 7.2.1 (Bernoulli meander)**.** *For $m \in \mathbb{Z}_{\geq 0}$, a Bernoulli meander of length m is a lattice walk $(x_k, y_k)_{k=0}^{2m}$ on $\mathbb{Z}^2$ such that $(x_0, y_0) = (0, 0)$, and $y_k \geq 0$ for all $k \in [m]$. Moreover, for $0 \leq k < 2m$, (x_k, y_k) is either $(x_k + 1, y_k + 1)$ or $(x_k + 1, y_k - 1)$, corresponding to an up- or down-step, respectively.*

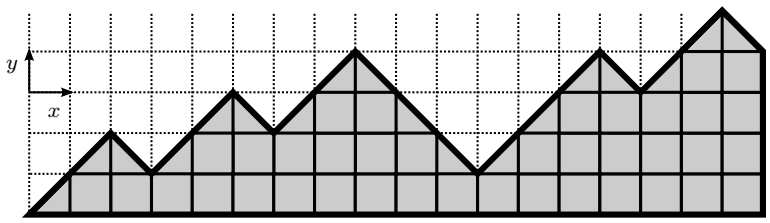

Figure 7.1: A Bernoulli meander of length 18 and area 49. The shaded squares have unit area. The dotted grid shows the underlying lattice, and the small arrows indicate the directions of the coordinate axes.

An example for a Bernoulli meander is shown in Fig. 7.1. We will refer to them as meanders from now on. The *length* of a meander is the number of steps it consists of and the *area* is here defined as the sum of the heights of all points on the trajectory. Here, the height of a point is its y-coordinate.

7.3 Functional equation and area-length generating function

First we note that the definition of the area as the sum of heights of all points on the trajectory coincides for Dyck paths with the total area under the path measured in units of lattice cells. Thus, the area-length generating function

$$\widetilde{D}(x,q) = \sum_{m=0}^{\infty}\sum_{n=0}^{\infty} d_{m,n} x^m q^n, \tag{7.1}$$

where $d_{m,n}$ is the number of Dyck paths with length m and area n, defined as the sum of heights of all points on the trajectory, was already considered in Chapter 3. Here we use the tilde to distinguish this generating function from the function $D(x,q)$ considered in Chapter 4, where a different parametrisation was used. Accordingly, $\widetilde{D}(x,q)$ satisfies the functional equation

$$\widetilde{D}(x,q) = 1 + x^2 q \widetilde{D}(qx,q)\widetilde{D}(x,q). \tag{7.2}$$

Comparing the above equation with Eq. (4.7), we see that $\widetilde{D}(x,q) = D(qx^2,q^2)$. Hence, we obtain from Eq. (4.12) the exact solution

$$\widetilde{D}(x,q) = \frac{\phi(q^3x^2,q^2)}{\phi(qx^2,q^2)}, \tag{7.3}$$

where $\phi(x,q) = {}_0\phi_1(-;0;q,-x)$.

Now we consider the generating function

$$M(x,q) = \sum_{m=0}^{\infty}\sum_{n=0}^{\infty} b_{m,n} x^m q^n, \tag{7.4}$$

where $b_{m,n}$ is the number of meanders of length m and area n. A functional equation for $M(x,q)$ is obtained by noting that a meander is either a Dyck

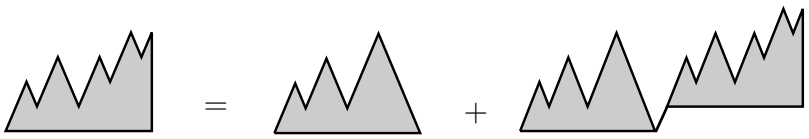

Figure 7.2: Graphical interpretation of Eq. (7.5). A meander is either a Dyck path, or a Dyck path followed by an up-step followed by a meander.

path, or a Dyck path followed by an up-step, followed by a meander. This leads to the functional equation

$$M(x,q) = \widetilde{D}(x,q) + xq\widetilde{D}(x,q)M(qx,q), \tag{7.5}$$

which was also given in [44]. Here the factor of q in the first argument of M on the rhs accounts for the fact that the meander is elevated by one, and the factor xq represents the weight connecting Dyck path and meander. Figure 7.2 shows a graphical interpretation of Eq. (7.5). Setting $q = 1$ in this equation and using $\widetilde{D}(x,1) = \frac{1}{2x^2}(1-\sqrt{1-4x^2})$, we obtain the length generating function $M(x,1) = M(x)$ of meanders as

$$M(x) = \frac{1}{\sqrt{\frac{1}{2}-x}}\frac{1}{\sqrt{\frac{1}{2}+x}+\sqrt{\frac{1}{2}-x}}. \tag{7.6}$$

Hence for $x \to \frac{1}{2}^-$, $M(x) = (\frac{1}{2}-x)^{-\frac{1}{2}} + \mathcal{O}(1)$. For arbitrary q, iterations of Eq. (7.5) yield

$$M(x,q) = \sum_{h=0}^{\infty} x^h q^{\binom{h+1}{2}} \prod_{k=0}^{h} \widetilde{D}(q^k x, q), \tag{7.7}$$

where each summand of the infinite series represents the generating function of meanders with a fixed height of the end point. Upon substituting

Eq. (7.3) into the above expression, we get after simplification

$$M(x,q) = \frac{1}{\phi(qx^2,q^2)} \sum_{h=0}^{\infty} \phi(q^{2h+3}x^2,q^2) x^h q^{\binom{h+1}{2}}. \tag{7.8}$$

7.4 The main result

We denote the integral of the Airy function Ai for $x \in \mathbb{R}$ as

$$\mathrm{I}(x) = \int_{-\infty}^{x} \mathrm{Ai}(y)dy. \tag{7.9}$$

In ([21, §9.10(iv)]), the values $\mathrm{I}(0) = \frac{2}{3}$ and $\lim_{x\to\infty} \mathrm{I}(x) = 1$ are given. The following is the main result of this chapter.

Proposition 7.4.1. *For $s \in (s_0, \infty)$ and $x = \frac{1}{2}\left(1 - s\epsilon^{\frac{2}{3}}\right)$,*

$$M(x, e^{-\epsilon}) = \frac{F(s)}{\epsilon^{\frac{1}{3}}} + \mathcal{O}(1) \qquad (\epsilon \to 0^+), \tag{7.10}$$

where $s_0 \approx 2^{-\frac{1}{3}} a_0$, with $a_0 \approx -2.34$ being the largest zero of $\mathrm{Ai}(s)$, and

$$F(s) = 2^{\frac{2}{3}} \frac{1 - 3\,\mathrm{I}(2^{\frac{1}{3}}s)}{\mathrm{Ai}(2^{\frac{1}{3}}s)}, \tag{7.11}$$

with $\mathrm{I}(s)$ defined in Eq. (7.9).

In the following sections we will carry out the calculations leading to this result.

7.5 Uniform asymptotics of $M(x,q)$

With $\phi_2(x,q) = \phi(q^2x,q)$, Eq. (7.8) can be rewritten as

$$M(x,q) = \frac{1}{\phi_2(q^{-3}x^2,q^2)} \sum_{h=0}^{\infty} \phi_2(q^{2h-1}x^2,q^2) x^h q^{\binom{h+1}{2}}. \tag{7.12}$$

The motivation for this step is that insertion of the asymptotic expression for $\phi(q^2x,q)$ will lead to an expression with the structure of a Jackson integral [37]. From Theorem 4.7.1, we define the leading asymptotic contribution to $\phi(q^2x,q)$ in the limit $q = e^{-\epsilon} \to 1^-$ as

$$\phi_2^{\mathrm{as}}(x,q) = (q;q)_\infty \exp\left(\frac{\beta(x)}{\epsilon}\right) H(x,q), \tag{7.13}$$

where $\alpha(x)$ and $\beta(x)$ are defined in Eq. (4.56) and

$$H(x,q) = p_2(x)\epsilon^{\frac{1}{3}} \operatorname{Ai}\left(\frac{\alpha(x)}{\epsilon^{\frac{2}{3}}}\right) + q_2(x)\epsilon^{\frac{2}{3}} \operatorname{Ai}'\left(\frac{\alpha(x)}{\epsilon^{\frac{2}{3}}}\right), \tag{7.14}$$

with the coefficients p_2 and q_2 given in Eq. (4.57). Theorem 4.7.1 asserts that in the limit $q = e^{-\epsilon} \to 1^-$,

$$\phi_2(x,q) = \phi_2^{\mathrm{as}}(x,q)(1+\mathcal{O}(\epsilon)), \tag{7.15}$$

and there exists a $x_2 > \frac{1}{4}$ such that the asymptotics are uniform for $x \in [x_1,x_2]$ if $0 < x_1 < x_2$. With this we prove the following result.

Lemma 7.5.1. *For $x \in (0,\frac{1}{2}]$ and $q = e^{-\epsilon} \to 1^-$,*

$$M(x,q) = \left(\sum_{h=0}^{\infty} \frac{H(q^{2h-1}x^2,q^2)}{H(q^{-3}x^2,q^2)} \frac{q^{h+1}}{x}\right)(1+\mathcal{O}(\epsilon)), \tag{7.16}$$

uniformly for $x \in [x_1,\frac{1}{2}]$ if $0 < x_1 < \frac{1}{2}$.

Proof. Let $x \in (0, \frac{1}{2}]$ and $\delta \in (0, x)$. Then $q^h x < \delta$ if $h \geq h_0(q)$, where

$$h_0(q) = \left\lceil \frac{1}{\ln(q)} \ln\left(\frac{\delta}{x}\right) \right\rceil . \tag{7.17}$$

Now we consider the sum

$$M^{(t)}(x,q) = \sum_{h=h_0(q)}^{\infty} \frac{\phi_2(q^{2h-1}x^2, q^2)}{\phi_2(q^{-3}x^2, q^2)} x^h q^{\binom{h+1}{2}} \tag{7.18}$$

Since $\widetilde{D}(x,1) \leq 2$ for $x \leq \frac{1}{2}$, we see from Eq. (7.7) that

$$\begin{aligned} M^{(t)}(x,q) &\leq 2 \sum_{h=h_0(q)}^{\infty} q^{\binom{h+1}{2}} = 2q^{\binom{h_0+1}{2}} \sum_{k=0}^{\infty} q^{kh_0 + \frac{k^2}{2} - \frac{k}{2}} \\ &\leq 2\, q^{\frac{h_0^2}{2}} \sum_{k=0}^{\infty} q^k \leq 2 \frac{e^{-\frac{1}{2\epsilon}\ln\left(\frac{\delta}{2}\right)^2}}{1-q} \end{aligned} \tag{7.19}$$

with $h_0 = h_0(q)$ and $\epsilon = -\ln(q)$. The right term in the second line tends to 0 exponentially as $q \to 1^-$. Since $M(x,1) \geq 1$ for $x \in (0, \frac{1}{2}]$, this implies

$$M(x,q) = \left(\sum_{h=0}^{h_0(q)} \frac{\phi_2(q^{2h-1}x^2, q^2)}{\phi_2(q^{-3}x^2, q^2)} x^h q^{\binom{h+1}{2}} \right) \big(1 + o(\epsilon)\big). \tag{7.20}$$

Since $q^{2h-1}x^2 > \delta^2 > 0$ for $0 \leq h \leq h_0(q)$, in the limit $q = e^{-\epsilon} \to 1^-$,

$$\frac{\phi_2(q^{2h-1}x^2, q^2)}{\phi_2(q^{-3}x^2, q^2)} = \frac{\phi_2^{\mathrm{as}}(q^{2h-1}x^2, q^2)}{\phi_2^{\mathrm{as}}(q^{-3}x^2, q^2)} \left(1 + \mathcal{O}(\epsilon)\right), \tag{7.21}$$

uniformly for all $h \in [0, h_0(q)]$. Inserting Eq. (7.13) into this expression and using Eq. (4.59) for $\beta = \beta(x)$, we arrive at Eq. (7.16).

□

For $x > 0$ and a bounded function $f : [0, x] \mapsto \mathbb{R}$, the Jackson integral

is defined in [37] to be

$$\int_0^x f(y)d_q y = x(1-q)\sum_{n=0}^{\infty} f(q^n x)q^n. \tag{7.22}$$

If f is continuous, then in the limit $q \to 1^-$, the Jackson integral converges towards the Riemann integral,

$$\lim_{q\to 1^-} \int_0^x f(y)d_q y = \int_0^x f(y)dy. \tag{7.23}$$

Concerning the difference between Jackson and Riemann integral, we have the following Lemma.

Lemma 7.5.2. *For $x > 0$, $q \in (0,1)$ and $f : [0,x] \mapsto \mathbb{R}$ differentiable,*

$$\left| \int_0^x f(y)dy - \int_0^x f(y)d_q y \right| \leq x^2(1-q)^2 \sum_{n=0}^{\infty} |f'(\xi_n)|q^{2n}, \tag{7.24}$$

where for $n \in \mathbb{Z}_{\geq 0}$, $\xi_n \in [q^{n+1}x, q^n x]$.

Proof. For continuous f, we have

$$\int_0^x f(y)d_q y - \int_0^x f(y)dy = \sum_{n=0}^{\infty} \left(xq^n(1-q)f(q^n x) - \int_{q^{n+1}x}^{q^n x} f(y)dy \right).$$

If f is also differentiable, then according to the mean value theorem [21], there exists for each $n \in \mathbb{Z}_{\geq 0}$ a $\eta_n \in [q^{n+1}x, q^n x]$, such that

$$\int_{q^{n+1}x}^{q^n x} f(y)dy = xq^n(1-q)f(\eta_n). \tag{7.25}$$

Hence, we obtain that

$$\int_0^x f(y)dy - \int_0^x f(y)d_q y = x(1-q)\sum_{n=0}^{\infty}(f(q^n x) - f(\eta_n))q^n. \tag{7.26}$$

Again it follows from the mean value theorem that for each $n \in \mathbb{Z}_{\geq 0}$, there exists a $\xi_n \in [\eta_n, q^n x]$, such that $f(q^n x) - f(\eta_n) = f'(\xi_n)(q^n x - \eta_n)$, hence

$$\int_0^x f(y)dy - \int_0^x f(y)d_q y = x(1-q)\sum_{n=0}^{\infty} f'(\xi_n)(q^n x - \eta_n)q^n. \tag{7.27}$$

Taking the absolute values on both sides of Eq. (7.27) and estimating $q^n x - \eta_n \leq q^n(1-q)$, we obtain Eq. (7.24). □

Now we define for $x \in (0, \frac{1}{4}]$ and $q = e^{-\epsilon} \in (0,1)$ the functions

$$g(x,q) = p_2(x)\,\mathrm{Ai}\left(\frac{\alpha(x)}{\epsilon^{\frac{2}{3}}}\right) \text{ and } h(x,q) = q_2(x)\,\mathrm{Ai}'\left(\frac{\alpha(x)}{\epsilon^{\frac{2}{3}}}\right). \tag{7.28}$$

Comparing the definition of the Jackson integral with Eq. (7.16), we see that for $q = e^{-\epsilon} \to 1^-$,

$$M(x,q) = \frac{\displaystyle\int_0^x \big(g(q^{-1}y^2,q^2) - h(q^{-1}y^2,q^2)(2\epsilon)^{\frac{1}{3}}\big)d_q y}{x^2(1-q)\big(g(q^{-3}x^2,q^2) - h(q^{-3}x^2,q^2)(2\epsilon)^{\frac{1}{3}}\big)}(1+\mathcal{O}(\epsilon)), \tag{7.29}$$

The following Lemma gives an estimate of the error made when the Jackson integral in Eq. (7.29) is replaced by a Riemann integral.

Lemma 7.5.3. *For $x \in (0, \frac{1}{2}]$ and $q = e^{-\epsilon} \to 1^-$,*

$$\int_0^x g(q^{-1}y^2,q^2)d_q y = \int_0^x g(q^{-1}y^2,q^2)dy + \mathcal{O}(\epsilon) \tag{7.30a}$$

$$\int_0^x h(q^{-1}y^2,q^2)d_q y = \int_0^x h(q^{-1}y^2,q^2)dy + \mathcal{O}(\epsilon) \tag{7.30b}$$

uniformly with respect to x.

Proof. Since $f(z_-) > f(z_+)$ for $x \in (0, \frac{1}{4})$, we have $\alpha(q^{-1}y^2) > 0$ for

$y \in (0, \frac{\sqrt{q}}{2})$, and in the limit $y \to 0^+$,

$$\alpha(q^{-1}y^2) \sim \left(\frac{3}{2}\right)^{\frac{2}{3}} \ln(y)^{\frac{4}{3}} \text{ and } \alpha'(q^{-1}y^2) = \mathcal{O}\big(y^{-2}\ln(y)^{\frac{1}{3}}\big). \tag{7.31}$$

From Eq. (4.57), we get in the same limit,

$$p_2(q^{-1}y^2) = \mathcal{O}(y^{-2}\ln(y)^{\frac{1}{3}}) \text{ and } p_2'(q^{-1}y^2) = \mathcal{O}(y^{-4}\ln(y)^{\frac{1}{3}}). \tag{7.32}$$

Substituting the above estimation for $p_2(q^{-1}y^2)$ and the asymptotic expression (4.66) for the Airy function into Eq. (7.28), we conclude that for $q < 1$,

$$\lim_{y\to 0^+} g(q^{-1}y^2, q^2) = 0,$$

and since for $y \in (0, \frac{1}{2})$, $g(q^{-1}y^2, q^2) \to 0$ pointwise for $q \to 1^-$, this implies that the Riemann integral on the RHS of Eq. (7.30a) is bounded by a constant for all $x \in (0, \frac{1}{4}]$ and $q \in (0, 1)$.

For the remainder we get from Lemma 7.5.2

$$\begin{aligned} &\left|\int_0^x g(q^{-1}y^2, q^2)d_q y - \int_0^x g(q^{-1}y^2, q^2)dy\right| \\ &\leq x^2(1-q)^2 \sum_{n=0}^{\infty} \left|g'(q^{-1}\xi_n^2, q^2)\right| q^{2n}, \end{aligned} \tag{7.33}$$

where $g'(q^{-1}y^2, q^2) = \frac{\partial}{\partial y} g(q^{-1}y^2, q^2)$ and $\xi_n \in [q^{n+1}x, q^n x]$ for $n \in \mathbb{Z}_{\geq 0}$. We need to find a sufficient bound for this derivative, which is given by

$$\begin{aligned} g'\left(\frac{y^2}{q}, q^2\right) = \frac{2y}{q}\Bigg[&p_2'\left(\frac{y^2}{q}\right) \mathrm{Ai}\left(\frac{\alpha(q^{-1}y^2)}{(2\epsilon)^{\frac{2}{3}}}\right) + \\ &+ p_2\left(\frac{y^2}{q}\right) \mathrm{Ai}'\left(\frac{\alpha(q^{-1}y^2)}{(2\epsilon)^{\frac{2}{3}}}\right) \frac{\alpha'(q^{-1}y^2)}{(2\epsilon)^{\frac{2}{3}}}\Bigg]. \end{aligned} \tag{7.34}$$

Using the estimations (7.31) and (7.32) in Eq. (7.34), we obtain that for $q \in (0,1)$, $\lim_{y\to 0^+} g'\left(q^{-1}y^2, q^2\right) = 0$. Moreover, since $\alpha(x) \sim 1 - 4x$ for $x \to \frac{1}{4}$, we have for $y = \frac{1}{2}(1-\epsilon^{\phi'})^{\frac{1}{2}}$ with $0 < \phi' < \frac{2}{3}$, and $q = e^{-\epsilon} \to 1^-$,

$$\frac{\alpha(q^{-1}y^2)}{\epsilon^{\frac{2}{3}}} \sim \epsilon^{\phi' - \frac{2}{3}} \to \infty.$$

From Eq. (4.66) it follows that $g'(q^{-1}y^2, q^2)$ is bounded by a constant if $y \in \left(0, \frac{1}{2}(1-\epsilon^{\phi'})^{\frac{1}{2}}\right]$ where $0 < \phi' < \frac{2}{3}$. For $y \in \left[\frac{1}{2}(1-\epsilon^{\phi'})^{\frac{1}{2}}, \frac{1}{2}\right]$, we have the weaker bound $g'(q^{-1}y^2, q^2) = \mathcal{O}(\epsilon^{-\frac{2}{3}})$ as $q = e^{-\epsilon} \to 1^-$.

Now assume $0 < \phi' < \frac{2}{3}$. We split up the sum on the RHS of Eq. (7.33) as

$$\sum_{n=0}^{\infty} \left|g'(q^{-1}\xi_n^2, q^2)\right| q^{2n} = \sum_{n=0}^{N-1} \left|g'(q^{-1}\xi_n^2, q^2)\right| q^{2n} + \sum_{n=N}^{\infty} \left|g'(q^{-1}\xi_n^2, q^2)\right| q^{2n},$$

where $N = N(q)$ is chosen such that $\xi_n < \frac{1}{2}(1-\epsilon^{\phi'})^{\frac{1}{2}}$ if $n > N(q)$. Since $\xi_n \in [q^{n+1}x, q^n x]$, this is satisfied if

$$xq^n < \frac{1}{2}(1-\epsilon^{\phi'})^{\frac{1}{2}}, \tag{7.35}$$

which certainly holds if $n > N(q) = \left\lceil \epsilon^{\phi'-1} \right\rceil$. With this we get

$$\sum_{n=0}^{N-1} \left|g'(q^{-1}\xi_n^2, q^2)\right| q^{2n} = N c_1 \epsilon^{\frac{2}{3}} = \mathcal{O}(\epsilon^{-1}), \text{ and} \tag{7.36a}$$

$$\sum_{n=N}^{\infty} \left|g'(q^{-1}\xi_n^2, q^2)\right| q^{2n} \leq \sum_{n=0}^{\infty} c_2 q^{2n} = \mathcal{O}(\epsilon^{-1}), \tag{7.36b}$$

where c_1 and c_2 are constants. Substituting the above bounds into Eq. (7.33), we conclude the proof of Eq. (7.30a). In a completely analogous way, one also shows Eq. (7.30b). □

With the definition of the function I in Eq. (7.9), we now formulate the following result.

Lemma 7.5.4. *For $s \in \mathbb{R}$, $x = \frac{1}{2}(1 - s\epsilon^{\frac{2}{3}})$ and $q = e^{-\epsilon} \to 1^-$,*

$$\int_0^x g(q^{-1}y^2, q^2)dy = \frac{(2\epsilon)^{\frac{2}{3}}}{\sqrt{2}} \left(\frac{1}{3} - \mathrm{I}(2^{\frac{1}{3}}s)\right) \left(1 + \mathcal{O}(\epsilon^{\frac{2}{3}})\right), \tag{7.37a}$$

$$\int_0^x h(q^{-1}y^2, q^2)dy = -\frac{(2\epsilon)^{\frac{2}{3}}}{2^{\frac{3}{2}}} \mathrm{Ai}\left(2^{\frac{1}{3}}s\right) \left(1 + \mathcal{O}(\epsilon^{\frac{2}{3}})\right). \tag{7.37b}$$

Proof. From the definition (2.12) of the Airy function we get, by applying Fubini's theorem,

$$\int_0^x g(q^{-1}y^2, q^2)dy = \int_0^x p_2(q^{-1}y^2)\,\mathrm{Ai}\left(\frac{\alpha(q^{-1}y^2)}{(2\epsilon)^{\frac{2}{3}}}\right) dy$$

$$= \frac{1}{2\pi i} \int_{e^{-i\frac{\pi}{3}}\infty}^{e^{i\frac{\pi}{3}}\infty} e^{\frac{u^3}{3}} \left[\int_0^x p_2(q^{-1}y^2) \exp\left(-\frac{\alpha(q^{-1}y^2)}{(2\epsilon)^{\frac{2}{3}}}u\right) dy\right] du. \tag{7.38}$$

Since $\alpha(q^{-1}y^2)$ is monotonic for $y \in \left(0, \frac{1}{2}\right]$, the integral in the second line of Eq. (7.38) can be transformed by setting $t = \alpha(q^{-1}y^2)$. This gives us

$$\int_0^x p_2(q^{-1}y^2) \exp\left(-\frac{\alpha(q^{-1}y^2)}{(2\epsilon)^{\frac{2}{3}}}u\right) dy$$

$$= -\int_{\alpha(x^2)}^{\infty} p_2(y(t)^2) \exp\left(\frac{-tu}{(2\epsilon)^{\frac{2}{3}}}\right) \frac{dy}{dt} dt. \tag{7.39}$$

Applying Watson's Lemma (2.2.1), we get for $x = \frac{1}{2}(1 - s\epsilon^{\frac{2}{3}})$,

$$\begin{aligned}
&\int_{\alpha(x^2)}^{\infty} p_2(y(t)^2) \exp\left(\frac{-tu}{(2\epsilon)^{\frac{2}{3}}}\right) \frac{dy}{dt} dt. \\
&= \left(p_2(x^2) \left.\frac{dy}{dt}\right|_{t=\alpha(x^2)} \int_{\alpha(x^2)}^{\infty} \exp\left(\frac{-tu}{(2\epsilon)^{\frac{2}{3}}}\right) dt\right) \left(1 + \mathcal{O}(\epsilon^{\frac{2}{3}})\right) \\
&= \left(\frac{1}{\sqrt{2}} \int_{2s\epsilon^{\frac{2}{3}}}^{\infty} \exp\left(\frac{-tu}{(2\epsilon)^{\frac{2}{3}}}\right) dt\right) \left(1 + \mathcal{O}(\epsilon^{\frac{2}{3}})\right) \\
&= \left(\frac{(2\epsilon)^{\frac{2}{3}}}{\sqrt{2}} \int_{2^{\frac{1}{3}}s}^{\infty} \exp\left(-vu\right) dv\right) \left(1 + \mathcal{O}(\epsilon^{\frac{2}{3}})\right), \qquad (7.40)
\end{aligned}$$

where we used in the third line that $p_2(\frac{1}{4}) = 2\sqrt{2}$ and $\alpha(x)^2 \sim 1 - 4x^2$ for $x \to \frac{1}{2}$, and therefore

$$p_2(x^2) \left.\frac{dy}{dt}\right|_{t=\alpha(x)^2} = \frac{1}{\sqrt{2}}\left(1 + \mathcal{O}(\epsilon^{\frac{2}{3}})\right) \quad (\epsilon \to 0^+). \qquad (7.41)$$

Inserting Eq. (7.40) into Eq. (7.38), and reversing the order of integration again, we arrive at Eq. (7.37a). By using $q_2(\frac{1}{4}) = -\sqrt{2}$, one similarly obtains Eq. (7.37b).

□

From Lemma 7.5.2 it follows that the Jackson integrals in Eq. (7.29) can be replaced by Riemann integrals in the scaling limit where $x = \frac{1}{2}(1 - s\epsilon^{\frac{2}{3}})$ and $q = e^{-\epsilon} \to 1^-$. Inserting Eqs. (7.14), (7.37a) and (7.37b) into Eq. (7.29), we arrive at Prop. 7.4.1. We note that this result can also be checked for consistency by inserting it into the functional equation Eq. (7.5) and using the known result for the scaling behaviour of Dyck paths.

8 Higher-order Airy scaling in deformed Dyck paths

8.1 Introduction

In the previous chapters we considered different models of directed two-dimensional polygon and walk models. As a common property, these models showed a tricritical point in their phase diagram, around which their area-length (or -width) generating functions admit a simple scaling form. For Dyck and Schröder paths and directed column-convex polygons, the associated scaling function was found to be the logarithmic derivative of the Airy function, and on the basis of exact enumeration data, Richard, Guttmann and Jensen conjectured the same kind of scaling behaviour to also hold for unrestricted, rooted self-avoiding polygons [59].

In [14], it was postulated that for SAP, there exists an entire hierarchy of higher-order scaling functions given for $k \geq 3$ by the logarithmic derivative $(\partial/\partial s_1)\Theta_k(s_1, \ldots, s_{k-2})$, where for $s_1, s_2, \ldots, s_{k-2} \in \mathbb{C}$, and

$$\Theta_k(s_1, \ldots, s_{k-2}) = \frac{1}{2\pi i} \int_{e^{-i\pi/k}\infty}^{e^{i\pi/k}\infty} \exp\left(\frac{u^k}{k} - \sum_{j=1}^{k-2} s_j u^j\right) du \tag{8.1}$$

([21, §36.2]). This function can be seen as a generalised Airy function, since $\Theta_3(s) = \mathrm{Ai}(s)$. We present here the first concrete example of a lattice polygon model with a higher-order multicritical point characterised

by the two-variable scaling function

$$\Phi(s_1, s_2) = \frac{\partial}{\partial s_1} \ln\Big(\Theta_4(s_1, s_2)\Big), \tag{8.2}$$

where $\Theta_4(s_1, s_2)$ is also called a Pearcey function which also appears in the context of random matrix theory and determinantal processes [71]. It consists of a deformed version of Dyck paths (DDP), where additional to the steps $(1, 0)$ and $(0, 1)$ allowed for (standard) Dyck paths, 'jump' steps in the direction $(-1, 1)$ are allowed. We note that there also exists a bijection between DDP and rooted plane ordered binary-ternary trees, analogously to the bijection between Dyck paths and rooted plane ordered binary trees [65].

In Section 8.2, we will define DDP precisely and derive the functional equation for their generating function, weighted with respect to their area, length and number of jumps. An expression for the generating function in the form of a fraction of two basic hypergeometric series will be obtained in Section 8.3. The main result is given in Section 8.4, and the remaining sections contain the steps of its derivation. A contour integral representation for the series occurring in the generating function of DDP which in the limit $q \to 1^-$ has a leading contribution in the form of a saddle point integral is provided by the general results from Chapter 5. The location of the relevant saddle points depending on the parameters w and t is discussed in Section 8.6, and the geometry of the paths of steepest descent originating from them is investigated in Section 8.7. In Section 8.8, the integral expression for the basic hypergeometric series is then transformed into a canonical form, and the asymptotic behaviour of the coefficients of this transformation around the multicritical point is analysed. The

asymptotic expression for the basic hypergeometric series is then obtained by evaluating the transformed integral in Section 8.9, which directly leads to Theorem 8.4.1.

This chapter consists of joint work with Adri Olde Daalhuis and Thomas Prellberg.

8.2 The model

The model of DDP is defined as follows.

Definition 8.2.1. *For $m, s \in \mathbb{Z}_{\geq 0}$ and $s \geq 2m$, a deformed Dyck path (DDP) of half-width m is a walk $(x_k, y_k)_{k=0}^{s}$ on $\mathbb{Z}^2$, such that $(x_0, y_0) = (0, 0)$, $(x_s, y_s) = (m, m)$ and $y_k \geq x_k$ for all $0 \leq k \leq s$. Moreover, if $(x_k, y_k) = (x, y)$ for $0 \leq k < s$, then (x_{k+1}, y_{k+1}) is either $(x, y+1)$ or $(x+1, y)$ or $(x-1, y+1)$, which we call an up-step, a down-step or a jump, respectively.*

We consider the generating function

$$G(w, x, q) = \sum_{k=0}^{\infty} \sum_{m=0}^{\infty} \sum_{n=0}^{\infty} p_{k,m,n}\, w^k\, x^m\, q^n, \tag{8.3}$$

where $p_{k,m,n}$ is the number of DDP with k jumps, half-width m and area n, with the area being defined as the number of full lattice cells enclosed between the path and the main diagonal of the lattice. Figure 8.1 shows an example of a DDP with half-width 9, 3 jumps and area 12.

To obtain a functional equation for $G(w, x, q)$, we use the following factorisation argument. A DDP has either half-length zero, or it starts with an up-step followed by a DDP followed by a down-step and then another DDP, or it starts with a jump followed by a DDP followed by a down-step

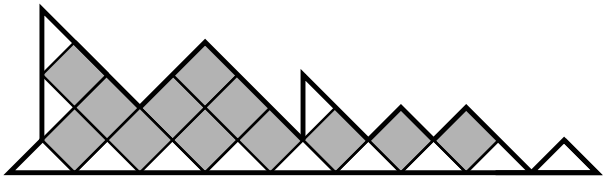

Figure 8.1: A DDP of half-width 9, 3 jumps and area 12. The lattice is rotated such that its main diagonal lies horizontally in the image.

followed by another DDP followed by a down-step and then another DDP – see Fig. 8.2 for an illustration.

Figure 8.2: Graphical decomposition of the set of DDP, leading to Eq. (8.4).

From this decomposition we obtain

$$wxG(q^2x)G(qx)G(x) + xG(qx)G(x) - G(x) + 1 = 0, \tag{8.4}$$

where $G(w, x, q) = G(x)$ for brevity. Equation (8.4) has a unique solution analytic at $x = 0$. For $w = 0$, it is satisfied by the generating function of Dyck paths, weighted with respect to their area and half-length, which was considered in Chapter 4.

We also note that every DDP can be mapped onto a (standard) Dyck path by replacing every jump step by two consecutive up-steps. In this way, each Dyck path represents a family of DDP – see Fig. 8.3. The function $G(w, x, q)$ can therefore alternatively be interpreted as the generating function of Dyck paths, weighted with respect to their half-length and their area, with an additional weight $F_k(w/x, 1/q)$ associated to each sequence of k consecutive up-steps, followed by a down-step. Here, $F_k(s, q)$ is the generating function of appropriately weighted dimer coverings of an interval of length k (for $q = 1$, see [76]).

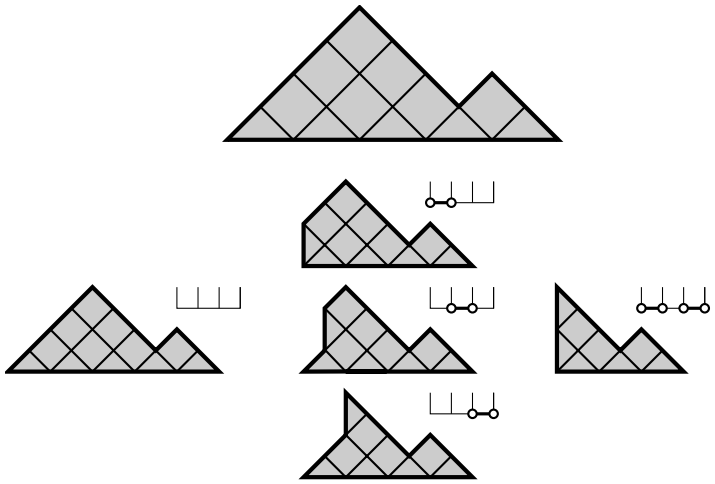

Figure 8.3: A Dyck path (top) and the family of DDP representing it, together with the corresponding dimer coverings.

The q-Fibonacci polynomials $F_k(s,q) \equiv F_k$ satisfy the recurrence

$$F_0 = F_1 = 1\ , \quad F_n = F_{n-1} + q^{n-1} s F_{n-2} \quad \text{for } n \geq 2 \tag{8.5}$$

and are given explicitly by

$$F_k(s,q) = \sum_{l=0}^{\lfloor k/2 \rfloor} \begin{bmatrix} k-l \\ l \end{bmatrix}_q q^{l^2} s^l\ , \tag{8.6}$$

see [15]. Using the dimer interpretation, a decomposition of Dyck paths by their left-most rise leads to an alternative functional equation for $G(w,x,q) = G(x)$,

$$G(x) = \sum_{k=0}^{\infty} x^k q^{\binom{k}{2}} F_k(w/x, 1/q) \prod_{l=0}^{k-1} G(q^l x)\ . \tag{8.7}$$

For $q = 1$, it follows from Viennot's Inversion Lemma [76] and the asymptotic behaviour of the number of dimer coverings [10] that $F_k(w/x, 1) \geq 0$ for $w/x \geq -1/4$.

8.3 Solution of the functional equation

Analogous to the case of Dyck and Schröder paths [26, 35], inserting the ansatz

$$G(w,x,q) = \frac{H(w,qx,q)}{H(w,x,q)}, \tag{8.8}$$

into Eq. (8.4) leads to the linearised functional equation

$$\big(x(1+w\sigma)\sigma^2 + (1-\sigma)\big)H(x) = 0, \tag{8.9}$$

where $H(x) = H(w,x,q)$ and $\sigma^n H(x) = H(q^n x)$ for $n \in \mathbb{Z}_{\geq 0}$. Comparing this equation with Eq. (5.4), we see that for $w, x, q \in \mathbb{C}$ and $|q| < 1$, Eq. (8.9) is solved by the basic hypergeometric series

$$H(w,x,q) = {}_1\phi_2(-w;0,0;q,-x) = \sum_{n=0}^{\infty} \frac{(-w;q)_n}{(q;q)_n}(-x)^n q^{n^2-n}. \tag{8.10}$$

In the following we write ${}_1\phi_2(-w;0,0;q,-x) = \phi(w,x,q)$. For $q \to 1^-$, both $\phi(w,x,q)$ and $\phi(w,qx,q)$ diverge and it is therefore not immediately clear which value $G(w,x,q)$ takes in this limit. But if we substitute $q = 1$ into Eq. (8.4), then we obtain a cubic equation for $G(w,x,1)$, which is readily solved. In the special case $w = -\frac{1}{9}$, the radius of convergence of $G(w,x,1)$ is determined by a cubic root singularity at $x = \frac{1}{3}$ and around this value we therefore expect an area-length scaling behaviour which is qualitatively different from the Airy function scaling found for Dyck and Schröder paths and staircase polygons. In order to analyse the asymptotics of the generating function in the vicinity of the point $w = -\frac{1}{9}$, $x = \frac{1}{3}$ as $q \to 1^-$, we apply the method of steepest descent, generalised to the case of several coalescing saddle points.

8.4 The main result

The principal result of this chapter is stated in the following theorem, which is an immediate consequence of Prop. 8.9.1.

Theorem 8.4.1. *Let* $q = e^{-\epsilon}$, $\delta = \mathcal{O}\big(\epsilon^{1/2}\big)$ *and* $\xi = \frac{3}{2}\delta + \mathcal{O}\big(\epsilon^{3/4}\big)$ *as* $\epsilon \to 0^+$. *Then*

$$G\left(\delta - \frac{1}{9}, \frac{1}{3} - \xi, q\right) = 3\left(1 + 2^{1/4}\,\Phi(s_1, s_2)\,\epsilon^{1/4} + \mathcal{O}\big(\epsilon^{1/2}\big)\right), \tag{8.11}$$

as $\epsilon \to 0^+$, *for all* $s_1, s_2 \in \mathbb{R}$ *such that* $|\Phi(s_1, s_2)| < \infty$, *where*

$$s_1 = 3\sqrt[4]{2}\left(\xi - \frac{3}{2}\delta\right)\epsilon^{-3/4} \text{ and } \; s_2 = \frac{27\sqrt{2}}{8}\left(\delta + \frac{1}{40}\xi^2\right)\epsilon^{-1/2}, \tag{8.12}$$

and where $\Phi(s_1, s_2)$ *is defined in Eq. (8.2).*

For example, Theorem 8.4.1 gives for all s such that $|\Phi(s, 0)| < \infty$,

$$G\left(-\frac{1}{9}, \frac{1}{3}\left(1 - s\epsilon^{\phi_c}\right), q\right) = 3\left(1 + F\big(s\big)\epsilon^{\theta_c} + \mathcal{O}\big(\epsilon^{1/2}\big)\right) \tag{8.13}$$

as $q = e^{-\epsilon} \to 1^-$, with $F(s) = \sqrt[4]{2}\Phi(\sqrt[4]{2}s, 0)$, $\theta_c = \frac{1}{4}$ and $\phi_c = \frac{3}{4}$.

The exponents θ_c and ϕ_c, together with $\gamma_c = \frac{\theta_c}{\phi_c} = \frac{1}{3}$ characterise the singular behaviour of $G(-\frac{1}{9}, x, q)$ around the multicritical point $(w, x, q) = (-\frac{1}{9}, \frac{1}{3}, 1)$. The singular behaviour of $G\left(-\frac{1}{9}, \frac{1}{3}, 1 - \epsilon\right)$ as $\epsilon \to 0^+$ is determined by θ_c, γ_c describes the singular behaviour of $G(-\frac{1}{9}, x, 1)$ as $x \to \frac{1}{3}^-$, and ϕ_c is called the crossover exponent of the model.

The multicritical point for $w = -\frac{1}{9}$ is the endpoint of a line of tricritical points $(w, x, q) = (w, x_c(w), 1)$ for $w > -\frac{1}{9}$, which are characterised by the exponents $\theta_c = \frac{1}{3}$, $\gamma_c = \frac{1}{2}$ and hence $\phi_c = \frac{2}{3}$. The special case $w = 0$ was analysed in Chapter 4. In Table 8.1 we summarise the values of the critical

w	γ_c	θ_c	ϕ_c
$-\frac{1}{9}$	$\frac{1}{3}$	$\frac{1}{4}$	$\frac{3}{4}$
$> -\frac{1}{9}$	$\frac{1}{2}$	$\frac{1}{3}$	$\frac{2}{3}$

Table 8.1: The critical exponents characterising the singular behaviour of the generating function of DDP around the multicritical point, depending on the value of w.

exponents for $w = -\frac{1}{9}$ and $w > -\frac{1}{9}$.

8.5 Contour integral representation of $\phi(a, q^k x, q)$

For $k \in \mathbb{Z}$, Lemma 5.4.2 gives a contour integral representation of the function $\phi(q^k x) \equiv \phi(a, q^k x, q) = {}_1\phi_2(a; 0, 0; q, -q^k x)$. In this special case, the functions in Eq. (5.25) are

$$f(z) = \ln(x)\ln(z) + \mathrm{Li}_2(z) - \frac{1}{2}\ln(z)^2 + \mathrm{Li}_2\left(\frac{a}{z}\right), \tag{8.14}$$

$$g_k(z, q) = \frac{1}{z^k}\left(\frac{z^2}{(1-z)(z-a)}\right)^{\frac{1}{2}} \exp\Big(\epsilon S(z, q)\Big), \tag{8.15}$$

where $\epsilon = -\ln(q)$ and $S(z, q)$ is bounded on the contour C. For $0 < a < 1$, $f(z)$ and $g_k(z, q)$ are real on the segment $a < z < 1$, therefore in this case, $f(z^*) = f(z)^*$ and $g_k(z^*, q) = g_k(z, q)^*$, and $f(z)$ is analytic for $z \in \mathbb{C} \setminus \big(-\infty, a\big] \cup \big[1, \infty\big)$. In Section 5.5, the saddle point landscape of a class of q-hypergeometric series was considered. In the following section, we provide a more detailed discussion for the specific series $\phi(a, q^k x, q)$.

8.6 Location of the saddle points

The saddle points of the function f given in Eq. (8.14) are the zeros of the derivative

$$f'(z) = \frac{1}{z} \ln \left(\frac{x\,(z-a)}{z^2(1-z)} \right), \tag{8.16}$$

which coincide with the zeros of the polynomial

$$s(z) = z^3 - z^2 + x\,z - x\,a. \tag{8.17}$$

Hence, $f(z)$ has (up to multiplicity) three saddle points z_i $(i = 1, 2, 3)$, which satisfy

$$\left.\begin{aligned} z_1 + z_2 + z_3 &= 1 \\ z_1 z_2 + z_2 z_3 + z_3 z_1 &= x \\ z_1 z_2 z_3 &= xa \end{aligned}\right\}. \tag{8.18}$$

If the parameter x takes one of the two values

$$x_c^{\pm} = \frac{1}{8} \left(1 + 18a - 27a^2 \pm (1-9a)\sqrt{9a^2 - 10a + 1} \right), \tag{8.19}$$

then two saddle points coalesce in one of the points

$$z_c^{\pm} = \frac{1}{4} \left(3a + 1 \pm \sqrt{9a^2 - 10a + 1} \right). \tag{8.20}$$

In Fig. 8.4 we show the dependence of the two critical values $x_c^{\pm}$ as functions of a. Concerning the location of the saddle points z_1, z_2 and z_3 in the complex plane, we distinguish the following 5 cases.

(i) If $a < 0$, then two saddle points coalesce for $x = x_c^+ < 1/4$, while the third one is negative.

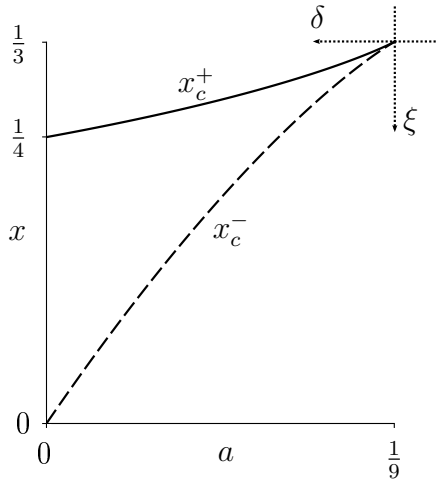

Figure 8.4: Plot of the critical values $x_c^{\pm}$ as functions of a. The picture also shows the orientation of the natural coordinates $\xi = 1/3 - x$ and $\delta = 1/9 - a$ which will be used later on.

(ii) If $a = 0$, then one saddle point is constantly zero while the other two coalesce in $z_c = 1/2$ for $x = x_c^+ = 1/4$.

(iii) If $0 < a < 1/9$, then two saddle points are mutually complex conjugates for $0 < x < x_c^- < 1/3$ and coalesce on the positive real line for $x = x_c^-$ in the point z_c^-, where $a < z_c^- < 1/3$. For $x_c^- < x < x_c^+$, all three saddle points are real and for $x = x_c^+ < 1/3$, two saddle points coalesce in the point $1/3 < z_c^+ < 1/2$. For $x > x_c^+$, again one saddle point is real and the other two are mutually complex conjugates.

(iv) If $a = 1/9$, then $x_c^- = x_c^+ = 1/3$, hence all three saddle points coalesce in the same point, $z_c^- = z_c^+ = 1/3$.

(v) If $a > 1/9$, then there is no saddle point coalescence for $x > 0$.

8.7 Geometry of the paths of steepest descent

In this section we are going to discuss the geometry of the paths of steepest descent of f since, for $a > 0$, this case is not covered by Lemma 5.5.5.

Note that for real z, real $x > 0$ and $0 < a < 1$,

$$\mathrm{Im}(f(z)) = \begin{cases} \pi \ln(x/|z|) & (z < 0) \\ \pi \ln(z/a) & (0 < z \leq a) \\ 0 & (a \leq z \leq 1) \\ -\pi \ln(z) & (z \geq 1) \end{cases}. \tag{8.21}$$

From the sign of the imaginary part of $f'(z)$, we can conclude that paths of steepest descent of the function $\mathcal{R}(z) = \mathrm{Re}(f(z))$ cannot end at the branch cut of the logarithm. Using Lemma 5.5.1 we prove the following result.

Lemma 8.7.1. *For real $a \leq 1/9$ and $0 < x \leq x_c^+(a)$, there exists a continuous curve $c : \mathbb{R} \to \mathbb{C}$, with $c(0) = z_3$ and $\mathrm{Im}\big(c(\lambda)\big) \gtrless 0$ for $\lambda \gtrless 0$, such that*

$$\mathcal{I}(z) = \mathrm{Im}\big(f\big(c(\lambda)\big)\big) = 0 \tag{8.22}$$

for $\lambda \in \mathbb{R}$, $|c(\lambda)| \to \infty$ for $\lambda \to \pm\infty$ and

$$\lim_{\lambda \to \pm\infty} \arg\big(c(\lambda)\big) = \pm\frac{\pi}{2}. \tag{8.23}$$

Proof. Assume $a \leq 1/9$ and $0 < x \leq x_c^+(a)$. According to the discussion above, we label the saddle points in such a way that z_1 and z_2 are mutually complex conjugates for $x < x_c^-(a)$ with $\mathrm{Im}(z_1) > 0$ while z_3 is real, and z_2

coalesces with z_3 for $x = x_c^+(a)$. From the asymptotic behaviour of $f(z)$ stated in Lemma 5.5.1, we can conclude that paths of steepest descent of $\mathcal{R}(z) = \mathrm{Re}(f(z))$ can only end in $z = 0$ or at $\infty \exp(\pm i\pi/2)$. Since $f(z^*) = f(z)^*$, it is sufficient to consider the paths of steepest ascent and descent which lie in the upper half-plane. There are two cases to be distinguished.

1. $0 < x < x_c^-(a)$. In this case, z_3 is real while $\mathrm{Im}(z_1) > 0$. One of the two paths of steepest descents originating from z_1 ends in $z = 0$, while the other one ends at infinity. Since paths of steepest descent of $\mathcal{R}(z)$ can only cross in saddle points, it follows that the path of steepest descent emerging from z_3 necessarily ends at $\infty \exp(i\pi/2)$. Figure 8.5 (a) shows an example for this case.

2. $x_c^-(a) \leq x \leq x_c^+(a)$. In this case, all three saddle points are real. The path of steepest descent originating from z_1 necessarily ends at zero, while the path of steepest ascent of $\mathcal{R}(z)$ originating from z_2 ends in the point $z = -x$. Again it follows that the path of steepest descent of $\mathcal{R}(z)$ originating from z_3 ends at $\infty \exp(i\pi/2)$. Figure 8.5 (b) shows an example for $x_c^-(a) < x < x_c^+(a)$ for $a < 1/9$ and (c) shows the special case $a = 1/9$, for which the three saddle points coalesce.

For $0 < x \leq x_c^+(a)$, $\mathcal{I}(f(z_3)) = 0$. Since the paths of steepest descent are the contours on which the imaginary part of $f(z)$ is constant, the union of the two paths of steepest descent originating from z_3 and ending at $\infty \exp(i\pi/2)$ and $\infty \exp(-i\pi/2)$ respectively, has the properties of the curve $c(\lambda)$. □

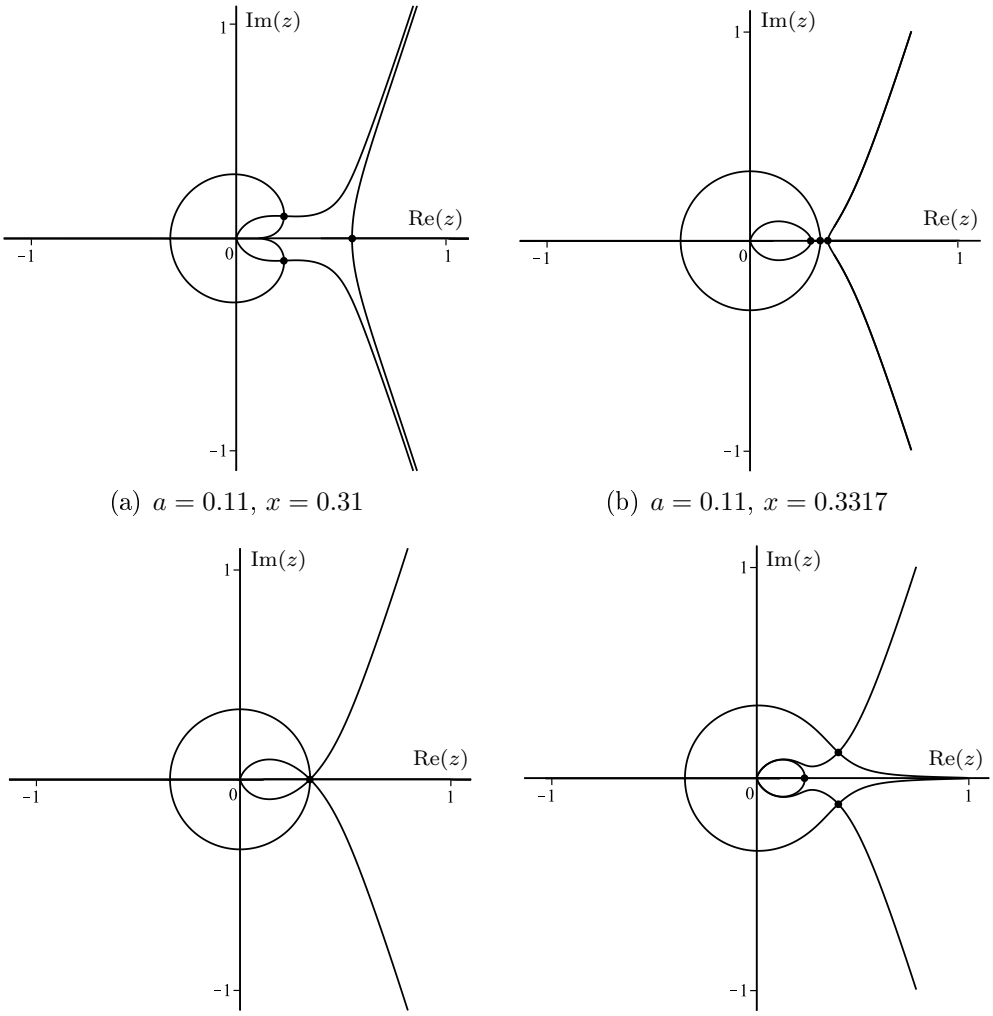

(a) $a = 0.11$, $x = 0.31$

(b) $a = 0.11$, $x = 0.3317$

(c) $a = 1/9$, $x = 1/3$

(d) $a = 0.11$, $x = 0.34$

Figure 8.5: The saddle points of the function $f(z)$ defined in Eq. (8.14) (marked by small black dots) and the paths of steepest descent and ascent of $\mathcal{R}(z) = \mathrm{Re}(f(z))$ originating from them. The case (d) is shown for completeness, though not considered in the text.

8.8 Transformation of $f(z)$ into a canonical form

As we discussed in Section 8.6, for $a = 1/9$, the three saddle points of $f(z)$ coalesce in the point $z_c = 1/3$ for $x = x_c^+(1/9) = 1/3$. We now define the natural coordinates

$$\xi = \frac{1}{3} - x \quad \text{and} \quad \delta = \frac{1}{9} - a, \tag{8.24}$$

and consider $f(z)$ and $g_k(z, q)$ as functions of z, ξ and δ from now on.

Theorem 2.2.3 states that there is a map $z \mapsto u(z)$, such that

$$f(z) = \frac{1}{4}\, u^4 - \alpha\, u^2 - \beta\, u + \gamma = p(u), \tag{8.25}$$

which is regular and bijective if $z - z_c$, ξ and δ are sufficiently close to zero. The coefficients α, β and γ are regular functions of ξ and δ. Thus,

$$\alpha = \sum_{j,k=0}^{\infty} \alpha_{j,k} \xi^j \delta^k \quad ; \quad \beta = \sum_{j,k=0}^{\infty} \beta_{j,k} \xi^j \delta^k \quad ; \quad \gamma = \sum_{j,k=0}^{\infty} \gamma_{j,k} \xi^j \delta^k. \tag{8.26}$$

Note that α and β are not unique, since the form of the RHS of Eq. (8.25) is invariant under rotations about the angle $k\pi/2$, where $k \in \mathbb{Z}$.

We denote the three saddle points of the polynomial $p(u)$ by u_1, u_2 and u_3, hence

$$p'(u) = u^3 - 2\alpha u - \beta = (u - u_1)(u - u_2)(u - u_3). \tag{8.27}$$

From Eq. (8.27) it follows that

$$u_1 + u_2 + u_3 = 0, \tag{8.28a}$$

$$u_1u_2 + u_2u_3 + u_3u_1 + 2\alpha = 0, \tag{8.28b}$$

$$u_1u_2u_3 - \beta = 0. \tag{8.28c}$$

As a necessary condition for the transformation defined in Eq. (8.25) to be regular, the saddle points of of $f(z)$ need to be mapped onto the saddle points of $p(u)$. For $\xi = \delta = 0$, the three saddle points of $f(z)$ coalesce and it follows from Eq. (8.28a) that $u_1 = u_2 = u_3 = 0$. With this we obtain from Eqs. (8.28b) and (8.28c) that $\alpha_{0,0} = \beta_{0,0} = 0$.

If we label the saddle points of $p(u)$ such that $u(z_j) = u_j$ for $j = 1, 2$ and 3, then from Eq. (8.25) it follows by differentiating twice that

$$\left.\frac{dz}{du}\right|_{u=u_i} = \left(\frac{3u_i^2 - 2\alpha}{f''(z_i)}\right)^{\frac{1}{2}}, \tag{8.29}$$

for $(\xi, \delta) \neq (0, 0)$. For $\xi = \delta = 0$, we get by taking higher derivatives that

$$\left.\frac{dz}{du}\right|_{u=0} = \frac{2^{\frac{1}{4}}}{3}, \quad \left.\frac{d^2z}{du^2}\right|_{u=0} = \frac{2^{\frac{1}{2}}}{3} \quad \text{and} \quad \left.\frac{d^3z}{du^3}\right|_{u=0} = \frac{2^{\frac{3}{4}}}{6}. \tag{8.30}$$

Since $u_j^3 = 2\alpha u_j + \beta$ for $j = 1, 2$ and 3, we have

$$f(z_j) = -\frac{1}{2}\,\alpha\, u_j^2 - \frac{3}{4}\,\beta\, u_j + \gamma. \tag{8.31}$$

Using Eqs. (8.28a) to (8.28c) and Eq. (8.31), we obtain the following set

of equations, where $\Sigma^{(k)} = \sum_{j=1}^{3} f(z_j)^k$ for $k = 1, 2$ and 3:

$$3\gamma - 2\alpha^2 = \Sigma^{(1)} \tag{8.32a}$$

$$3\gamma^2 + \frac{9}{2}\alpha\beta^2 - 4\alpha^2\gamma + 2\alpha^4 = \Sigma^{(2)} \tag{8.32b}$$

$$3\gamma^3 - \frac{81}{64}\beta^4 + \frac{27}{2}\alpha\beta^2\gamma - 6\alpha^2\gamma^2 - \frac{51}{4}\,\alpha^3\beta^2 + 6\,\alpha^4\gamma - 2\alpha^6 = \Sigma^{(3)}. \tag{8.32c}$$

From Eqs. (8.32a) to (8.32c) we derive

$$2\alpha^4 + \frac{27}{2}\alpha\beta^2 = 3\Sigma^{(2)} - \left(\Sigma^{(1)}\right)^2 \tag{8.33a}$$

$$\alpha^6 - \frac{135}{8}\alpha^3\beta^2 - \frac{729}{128}\beta^4 = \left(\Sigma^{(1)}\right)^3 + \frac{9}{2}\Big(\Sigma^{(3)} - \Sigma^{(1)}\Sigma^{(2)}\Big). \tag{8.33b}$$

With Eqs. (8.32a) to (8.32c), (8.33a) and (8.33b) we are now going to calculate the leading coefficients of the power series expansions (8.26). We will begin by considering the cases $\delta = 0$ and $\xi = 0$ separately.

8.8.1 Coefficient asymptotics for $\xi \to 0$ and $\delta = 0$

From the above discussion we know that for $\delta = 0$ and $\xi \to 0$, $\alpha \sim \alpha_{r_\alpha,0}\xi^{r_\alpha}$ and $\beta \sim \beta_{r_\beta,0}\xi^{r_\beta}$, where $r_\alpha, r_\beta \in \mathbb{N}$ and $\alpha_{r_\alpha,0}, \beta_{r_\beta,0} \neq 0$.

To determine r_β, we take the third derivative of Eq. (8.25) with respect to u and insert the saddle point values. This gives us

$$f'''(z_j)\left(\left.\frac{dz}{du}\right|_{u_j}\right)^3 + 3f''(z_j)\left.\frac{dz}{du}\right|_{u_j}\left.\frac{d^2z}{du^2}\right|_{u_j} = 6\,u_j \tag{8.34}$$

for $j = 1, 2$ and 3. Expanding both $f''(z_j)$ and $f'''(z_j)$ as series in ξ shows that for $\xi \to 0^+$, $f''(z_j) = o(\xi^{1/3})$. Moreover, for $k = 1, 2$ and 3,

$$f'''(z_k) = c_0 \exp\left(\frac{2k\pi i}{3}\right)\xi^{\frac{1}{3}} + \mathcal{O}(\xi^{\frac{2}{3}}), \tag{8.35}$$

where $c_0 = 81 \cdot 6^{1/3}$, and from this it follows together with (8.30) that

$$u_k = u_0 \exp\left(\frac{2k\pi i}{3}\right) \xi^{\frac{1}{3}} + \mathcal{O}(\xi^{\frac{2}{3}}), \tag{8.36}$$

where $u_0 = 6^{\frac{1}{3}}/2^{\frac{1}{4}}$. From Eq. (8.28c) we therefore conclude that $r_\beta = 1$. With this we can now determine r_α. From Eq. (8.33a), we obtain for $\delta = 0$ and $\xi \to 0$

$$2\,\alpha^4 + \frac{27}{2}\alpha\beta^2 = \frac{6561}{320}\xi^4 + \mathcal{O}(\xi^5). \tag{8.37}$$

It follows by the following dominant balance argument that $r_\alpha = 2$. There are three possibilities to be distinguished. The first possibility is that $\alpha^4 = o(\alpha\beta^2)$, from which it would follow that $r_\alpha + 2 = 4$, hence $r_\alpha = 2$. The second possibility is that $\alpha\beta^2 = o(\alpha^4)$, from which it would follow that $4\,r_\alpha = 4$, hence $r_\alpha = 1$. However, this would mean that $r_\alpha + 2 = 3$, which stands in contradiction to the assumption that $\alpha\beta^2 = o(\alpha^4)$. The third possibility is that the leading terms of α^4 and $\alpha\beta^2$ cancel each other. In that case, $4\,r_\alpha = r_\alpha + 2$, hence $r_\alpha = 2/3$, which is impossible. We conclude that $r_\alpha = 2$.

Expanding the RHS of Eq. (8.32a) for $\delta = 0$ in ξ, we get

$$\gamma_{0,0} = 2\,\mathrm{Li}_2\left(\frac{1}{3}\right) + \frac{1}{2}\ln(3)^2, \tag{8.38}$$

and using Eq. (8.37) and expanding Eq.(8.33b) in ξ for $\delta = 0$, we obtain $\alpha_{1,0}\beta_{1,0}^2$ and $\beta_{1,0}^4$. Choosing the real positive root for $\beta_{1,0}$, we arrive at

$$\alpha_{2,0} = \frac{27\sqrt{2}}{320} \quad \text{and} \quad \beta_{1,0} = 3\sqrt[4]{2}. \tag{8.39}$$

One can easily calculate further expansion coefficients, but here we will

only give the results for the leading orders.

8.8.2 Coefficient asymptotics for $\delta \to 0$ and $\xi = 0$

It follows from an argument analogous to the one given in the previous subsection that for $\xi = 0$ and $\delta \to 0$, $\alpha \sim \alpha_{0,1}\delta$ and $\beta \sim \beta_{0,1}\delta$, where $\alpha_{0,1}, \beta_{0,1} \neq 0$.

Again using Eqs.(8.33a-b), we obtain the values for $\alpha_{0,1}\beta_{0,1}^2$ and $\beta_{0,1}^4$. Since in the previous subsection we have chosen the positive root for $\beta_{1,0}$, we need to make sure to choose the correct root for $\beta_{0,1}$. Setting $\delta = -\xi$ and expanding the RHS of Eq. (8.33b) in ξ, we get $\beta_{1,0} - \beta_{0,1} = (15/2)\sqrt[4]{2}$. From this it follows that we need to choose the real negative root for $\beta_{0,1}$. We obtain

$$\alpha_{0,1} = \frac{27\sqrt{2}}{8} \quad \text{and} \quad \beta_{0,1} = -\frac{9}{2}\sqrt[4]{2}. \tag{8.40}$$

Combining Eqs. (8.39) and (8.40), we get that for $(\xi, \delta) \to (0, 0)$,

$$\alpha \sim \frac{27\sqrt{2}}{8}\left(\delta + \frac{1}{40}\xi^2\right) \quad \text{and} \quad \beta \sim 3\sqrt[4]{2}\left(\xi - \frac{3}{2}\delta\right). \tag{8.41}$$

8.9 Asymptotics of $\phi(a, q^k x, q)$

It follows from Lemma 8.7.1 together with Cauchy's theorem that for $0 < x \leq 1/3$ and $a \leq 1/9$, we can replace the integration contour in Eq. (5.25) by a contour C_0 originating from $\infty \exp(-i\frac{\pi}{2})$, passing through the real valued saddle point z_3 of $f(z)$ and ending at $\infty \exp(i\frac{\pi}{2})$, such that $\operatorname{Im} f(z) = 0$ on this contour and $\operatorname{Re} f(z)$ is maximal at z_3.

The correction due to restricting C_0 to the central part C_0' on which the transformation defined in Eq. (8.25) is regular decays exponentially in the limit $\epsilon \to 0^+$. The segment $u(C_0')$ is the central part of the contour

given by the union of the two paths of steepest descent of $p(u)$ ending at $\infty \exp(\pm i\pi/4)$. Extending the integration to the complete contour, we obtain

$$\phi(a, q^k x, q) = \frac{A(a,q)}{2\pi i} \int_{c_- \infty}^{c_+ \infty} \exp\left(\frac{1}{\epsilon} p(u)\right) G^{(k)}(u) \Big(1 + \mathcal{O}(\epsilon)\Big) du, \quad (8.42)$$

where $c_\pm = \exp\left(\pm i \frac{\pi}{4}\right)$, and

$$G^{(k)}(u) = \frac{g_0(z(u))}{z(u)^k} \frac{dz}{du}. \quad (8.43)$$

In order to calculate the leading asymptotic contribution to $\phi(a, q^k t, q)$, we use the ansatz [73]

$$G^{(k)}(u) = P^{(k)} + uQ^{(k)} + u^2 R^{(k)} + (u^3 - 2\alpha u - \beta) S^{(k)}(u), \quad (8.44)$$

where $S^{(k)}(u)$ is an analytic function of u, ξ and δ and $P^{(k)}$, $Q^{(k)}$ and $R^{(k)}$ are analytic functions of ξ and δ. Inserting the saddle point values into Eq. (8.44), we get for $j = 1, 2$ and 3,

$$G^{(k)}(u_j) = P^{(k)} + u_j Q^{(k)} + u_j^2 R^{(k)}. \quad (8.45)$$

Evaluating Eq. (8.44) and the first and second derivative with respect to u at $u = 0$ for $\xi = \delta = 0$ gives together with (8.30) for $\xi = \delta = 0$,

$$\begin{aligned} P^{(0)} &= \frac{2^{1/4}\sqrt{3}}{6}, \quad Q^{(0)} = \frac{\sqrt{6}}{4}, \quad R^{(0)} = \frac{5\, 2^{3/4}\sqrt{3}}{24}, \\ P^{(1)} &= \frac{2^{1/4}\sqrt{3}}{2}, \quad Q^{(1)} = \frac{\sqrt{6}}{4}, \quad R^{(1)} = \frac{2^{3/4}\sqrt{3}}{8}. \end{aligned} \quad (8.46)$$

From Eq. (8.1) we define the functions

$$\Theta_4^{(1)}(x,y) = \frac{\partial}{\partial x}\Theta_4(x,y) \quad \text{and} \quad \Theta_4^{(2)}(x,y) = \frac{\partial}{\partial y}\Theta_4(x,y). \tag{8.47}$$

Note that $\Theta_4(x,y)$ is related to the Pearcey integral

$$\mathcal{P}(x,y) = 2\exp\left(\frac{i\pi}{8}\right)\int_0^\infty \exp\left(-u^4 - yu^2\right)\cos(xu)du, \tag{8.48}$$

the asymptotics of which have been studied in [50], via the formula

$$\mathcal{P}(x,y) = \frac{\sqrt{2}\,\pi}{\exp\left(i\frac{\pi}{8}\right)}\left[\Theta_4\left(\frac{1-i}{2}x, \frac{iy}{2}\right) + i\,\Theta_4\left(\frac{1+i}{2}x, \frac{-iy}{2}\right)\right]. \tag{8.49}$$

Applying Theorem 2 from [73], we can now formulate the following result.

Proposition 8.9.1. *For $k \in \mathbb{Z}_{\geq 0}$, there exist constants $d_a, d_x > 0$ such that for $a \in \left[\frac{1}{9} - d_a, \frac{1}{9} + d_a\right]$ and $x \in \left[\frac{1}{3} - d_x, \frac{1}{3} + d_x\right]$ and $q = e^{-\epsilon} \to 1^-$, we have*

$$\begin{aligned}\phi(a, q^k x, q) = A(a,q)\,\exp\left(\frac{\gamma}{\epsilon}\right)\,\Big[&P^{(k)}\,\epsilon^{1/4}\,\Theta_4\left(\frac{\beta}{\epsilon^{3/4}}, \frac{\alpha}{\epsilon^{1/2}}\right) - \\ &- Q^{(k)}\,\epsilon^{1/2}\Theta_4^{(1)}\left(\frac{\beta}{\epsilon^{3/4}}, \frac{\alpha}{\epsilon^{1/2}}\right) - R^{(k)}\,\epsilon^{3/4}\,\Theta_4^{(2)}\left(\frac{\beta}{\epsilon^{3/4}}, \frac{\alpha}{\epsilon^{1/2}}\right)\Big]\big(1 + \mathcal{O}(\epsilon)\big),\end{aligned} \tag{8.50}$$

uniformly, where the coefficients α, β, γ and $P^{(k)}, Q^{(k)}, R^{(k)}$ are regular functions of a and x and $A(a,q) = (q;q)_\infty (a;q)_\infty$.

Substituting Eq. (8.50) into Eq. (8.8) for $k = 0$ and 1 and $a = -w$, we obtain the scaling behaviour of $G(w,x,q)$ around the critical point $(w,x,q) = (-\frac{1}{9}, \frac{1}{3}, 1)$ as stated in Theorem 8.4.1. In Fig. 8.6, we show the convergence of the asymptotic approximation of $F(s)$ obtained by rearran-

ging Eq. (8.13) against the exact scaling function.

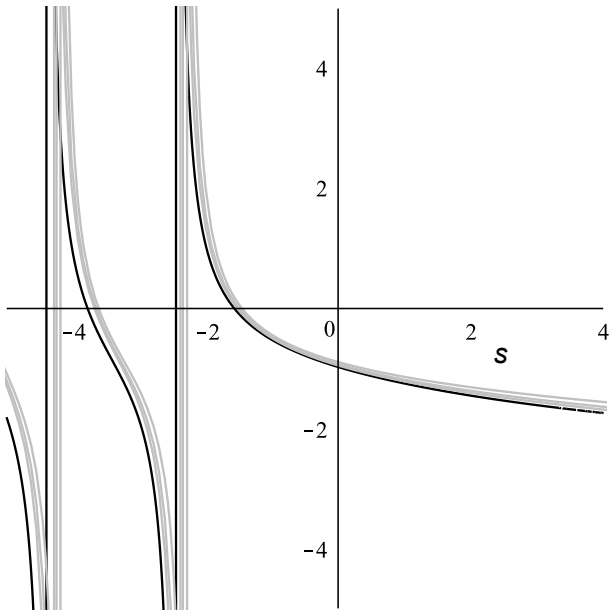

Figure 8.6: Plot of the scaling function $F\big(\sqrt[4]{2}\,s\big) = \Phi\big(\sqrt[4]{2}\,s, 0\big)$ (black) and the asymptotic approximation obtained from rearranging Eq. (8.13) for $\epsilon = 10^{-4}, 10^{-5}, 10^{-6}$ (grey, the smallest value corresponds to the closest approximation).

As discussed in Lemma 8.7.1, for $a < \frac{1}{9}$ and $0 < x < x_c^+(a)$, the integration contour C used in Eq. (5.25) can be deformed such that it consists of two paths of steepest descent, connecting a saddle point on the real axis with infinity, and the asymptotics of $\phi(a, q^k x, q)$ can be obtained via the ordinary method of steepest descent. According to Section 8.6, the relevant saddle point coalesces with another saddle point for $x = x_c^+(a) < \frac{1}{3}$. At this point, $\phi(a, q^k x, q)$ can be approximated in terms of Airy functions, with the special case $a = 0$ having been treated in Chapter 4.

9 Summary and Outlook

In Chapter 3, we made a conjecture on the tricritical scaling behaviour of the area-width generating function of a class of generalised Motzkin paths, subject to the assumption that their generating functions satisfy a certain scaling relation around the tricritical point. This class includes in particular Dyck paths, (standard) Motzkin paths and Schröder paths. Our argument consisted in substituting the conjectured asymptotic form of the generating function into the functional equation satisfied by it, leading to the unique determination of the tricritical exponents and the scaling function. For all models within the class of generalised Motzkin paths, the tricritical exponents were determined as $(\gamma_c, \theta_c, \phi_c) = (\frac{1}{2}, \frac{1}{3}, \frac{2}{3})$, and the scaling function is, up to model-dependent prefactors, the logarithmic derivative of the Airy function.

In Chapter 4 we used an expression for the area-width generating function of Dyck paths in terms of a fraction of q-hypergeometric series to obtain an asymptotic expression of it in terms of the Airy function and its derivative in the limit when the area generating variable tends to 1. The asymptotic expression is uniform for a range of values of the width generating variable, in particular in the region around the tricritical point. This confirmed in particular the scaling behaviour of Dyck paths derived non-rigorously in Chapter 3.

The asymptotic analysis of the q-hypergeometric series involved in the

area-width generating function of Dyck paths was generalised in Chapter 5 to a class of q-hypergeometric series. In Chapter 6 we used the general results to obtain asymptotic expressions for the area-width generating function of Schröder paths, the area-perimeter generating function of directed column-convex polygons and the length-interaction generating function of interacting partially directed self-avoiding walks. In all three cases, the expressions involve the Airy function and its derivative, and for Schröder paths, the scaling relation conjectured in Chapter 3 is confirmed.

In Chapter 7, we use the asymptotic expressions derived in Chapter 4 to analyse the scaling behaviour of the area-length generating function of Bernoulli meanders in the vicinity of the tricritical point. Here, the tricritical exponents are $(\gamma_c, \theta_c, \phi_c) = (-\frac{1}{2}, -\frac{1}{3}, \frac{2}{3})$ and the scaling function is expressible in terms of the Airy function and its integral.

In Chapter 8, we defined a model of Dyck paths with an enriched step set, which we called deformed Dyck paths. Precisely, apart from the diagonal steps allowed for Dyck paths, 'jumps' orthogonal to the preferred direction of the path are allowed. We considered the generating function of DDP, weighted with respect to their width, their number of jumps and their area. As in the previous chapters, we used the method of steepest descents to the q-hypergeometric series involved in the exact solution of the generating function. For a given set of values of the weights of the model, three saddle points coalesce in the kernel of the associated integral. This leads to an asymptotic expression for the generating function in terms of a bivariate, higher-order Airy function.

The obvious continuation of this thesis is to consider further models in statistical physics and combinatorics which are amenable to our set of methods. More concretely, the model of DDP can be extended further

by introducing jumps of different height. The generating function of these paths, which are weighted with respect to their width, their area and where additionally, the jumps obtain different weights according to their heights, has a solution in terms of q-hypergeometric series, of the same structure as the one of Dyck paths and DDP. The asymptotic analysis of this multivariate generating function in the limit of the area weight tending towards one can again be done via the method of steepest descents. For special values of the weights of the jumps, arbitrarily many saddle points coalesce in the corresponding integral kernel. This leads to asymptotic expressions in terms of generalised, multivariate Airy integrals. The details, however, require some more care. Technically, the biggest problem is to show that the paths of steepest descent of the integral kernel behave in a suitable way.

Bibliography

[1] M. Aigner. *A Course in Enumeration*. Springer–Verlag, Berlin Heidelberg, 2007.

[2] B. Alberts. Intracellular vesicular traffic. In *Molecular biology of the cell*, chapter 13. Garland Science, Taylor and Francis Group, 2007.

[3] T. M. Allen and P. R. Cullis. Liposomal drug delivery systems: From concept to clinical applications. *Advanced Drug Delivery Reviews*, 65:36–48, 2013.

[4] S. Banach. Sur les opérations dans les ensembles abstraits et leur application aux équations intégrales. *Fund. Math.*, 3:133–181, 1922.

[5] C. Banderier and P. Flajolet. Basic analytic combinatorics of directed lattice paths. *Theoretical Computer Science*, 281(1):37–80, June 2002.

[6] C. Banderier, P. Flajolet, G. Schaeffer, and M. Soria. Random maps, coalescing saddles, singularity analysis, and Airy phenomena. *Random Structures & Algorithms*, 19:194–246, 2001.

[7] C. Banderier and B. Gittenberger. Analytic combinatorics of lattice paths: Enumeration and asymptotics for the area. In *Fourth Colloquium on Mathematics and Computer Science, DMTCS Proceedings AG*, pages 345–356, 2006.

[8] R. Becker. *Theorie der Wärme*, volume 10 of *Heidelberger Taschenbücher*. Springer-Verlag, 1966.

[9] M. Bousquet-Mélou. A method for the enumeration of various classes of column-convex polygons. *Discrete Mathematics*, 154:1–25, 1996.

[10] M. Bousquet-Mélou and A. Rechnitzer. Lattice animals and heaps of dimers. *Discrete Mathematics*, 258:235–274, 2002.

[11] R. Brak and A. J. Guttmann. Exact solution of the staircase and row-convex polygon perimeter and area generating function. *Journal of Physics A: Mathematical and General*, 23(20):4581, 1990.

[12] R. Brak, A. L. Owczarek, and T. Prellberg. A scaling theory of the collapse transition in geometric cluster models of polymers and vesicles. *J. Phys. A: Math. Gen.*, 26:4565–4578, 1993.

[13] J. Cardy. *Scaling and renormalization in statistical physics*. Cambridge Lecture Notes in Physics. Cambridge University Press, 1996.

[14] J. Cardy. Exact scaling functions for self-avoiding loops and branched polymers. *Journal of Physics A: Mathematical and General*, 34(47):L665, 2001.

[15] L. Carlitz. Fibonacci Notes 4: q-Fibonacci Polynomials. *The Fibonacci Quarterly*, 13(2):97–102, 1975.

[16] P. Carmona, G. B. Nguyen, and N. Pétrélis. Interacting partially directed self-avoiding walk. From phase transition to the geometry of the collapsed phase. *Annals of Probability*, 44(5):3234–3290, 2016.

[17] P. Carmona and N. Pétrélis. Interacting partially directed self-avoiding walk: scaling limits. *Electronic Journal of Probability*, 21(49):1–52, 2016.

[18] P. Chassaing and G. Louchard. Reflected Brownian bridge area conditioned on its local time at the origin. *Journal of Algorithms*, 44(1):29–51, 2002.

[19] C. Chester, B. Friedman, and F. Ursell. An extension of the method of steepest descents. *Math. Proc. Cambridge Philos. Soc.*, 53:599–611, 1957.

[20] D. A. Darling. On the supremum of a certain Gaussian process. *The Annals of Probability*, 11:803–806, 1983.

[21] *NIST Digital Library of Mathematical Functions*. http://dlmf.nist.gov/, Release 1.0.13 of 2016-09-16. F. W. J. Olver, A. B. Olde Daalhuis, D. W. Lozier, B. I. Schneider, R. F. Boisvert, C. W. Clark, B. R. Miller and B. V. Saunders, eds.

[22] P. Duchon. Q-grammars and wall polyominoes. *Annals of Combinatorics*, 3:311–321, 1999.

[23] B. Duplantier and H. Saleur. Exact tricritical exponents for polymers at the Θ point in two dimensions. *Physical Review Letters*, 59(5):539–542, 1987.

[24] M. E. Fisher. Shape of a self-avoiding walk or polymer chain. *The Journal of Chemical Physics*, 44(2):616–622, 1966.

[25] M. E. Fisher, A. J. Guttmann, and S. G. Whittington. Two-

dimensional lattice vesicles and polygons. *Journal of Physics A: Mathematical and General*, 24:3095–3106, 1991.

[26] P. Flajolet. Combinatorial Aspects of Continued Fractions. *Discrete Mathematics*, 32:125–161, 1980.

[27] P. Flajolet and G. Louchard. Analytic Variations on the Airy Distribution. *Algorithmica*, 31(3):361–377, 2001.

[28] P. Flajolet, P. Poblete, and A. Viola. On the analysis of linear probing hashing. *Algorithmica*, 22:490–515, 1998.

[29] P. Flajolet and R. Sedgewick. *Analytic Combinatorics*. Cambridge University Press, 2009.

[30] P. J. Flory. Configuration of polymer chains. In *Principles of Polymer Chemistry*, chapter 10. Cornell University Press, 1953.

[31] G. Gasper and M. Rahman. *Basic Hypergeometric Series*, volume 96 of *Encyclopedia of Mathematics and its Applications*. Cambridge University Press, 1990.

[32] S. W. Golomb. Checker Boards and Polyominoes. *The American Mathematical Monthly*, 61:675–682, 1954.

[33] N. Haug, A. Olde Daalhuis, and T. Prellberg. Higher-order Airy scaling in deformed Dyck paths. *Journal of Statistical Physics*, 166(5):1193–1208, 2017.

[34] N. Haug and T. Prellberg. Uniform asymptotics of area-weighted Dyck paths. *Journal of Mathematical Physics*, 56:043301, 2015.

[35] N. Haug, G. Siudem, and T. Prellberg. Area-width scaling in generalised Motzkin paths. *Physica A*, 482:611–620, 2017.

[36] S. Janson, D. E. Knuth, T. Łuczak, and B. Pittel. The birth of the giant component. *Random Structures & Algorithms*, 4(3):233–358, 1993.

[37] V. Kac and P. Cheung. *Quantum Calculus*. Springer-Verlag New York, first edition, 2002.

[38] S. Leibler, R. R. P. Singh, and M. E. Fisher. Thermodynamic behavior of two-dimensional vesicles. *Physical Review Letters*, 59:1989–1992, Nov 1987.

[39] N. Levinson. Transformation of an analytic function of several variables to a canonical form. *Duke Mathematical Journal*, 28:345–353, 1961.

[40] G. Louchard. Kac's formula, Levy's local time and Brownian excursion. *Journal of Applied Probability*, 21(3):479–499, 1984.

[41] N. Madras and G. Slade. *The Self-Avoiding Walk*. Birkhäuser, New York, NY, 2013.

[42] S. N. Majumdar and A. Comtet. Airy distribution function: From the area under a Brownian excursion to the maximal height of fluctuating interfaces. *Journal of Statistical Physics*, 119(3/4), 2005.

[43] G. B. Nguyen and N. Pétrélis. A variational formula for the free energy of the partially directed polymer collapse. *J. Stat. Phys.*, 151:1099–1120, 2013.

[44] M. Nguyên Thê. Area of Brownian motion with generatingfunctionology. *Discrete Mathematics and Theoretical Computer Science*, AC:239–242, 2003.

[45] OEIS Foundation Inc. The On-Line Encyclopedia of Integer Sequences. `http://oeis.org`, 2016.

[46] F. W. J. Olver. *Asymptotics and special functions*. Computer Science and Applied Mathematics. Academic Press, 1974.

[47] A. C. Oppenheim, R. Brak, and A. L. Owczarek. Anisotropic step, surface contact, and area weighted directed walks on the triangular lattice. *Int. J. Mod. Phys. B*, 16(9):1269–1299, 2002.

[48] A. L. Owczarek and T. Prellberg. Pressure exerted by a vesicle on a surface. *J. Phys. A: Math. Gen.*, 47:215001, 2014.

[49] A. L. Owczarek, T. Prellberg, and R. Brak. The Tricritical Behavior of Self-Interacting Partially Directed Walks. *J. Stat. Phys.*, 72:737–72, 1993.

[50] R. B. Paris. The Asymptotic Behaviour of Pearcey's Integral for Complex Variables. *Proceedings: Mathematical and Physical Sciences*, pages 391–426, 1991.

[51] E. Pergola, R. Pinzani, S. Rinaldi, and R. A. Sulanke. A bijective approach to the area of generalized Motzkin paths. *Advances in Applied Mathematics*, 28(3):580 – 591, 2002.

[52] T. Prellberg. Uniform q-series asymptotics for staircase polygons. *Journal of Physics A: Mathematical and General*, 28:1289–1304, 1995.

[53] T. Prellberg and R. Brak. Critical exponents from nonlinear functional equations for partially directed cluster models. *Journal of Statistical Physics*, 78(3-4):701–730, 1995.

[54] T. Prellberg and A. L. Owczarek. Stacking models of vesicles and compact clusters. *Journal of Statistical Physics*, 80(3):755–779, 1995.

[55] T. Prellberg, A. L. Owczarek, R. Brak, and A. J. Guttmann. Finite-length scaling of collapsing directed walks. *Physical Review E*, 48(4):2386–2396, 1993.

[56] C. Richard. Scaling behaviour of two-dimensional polygon models. *Journal of Statistical Physics*, 108(3):459–493, 2002.

[57] C. Richard. Limit distributions and scaling functions. In A. J. Guttmann, editor, *Polygons, Polyominoes and Polycubes*, volume 775 of *Lecture Notes in Physics*, pages 247–299. Springer Netherlands, 2009.

[58] C. Richard. On q-functional equations and excursion moments. *Discrete Mathematics*, 309:207–230, 2009.

[59] C. Richard, A. J. Guttmann, and I. Jensen. Scaling function and universal amplitude combinations for self-avoiding polygons. *Journal of Physics A: Mathematical and General*, 34(36):L495–L501, 2001.

[60] C. Richard, I. Jensen, and A. J. Guttmann. Scaling prediction for self-avoiding polygons revisited. *Journal of Statistical Mechanics: Theory and Experiment*, page P08007, 2004.

[61] U. Schwerdtfeger. Linear functional equations with a catalytic variable

and area limit laws for lattice paths and polygons. *Eur. J. Comb.*, 36:608–640, 2014.

[62] U. Schwerdtfeger, C. Richard, and B. Thatte. Area limit laws for symmetry classes of staircase polygons. *Combinatorics, Probability and Computing*, 19(3):441–461, 2010.

[63] U. Seifert. Configurations of fluid membranes and vesicles. *Advances in Physics*, 46:13–137, 1997.

[64] J. Spencer. Enumerating graphs and Brownian motion. *Communications on Pure and Applied Mathematics*, 50(3):291–294, 1997.

[65] L. Takács. A Bernoulli excursion and its various applications. *Advances in Applied Probability*, 23:557–585, 1991.

[66] L. Takács. On a probability problem connected with railway traffic. *Journal of Applied Mathematics and Stochastic Analysis*, 4(1):1–27, 1991.

[67] L. Takács. On the distribution of the integral of the absolute value of the Brownian motion. *Annals of applied probability*, 3(1):186–197, 1993.

[68] L. Takács. On the total heights of random rooted binary trees. *Journal of Combinatorial Theory*, Series B 61:155–166, 1994.

[69] L. Takács. Limit distributions for the Bernoulli meander. *Journal of Applied Probability*, 32(2):375–395, 1995.

[70] C. A. Tracy and H. Widom. Level-spacing distributions and the Airy kernel. *Communications in Mathematical Physics*, 159:151–174, 1994.

[71] C. A. Tracy and H. Widom. The Pearcey process. *Communications in Mathematical Physics*, 263(2):381–400, 2006.

[72] F. Ursell. Integrals with a large parameter. The continuation of uniformly asymptotic expansions. *Mathematical Proceedings of the Cambridge Philosophical Society*, 61:113–128, 1965.

[73] F. Ursell. Integrals with a large parameter. Several nearly coincident saddle points. *Mathematical Proceedings of the Cambridge Philosophical Society*, 72:49–65, 7 1972.

[74] O. Vallée and M. Soares. *Airy functions and applications to physics*. World Scientific, 2004.

[75] E. M. Wright. The number of connected sparsely edged graphs. *Journal of graph theory*, 1:317–330, 1977.

[76] X. G. Viennot. Heaps of pieces, I: Basic Definitions and Combinatorial Lemmas. *Annals of the New York Academy of Sciences*, 576:542–570, 1989.

[77] C. H. Yeung, D. Saad, and K. Y. M. Wong. From the physics of interacting polymers to optimizing routes on the London underground. *Proceedings of the National Academy of Sciences of the United States of America*, 110(34):13717–13722, 2013.